Investigation of complexation and antimicrobial activity of gramicidin S in the presence of lipopeptides from Bacillus subtilis

By

Nicolaas Maré Vlok
BSc (Hons) Biochemistry

Dissertation approved for the degree

Doctor of Philosophy (Biochemistry)

in the

Faculty of Science

University of Stellenbosch

Supervisor: Dr. M. Rautenbach

Co-supervisor Prof J. Snoep

Department of Biochemistry

University of Stellenbosch

April 2005

Declaration

I, the undersigned, hereby declare that the work contained in this dissertation is my own, original work and that I have not previously, in its entirety or in part submitted it at any other university for a degree.

Nicolaas Maré Vlok

Summary

The implication of biologically active peptides from different organisms on one another in complex ecological communities is largely unknown at this stage. The elucidation of the nature of this influence may have practical implications in terms of organism resistance and the conservation of an optimal agricultural environment. This study was aimed to elucidate the effect of antimicrobial peptides from different co-habitational organisms, on each other, both in terms of bioactivity and interaction. The two peptides investigated were gramicidin S, a decapeptide from *Bacillus brevis*, and surfactin, a heptalipopeptide from *Bacillus subtilis.* Preliminary studies were also done on iturin A and synthetic analogues of iturin A and iturin C, both octalipopeptides from *Bacillus subtilis.*

Analytical antimicrobial assay systems were used to study the effect of surfactin on the antibiotic action of gramicidin S towards three different target cells namely, a Gram-positive bacterium (*Micrococcus luteus*), a Gram-negative bacterium, (*Escherichia coli*) and a fungus (*Penicillium corylophilium*). The investigation of the antifungal activity was hampered by the insensitivity and subjectivity of the majority of antifungal assays and necessitated the development of two new testing methodologies.

The investigation showed that surfactin had an antagonistic effect on the antimicrobial activity of gramicidin S against all three of the target cells. This antagonism is dose-dependent at concentrations lower than required for surfactin to exert biological activity. Electrospray mass spectrometry (ESMS) showed the formation of surfactin-gramicidin S complexes in 1:1 and 2:1 ratios with enhanced complex formation in an apolar environment. Dissociation experiments indicated that the peptide complexes were slightly less stable than the peptides alone. The presence of NaCl up to 80 mM had little effect on the stability of preformed complexes. Incubating surfactin with NaCl and $CaCl_2$ before titration with gramicidin S also did not affect complex formation. Furthermore, results from the pre-incubation studies with $CaCl_2$ indicated that surfactin-gramicidin S complexes might be formed through the displacement of the metal ion. The mechanism of this displacement is unlikely to be direct competition but rather the result of conformational changes induced by peptide-peptide interaction/interactions. A likely point of interaction the β-turns in the peptide ring.

Linear iturin A_2 and iturin C analogues were synthesised (8-Beta and 8-$Beta_c$) with solid phase peptide synthesis and purified using self-assembly and high performance liquid

chromatography. The products of the syntheses were analysed by ESMS and found to be correct. The products, together with commercially obtained iturin A, were used in biological assays and it was found that iturin A antagonises the antibiotic activity of gramicidin S but the linear analogues had no effect. Complex formation between iturin A and gramicidin S was observed using ESMS but no complexes were detected for the analogues, which reinforces the hypothesis that antagonism is related to the formation of inactive complexes.

In general, the formation of peptide-gramicidin S complexes may indicate that a defence mechanism may be present in which toxic peptides of the competitor organism are inactivated by peptides from co-habiting organisms.

chromatography. The products of the syntheses were analysed by ESMS and found to be correct. The products, together with commercially obtained iturin A, were used in biological assays and it was found that iturin A antagonises the antibiotic activity of gramicidin S but the linear analogues had no effect. Complex formation between iturin A and gramicidin S was observed using ESMS but no complexes were detected for the analogues, which reinforces the hypothesis that antagonism is related to the formation of inactive complexes.

In general, the formation of peptide-gramicidin S complexes may indicate that a defence mechanism may be present in which toxic peptides of the competitor organism are inactivated by peptides from co-habiting organisms.

Opsomming

Die invloed wat biologiese aktiewe verbindings van verskillende mikro-organismes in komplekse ekologiese omgewings op mekaar het, is onbekend. Die ontrafeling van die rol mag verskeie vrae ten opsigte van weerstandbiedenheid en ontwrigting van ekologiese landbou-omgewings beantwoord. Die doel van hierdie studie was om die invloed wat antimikrobiese peptiede, afkomstig van verskillende ko-habiterende organismes, op mekaar het te ondersoek– beide in terme van biologiese aktiwiteit en interaksie. Die twee peptiede wat ondersoek is, was gramisidien S, 'n dekapeptied geproduseer deur *Bacillus brevis* en surfaktien, 'n heptalipopeptied, geproduseer deur *Bacillus subtilis*. Voorlopige ondersoeke is ook uitgevoer op iturin A, en sintetiese iturin A en iturin C analoë, beide oktalipopeptiede van *B. subtilis*.

Analitiese antimikrobiese toetsstelsels is gebruik om die effek van surfaktien op die biologiese aktiwiteit van gramisidien S te bepaal. Drie teikenselle is gebruik nl. 'n Gram-positiewe bakterium (*Micrococcus luteus*), 'n Gram-negatiewe bakterium (*Escherichia coli*) en 'n fungus (*Penicillium corylophilium*) Die gebrek aan sensitiwiteit van bestaande antifungiese toetsstelsels het die ontwikkelling van twee nuwe toetstelsels genoodsaak.

Die ondersoek het aangetoon dat surfaktien 'n antagonistiese effek op gramisidien S se antimikrobiese werking teen al drie teikenselle het. Die antagonisme is waarneembaar by surfaktien konsentrasies veel laer as wat nodig is vir biologiese aktiwiteit. Elektrosproei-massaspektrometrie (ESMS) van surfaktien en gramisidien S mengsels het aangedui dat komplekse in 'n 1:1 en 2:1 stoichiometrie voorkom. Die vorming van peptiedkomplekse word ook deur 'n nie-polêre omgewing bevorder. Die stabiliteit van die peptiedkomplekse is ook geëvalueer met dissosiasie eksperimente en daar is gevind dat die komplekse minder stabiel is as die peptiede alleen - dit is 'n aanduiding van kompleksdissosiasie. Die teenwoordigheid van NaCl tot en met 80 mM het 'n minimale invloed op die stabiliteit van voorafgevormde peptiedkomplekse gehad. Inkubasie van surfaktien met NaCl en $CaCl_2$ voor titrasie met gramisidien S, het ook nie die vorming van peptiedkomplekse beïnvloed nie en die studies het aangetoon dat die komplekse moontlik gevorm word deur die verplasing van die alkalie-metaalioon. Dit is onwaarskynlik dat die meganisme van ioon-verplasing direkte kompetisie is, maar eerder as gevolg van interaksie in een van die β-draaie.

Linière iturin A_2 en linière iturin C analoë (8-Beta en 8-$Beta_c$) is gesintetiseer met behulp van soliede fase peptiedsintese en gesuiwer deur middel van "self-assembly" en "high performance liquid chromatography (HPLC)". Volgens die ESMS analise is die korrekte produkte verkry. Die analoë en kommersieel beskikbare iturin A is aan biologiese toetsing onderwerp en daar is gevind dat iturin A, maar nie die analoë nie, die antibiotiese effek van gramisidien S ophef. Die vorming van iturin en gramisidien S komplekse, wat met ESMS waargeneem is, versterk die teorie dat opheffing van aktiwiteit verband hou met die vorming van inaktiewe komplekse. Verder, die analoë het nie komplekse met gramisidien S gevorm nie.

Dit blyk vanuit hierdie studies dat die vorming van peptied komplekse moontlik deel kan uitmaak van 'n tipe verdedigingsmeganisme waar toksiese peptiede van kompeterende organismes, deur peptiede van ko-habiterende organismes, geïnaktiveer word.

"If I have seen farther than others, it is because I was standing on the shoulders of giants."
-- Isaac Newton

I dedicate this work to all the giants in my life - most of all, my mother a giant standing 1.6 meters tall.

Acknowledgements

I would like to extend my most sincere gratitude to the following persons for their invaluable assistance without which this work would not have been possible:

1. Dr. Marina Rautenbach, my supervisor for the guidance offered, lessons taught in science and in life, regular critical evaluation of this work and preparation of this manuscript.

2. Dr. Thinus van der Merwe for the mass spectrometric analyses, expert advice in planning experiments, and analysis of the data obtained as well as infinite patience and almost as many hours.

3. Ms Sandra Coetzer from the department of Plant Pathology for supplying the fungi and for advice on all things fungal.

4. My fellow students, especially Navin Naidoo and Getrude Gersner for instruction, advice, and motivation.

5. Dr Gawie Malherbe for 10 years of support through good and very difficult times.

6. My friends who remained my friends in spite of the neglect they suffered and all those who helped me without being aware of doing so.

7. A special word of thanks to Karin Joubert, for everything she did and did not do.

8. Peter Willemse who supplied the bricks and mortar for my castle in the sky.

9. Last but not least, my family and in particular my mother, Sumari Vlok, who supported me and believed in me even before I can remember.

Table of Contents

List of Abbreviations and Acronyms

A	Alanine
ACN	acetonitrile
AFM	Atomic Force Microscopy
Ala	Alanine
Asn	Asparagine
Asp	Aspartic acid
B. brevis	*Bacillus brevis*
B. subtilis	*Bacillus subtilis*
β-NC_{14}	β-aminotetradecanoic acid
BOC-ON	2-(BOC-oxyimino)-2-phenylacetonitrile
B-OH	B-hydroxy fatty acid
BOP	benzotriazol-1-yl-oxy-tris-dimethylaminophosphonium hexafluorophosphate
CFU	colony forming units
D	Aspartic acid
DCC	dicyclohexylcarbodiimide
DCM	dichloromethane
Dhbt	3,4-dihydro-4-oxo-1,2,3-benzotriazin-3-yl
DIPCDI	Diisopropylcarbodiimide
DIPEA	N, N'-diisopropylethyl amine
DMF	N, N'-dimethylformamide
DMPC	dimyristoylphosphatidylcholine
DPPC	dimyristoylphosphatidylcholine
DSC	differential scanning calorimetry
E	Glutamine

E. coli	*Eschericia coli*
ESMS	electro-spray mass spectrometry
F	Phenylalanine
FDNB	1-fluoro-2, 4-dinitrobenzene
Fmoc	N^9-fluoroenylmethyloxycarbonyl
FTIR	Fourier Transform Infra-red spectroscopy
Gln	Glutamine
Glu	Glutamic acid
GS	gramicidin S
HF	hydrofluoric acid
HOBt	1-hydroxy-benzotriazole
HPLC	High performance liquid chromatography
I	Isoleucine
IC_{50}	50 % Inhibitory concentration
ICmax	Maximal inhibitory concentration
Ile	Isoleucine
KCN	potassium cyanide
L	Leucine
LA	Luria agar
LB	Luria Broth
Leu	Leucine
M. luteus	*Micrococcus luteus*
m/z	mass to charge ratio
MIC	Minimum Inhibitory Concentration
N	Asparagine
NMR	nuclear magnetic resonance

O	Ornithine
Orn	Ornithine
P	Proline
P. corylophilium	*Penicillium cf. corylophilium*
PBS	phosphate buffered saline
PDA	potato dextrose agar
PDB	Potato dextrose broth
pfp	pentafluorophenyl
Phe	Phenylalane
Pro	Proline
PyBOP®	benztriazol-1-yl-oxy-tris-pyrrolidinophosphonium hexafluorophosphate
S	Serine
Ser	Serine
SPPS	Solid phase peptide synthesis
Surf	surfactin
t-amyl alcohol	2-methyl-butan-2-ol
tBoc	N^{α}-tertiary-butyloxycarbonyl
TFA	trifluoroacetic acid
TOFMS	Time of flight mass spectrometry
TSA	tryptone soy agar
TSB	Tryptone soy broth
Tyr	Tyrosine
UV	ultraviolet
V	Valine
Val	Valine
Y	Tyrosine

Preface

The Second World War was certainly one of the defining moments in the history of humankind. A moment that gave us the A-bomb, the cold war and unbeknown to many, a new war – a war not fought on the battlefields but a war fought everyday in and around us. The Second World War saw the introduction of penicillin in 1940 and the first case of clinical immunity was observed in 1942. Five years later 38% *Staphylococcus aureus* strains were penicillin-resistant - and thus the battle lines were drawn. Human beings are at a distinct disadvantage in this war for survival, as we do not fully comprehend the intricacies and complexity of the microbial environment -the same environment in which the battles are fought.

The antimicrobial peptides used in this investigation, gramicidin S, surfactin and iturin A, are produced under stress conditions, specifically oxygen stress. This study was launched to elucidate the influence of the peptides on each other and relate this to organism survival A multitude of studies have been initiated to elucidate the mechanisms of action for the peptides in isolation. The studies were initiated to explore clinical, agricultural, and industrial applications of the peptides and peptide analogues. However, not a single study investigated the influence that the peptides might have on one another in terms of biological activity. Although the peptides are of great commercial importance, their fundamental purpose should never be forgotten. These peptides are created by nature to facilitate producer survival in complex ecological communities and are as such secreted not in isolation but together with numerous other compounds from a variety of organisms.

This thesis describe a possible alternative bacterial defense mechanism and by implication an alternative model for bacterial resistance. The first chapter is dedicated to a short overview of the antibiotic peptides used in this study and the following five chapters will describe and discuss the experimental results obtained. To facilitate future publication of this work, each chapter is written with publication format in mind and therefore is, to a certain extent, independent units. Unfortunately, this approach does lead to a repetition, but every attempt was made to keep this to a minimum.

In summary, the aim of this thesis is to elucidate a possible alternative function for surfactin in host-defence and to evaluate the feasibility of extending this project to include iturin A and C. The following objectives were set to meet this aim:

1. The synthesis of iturin C (8-Beta$_c$) and iturin A_2 (8-Beta) analogues as well as the analyses of commercially available compounds used in this study (Chapter 2)

2. Development of an antifungal assay system with sufficient sensitivity (Chapter 3);

3. Investigation of the influence of surfactin on gramicidin S antimicrobial activity using the developed assay system (Chapter 4);

4. Mass spectrometric investigations of peptide interactions to explain the results observed with biological testing (Chapter 5).

5. Investigation of the influence of iturin A and iturin analogues on gramicidin S antimicrobial activity (Chapter 6)

Chapter 1

Literature overview on selected cyclic peptides produced by Bacillus subtilis and Bacillus brevis

1.1 Introduction

In complex ecological communities, as found in soil and aquatic ecosystems, many defence strategies have evolved among co-inhabitants in the fight for survival. These strategies involve both the physical environment and the active production of compounds. The physical environment can be used as a weapon through adaptation such as sporulation to withstand conditions that competitors cannot. Active resistance revolves around antibiotic production that includes extra-cellular enzymes such as proteases, DNA replication inhibitors, and antimicrobial peptides [1, 2, 3]. Antibiotic production is a characteristic of many micro-organisms including Gram-positive bacteria from staphylococcus, streptomyces, and bacilli species [4]. This study will focus on one defence strategy – antimicrobial peptides – produced by two co-habiting bacilli, *Bacillus brevis* and *Bacillus subtilis*. Furthermore, a newly discovered defence strategy involving the antimicrobial peptides from the bacilli will be presented in this thesis.

1.2 Cyclic Peptides from *Bacillus*

Antimicrobial peptides can be classified into two broad categories: 1) gene products and 2) secondary metabolites. Peptides belonging to the first group are directly translated from the organism genome and synthesised through the ribosomal mechanism. Magainins, melittin, and secropins are representatives of this class [5, 6]. The second group of peptides are synthesised through non-ribosomal multi-subunit synthetases, which activate, isomerise, modify amino acids, and incorporate non-amino acid moieties in the primary peptide structure. The synthetases are also responsible for cyclisation of the primary sequence to form the peptide ring structure - gramicidin S, surfactin, and the iturin family of peptides

represent this group. Gramicidin S, together with tyrocidin A-E is produced by B. brevis [7, 8, 9, 10, 11]. Both surfactin and iturin A is produced by *B. subtilis*. Furthermore, iturin A together with iturin A_L and C, mycosubtilin, bacillomycin F, D and L and bacillopeptin/bacillomycin L_c belongs to the iturin group of peptides [12, 13, 14, 15, 16, 17]. The iturins share many structural features such as a constant LDDLLDL chiral sequence, a β-D-amino acid residue, and a ring structure closed by a lactam ring. Peptidic variants of surfactin have been isolated from *Bacillus licheniformis* (lichenysin [18, 19, 20, 21] and antiadhesin [22]) and *Bacillus pumilus* (pumilacidin [23]). The common denominator to all these peptides is the pronounced amphipatic character that is essential to peptide function.

This discussion will be limited to four cyclic peptides produced by soil-borne saprophytic bacteria from the genus *Bacillus* namely gramicidin S from *B. brevis* as well as iturin A, iturin C and surfactin from *B. subtilis*. Phylo-genetically the genus is divided into five groups of endosporulating bacteria with *B. subtilis* in group II and *B. brevis* in group III [4]. The bacteria of group II all produce acids from sugars and are facultative aerobes and can therefore grow and sporulate under strict anaerobic conditions given glucose and nitrate as terminal electron acceptor [4]. The bacilli of group III are strictly aerobic and do not utilise sugars as major carbon or energy source. Their energy requirements are met by acetate and amino acids, especially glutamate [4].

The history of the four cyclic peptides date back more than half a century. Investigation into two of the *B. subtilis* peptides, iturin A and surfactin began in 1946 and 1968 respectively [13, 24]. Gramicidin S was first isolated from *B. brevis* cultures in 1944 [25]. These peptides generated considerable interest from pharmaceutical, agricultural, and industrial sources as alternatives to current antibiotics and synthetic surfactants. Unfortunately, interest waned as the complicated nature of biological interaction and high production cost became apparent.

1.2.1 Chemical Structures

1.2.1.1 Gramicidin S

Gramicidin S is a cyclic amphipatic decapeptide [26] consisting of two antiparallel pentapeptides, D-Phe-Pro-Val-Orn-Leu, linked between D-Phe and Leu (*Figure 1*). The two tetrapeptide sequences Val-Orn-Leu assumes a double stranded β-sheet structure which

terminates in two type II β-turns defined by Pro-D-Phe residues. Intra-molecular hydrogen bonds between the two Val and Leu residues stabilise the rigid structure. The four hydrophobic side chains of the valine and leusine residues are on one side of the ring structure plane, and the two hydrophilic ornithine residues on the other, thereby conferring an amphipatic character on the molecule [27, 28, 29, 30].

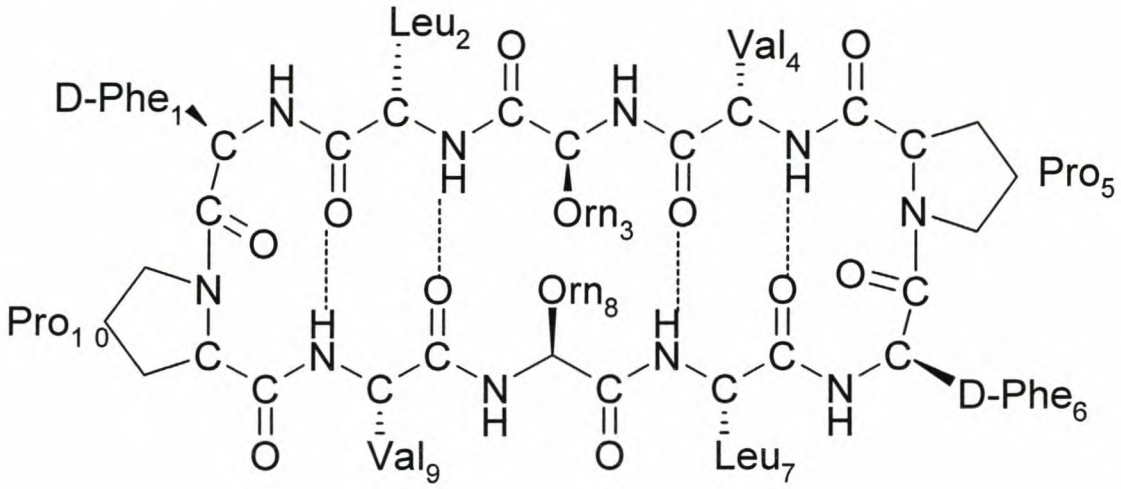

Figure 1 The structure of gramicidin S with the basic ornithine residues located on one side of the plane and the hydrophobic valine and leucine on the opposing side of the plane [26].

1.2.1.2 The Iturins

The iturin family of peptides share several common features such as a constant LDDLLDL chiral sequence of seven residues and a cyclic structure closed by a lactam ring at the β-D-amino acid (*Figure 2*). The β-D-amino fatty acyl-L-Asn_2-D-Tyr_3-D-Asn_4 peptide moiety is common to all the iturins except iturin C and bacillomycin F [31, 32].

The two iturins under investigation, iturin A and C, contain the following amino acid sequences: iturin A; L-Asn-D-Tyr-D-Asn-L-Gln-L-Pro-D-Asn-L-Ser and iturin C; L-Asp-D-Tyr-D-Asn-L-Gln-L-Pro-D-Asn-L-Ser (Table 1).

Table 1 Variations in the amino acid sequence of natural occurring iturin variants [12, 13, 14, 15, 16]

	Peptide sequence (N→C)							
	Position 1	2	3	4	5	6	7	8
Iturin A	*n*-C_{14}, *i*-C_{15}, *a*-C_{15}	L-Asn	D-Tyr	D-Asn	L-Gln	L-Pro	D-Asn	L-Ser
Iturin A_L	*i*-C_{16}, *a*-C_{16}	L-Asn	D-Tyr	D-Asn	L-Gln	L-Pro	D-Asn	L-Ser
Iturin C	*n*-C_{14}, *i*-C_{15}, *a*-C_{15}	L-Asp	D-Tyr	D-Asn	L-Gln	L-Pro	D-Asn	L-Ser

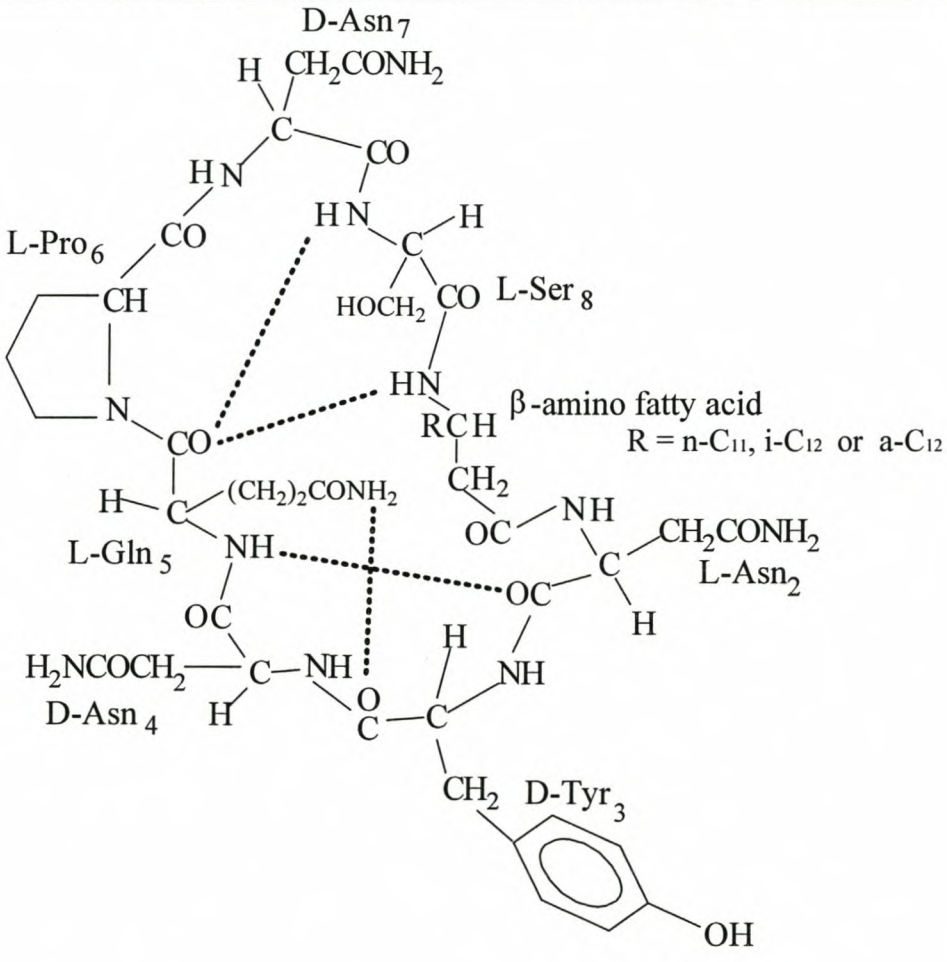

Figure 2 The structure if iturin A, The L-Asn_2 residue is replaced by L-Asp_2 in iturin C [31].

The structures of only two of the iturins, iturin A and bacillomycin F, have been elucidated through NMR spectroscopy and molecular modelling techniques [33, 34]. Garbay-

Jaureguiberry *et al.* [33] proposed the first three-dimensional structure for iturin A that was later further refined by Marion *et al.* [33 16]. Two type II β-turns in the tetrapeptide units stabilises the cyclic structure of iturin A in the tetrapeptide moieties β-amino fatty acyl-Asn_2-D-Tyr_3-D-Asn_4 (turn A) and Gln_5-Pro_6-Asn_7-Ser_8 (turn B). The two turns are linked by a third turn (turn C) consisting of Asn_2-D-Tyr_3-D-Asn_4-Gln_5. This turn can be classified as a type I' or III' β-turn; alternatively the beginning of a 3_{10}-helix with distorted hydrogen bonds in the turns. The peptide backbone confers a rigid conformation on the molecule, but the polar residues have a larger decree of freedom that allows interaction with an aqueous environment [31]. This conformation has also been referred to as an S conformation.

1.2.1.3 Surfactin

Surfactin, is an heptalipopeptide with the chiral sequence LLDLLDL that is similar to that of the iturins (*Figure 3*). The ring structure with sequence L-Glu-L-Leu-D-Leu-L-Val-L-Asp-D-Leu-L-Leu is closed by a β-hydroxy fatty acid by means of a lactone bond [35]. The spectrum of the fatty acid moiety has been elucidated as *iso*, *anteiso* C_{13}, *iso*, *normal* C_{14} and *iso*, *anteiso* C_{15} and *iso* C16 [36, 37, 38]. Natural occurring variant forms of surfactin differ at residue seven with L-Leu being substituted with either L-Ile or L-Val [39, 40]. In addition to these natural variants, Peypoux and co-workers isolated a surfactin with Val_4 substituted with alanine when surfactin was produced with alanine as sole nitrogen source in the growth medium [41] (Table 2). Although considerable variation is possible in the primary structure of surfactin, according to some sources surfactin are classified based on amino acid sequence as surfactin A (Leu_7), surfactin B (Ile_7) and surfactin C (Val_7) with the fatty acid moiety as C_{14} – C_{15} [42].

High-resolution ^1H NMR together with molecular modelling techniques led to the elucidation of the three-dimensional structure of surfactin [43]. The compact topology of the molecule is dictated by the cyclisation requirements, the chiral sequence, and favourable intra-molecular interactions. Two conformational states, S1 and S2, have been identified for surfactin [44]. In the S1 state the ring structure is stabilised by a hydrogen bond between NH of Glu_1 and C=O of Val_5. Three hydrogen bonds between NH of Leu7 and C=O of Asp5, NH of Val4 and C=O of Leu2, and the NH of Leu6 and the C=O of the β-hydroxy fatty acid stabilise the peptide ring in the S2 conformation. As a result, the backbone of the molecule folds into what has been called a W conformation or alternatively a β-sheet conformation that is retained in an

aqueous environment. It is interesting to note the similarities between the 3-dimensional structures of iturin A and surfactin, both forming β-pleated structures [34, 43, 45].

Table 2. Variations in amino acid sequence of natural occurring surfactin variants [39, 40, 41]

Peptide sequence (N→C)							
1	2	3	4	5	6	7	Fatty acid
Glu	Leu	D-Leu	Val	Asp	D-Leu	Leu	C13-16
Glu	Leu	D-Leu	Val	Asp	D-Leu	Ile	C13-15
Glu	Leu	D-Leu	Val	Asp	D-Leu	Val	C13-15
Glu	Leu	D-Leu	Ala	Asp	D-Leu	Leu	C13-15

The spatial arrangement of the constituent residues is such that the hydrophobic residues Leu_2 and D-Leu_6 face each other in the region of the acidic residues Glu_1 and Asp_5, which forms a minor polar domain. On the other side of the ring structure the Val_4 faces the lipidic chain, which constitutes a major hydrophobic domain. This spatial arrangement results in a pronounced amphipatic character.

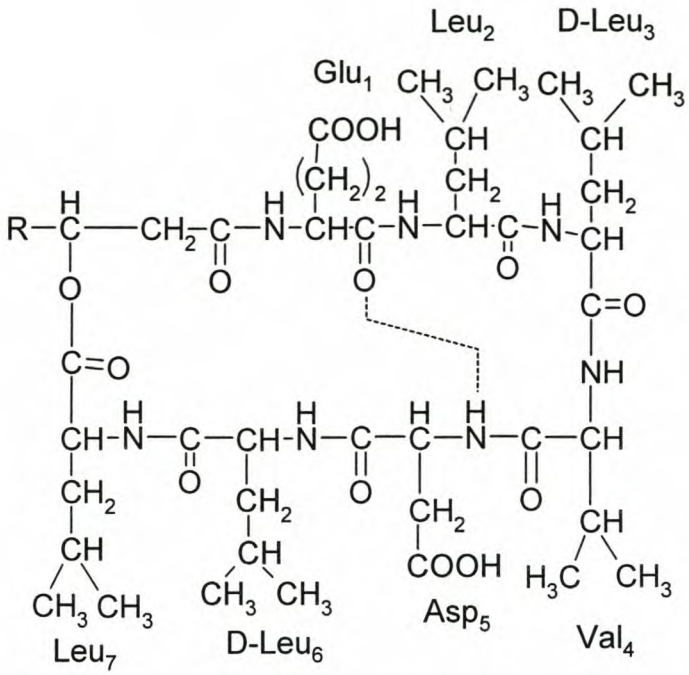

Figure 3 The structure natural occurring surfactin with variation caused by L- Ile and L-Val substitutions at D-Leu$_3$. R=*n*, *i*, *a* C_{11-14} [38].

1.2.2. Biosynthesis

Antibiotic peptides can be synthesised *via* two mechanisms, either through ribosomal synthesis or non-ribosomal synthesis. The non-ribosomal synthesis route is also known as the multienzyme thiotemplate mechanism [46, 47, 48, 49, 50]. All four peptides used in this study are produced using the non-ribosomal mechanism, which involves the gramicidin S, iturin, and surfactin synthetases. This type of peptide synthesis is catalysed by large, multifunctional enzyme of modular design. The biosynthetic pathway requires the activation of the amino acid residues at the activation domain of the minimal module by ATP to form amino-acyl residues, which are aligned in order of addition to the growing peptide chain. Activated amino acids are covalently linked as a carboxy-thioester to an enzyme bound 4'-phosphopantetheine (modifications to the residues such as epimerisation occur at this stage). Transpeptidation is facilitated by a multiple carrier mechanism, which implies multiple 4'-phosphopantetheinyl co-factors instead of a single arm mechanism. The peptide intermediate is transferred and linked to another acyl-amino acid intermediate on the adjacent downstream condensation domain to form a peptide bond. Synthesis is terminated by cyclisation, di- and trimerisation of

peptide precursors or transfer of the peptide to functional groups such as a fatty acid.

1.2.2.1 Gramicidin S

Gramicidin S synthetase II and I synthesise gramicidin S in the presence of ATP and Mg^{2+} [49, 50, 51]. Isolation of the nucleotide sequence of the genes involved in enzyme synthesis indicates that three genes denoted *grsA*, *grsB* and *grsT* encode the synthetase I, and synthetase II proteins with a high homology to a thioesterase of fatty acid synthetase complexes [52, 53, 54, 55]. The genes for the synthetase complexes are arranged in the order *grsA-grsB-grsT* and transcribed from a single promoter [53]. Synthetase I and II are responsible for the activation and racemisation of L-Phe to D-Phe and the activation of Pro, Val, Orn, and Leu respectively. The nucleotide sequence determination resulted in the accurate estimation of their respective molecular weights (126 663 Da for synthetase I and 510 287 for synthetase II) [56, 57]. The synthetase produces gramicidin S during the transition period between log and stationary phase after which the peptide rapidly disappears [58].

Antibiotic production is dependent on the interaction between several factors such as medium composition, temperature, and growth phase. Determination of optimal growth conditions is especially important when culturing the organism for large-scale peptide production. Even though oxygen has a pronounced effect on peptide production [59] most of the research has been directed at finding optimal carbon and nitrogen sources for chemically defined media. This situation is further complicated by different responses by the various strains of *B. brevis* to the same medium [60]. It must be noted that none of the sources quoted investigated the effect of oxygen limitation on gramicidin S production. This is of particular importance given that gramicidin synthetase is inactivated through oxidation and activated through reduction [59].

1.2.2.2 Iturin A

Except for iturin A synthetase, none of the other iturin synthetases have been fully characterised. Iturin A synthetase consists of two subunits, *Its* and *ITagp*. The activation of L-Ser is catalysed by *Its* and *ITagp* catalyses the activation of L-Asn, D-Asn, L-Gln and L-Pro [61]. The precise structure and mechanism of the iturin A multienzyme complex is still unknown as is the mechanism of storage and secretion.

1.2.2.3 Surfactin

Surfactin biosynthesis has been under investigation since 1968 when Kluge *et al.* [62] proposed a thiotemplate synthesis mechanism. The surfactin synthetase consists of four subunits, E_{1A}, E_{1B}, E_2, and E_3 with molecular masses of 460 kDa, 435 kDa and 160 kDa for E_{1A}, E_{1B}, and E_2 respectively [63, 64]. The forth subunit, E_3 has not been purified to homogeneity but the M_r is estimated at 40 kDa [64]. The genetic organisation of biosynthetic genes consist of a two operons of 25 kDa denoted *srfA* and a 4 kDa, *sfp* segment located downstream of *srfA* [65, 66]. The *srfA* operon consists of four modular open reading frames denoted ORF1 (*srfA-A*), ORF2 (*srfA-B*), ORF3, (*srfA-C*) and ORF4 (*srfA-D*). The first three reading frames encode the enzymes E_{1A}, E_{1B}, and E2 [67], and the fourth a protein with sequence homology to mammalian type II thioesterases [66]. Associated, but not integrated with *srfA* is *sfp,* which is essential for surfactin production. The encoded protein, termed sfp, belongs to the 4'-PPTases that function as a primer for non-ribosomal synthesis [68]. All the subunits are of cytoplasmic origin. The initiation intermediate of surfactin biosynthesis is β-hydroxyacyl-L-Glu produced by an acyltransferase with E_3 involved. The subunits E_{1A} and E_{1B} catalyse the elongation of the initiation product into a lipopeptide followed by the formation of a lipohexapeptide. This is achieved through a series of thioester bond cleavages and simultaneous transpeptidation reactions. Termination of synthesis occurs when subunit E_2 condensates Leu_7 to the lipopeptide and the release of the lipopeptidyl intermediate from the enzyme complex [47]. Three genes have been identified that controls swarming in *B. subtilis* [69]. Although these genes are not directly related to surfactin production it is interesting to note that one of the genes, swrC, confers resistance to surfactin.

Most of the research into the nutritional requirements of surfactin production was done with batch cultures, usually in shake flasks [70, 71]. Synthetic and organic media were developed from these experiments and the need for a nitrogen/iron/manganese molar ratio of 920:7.7:1.0 were established [72]. Acidification of growth medium was observed during iron enrichment and necessitated pH control as demonstrated by Wei *et al.* [73]. The best carbon sources were established as glucose, fructose, and saccharose, while glycerol greatly reduced surfactin production. The developed media supported bacterial growth very well, but had little success in stimulating surfactin production. The surfactin yield with these media ranged between 0.1 g/L and 1.1 g/L [72, 74]. In contrast to other biosurfactants, surfactin biosynthesis was not stimulated by hexadecane [70]. However, successful surfactin production was also achieved by oxygen limitation in which case the production increased to 7 g/L [75]. The importance of oxidative processes in the production of surfactin was further illustrated by the work of

Roubin *et al.* [76]. The authors have shown surfactin over production in a mutant strain with isocitrate dehydrogenase activity 30 times lower than the parent strain. This mutation resulted in a four-fold increase of surfactin production. The same effect was also achieved by adding citric acid to the medium and oxygen limitation. Equally important is the source of nitrogen as terminal electron acceptor. Davies *et al.* [77] found that nitrate depletion resulted in a dramatic increase in surfactin. Using nitrate as sole nitrogen source did not benefit surfactin production but the transition from oxygen to ammonia to nitrate as electron acceptors was necessary for optimal production. Unfortunately, these studies were performed with different strains of *B. subtilis* and no comparative studies exist to objectively evaluate the influence of media and oxygen limitation on a specific strain.

1.2.3 Structure-function relationships and mechanism of action

The amphipatic character of the peptides endows them with a natural ability to disrupt membranes and as such be antibiotic. However, recent research suggests that these molecules are more than mere "glorified detergents". This idea is supported by the identification of intracellular targets for the peptides [78, 79, 80, 81, 82]. The mechanism of action of most antimicrobial peptides follows a fixed sequence which, involves: a) recognition of the target cell membrane, b) interaction with or transport across the cytoplasmic membrane, c) the formation of active complexes, and d) disruption and/or inhibition of normal physiological processes that lead to cell death.

Gramicidin S has a broad-spectrum antibacterial and antifungal activity [83, 84, 85]. Iturin A is active against many plant and animal fungi, but has limited antibacterial activity where as surfactin is active against mycoplasma and Gram positive bacteria [13, 85, 86, 87]. In addition, iturin A and surfactin has been shown to have a profound synergistic activity [88, 89].

1.2.3.1 Gramicidin S

The absence from of a fatty acid moiety - as found in the other peptides – in the gramicidin S structure necessitate the incorporation of the amphipatic character in the spatial orientation of the residues. This achieved by orientating the hydrophobic residues to one side of the plane and the charged residues in the other side of the half-chair β-pleated conformation [25] of the

peptide ring. To investigate the structure-function relationship the native peptide, as well as substitution, insertion, and deletion analogues were investigated [83, 90, 91, 92, 93, 94]. From these studies, it became clear that the δ-amino group of the Orn residues as well as the D-Phe-Pro residues at the β-turn are essential for activity. A series of cyclic gramicidin S analogues were synthesised with the number of residues varying from 6–21. Of the analogues containing ten or less residues, only those with 6, 8 and 10 residues showed activity against gram-positive bacteria. It was found that gramicidin S analogues containing 10, 11 and 12 residues had markedly higher activity than those containing less than 10 or more than 12. It is also interesting to note that of the analogues synthesised with residues varying from 6–14 those with less than eight residues and the analogue in which D-Phe was omitted showed no activity. Furthermore, Grotenbreg *et al.* [95] illustrated the importance of the proline residue in the peptide structure by synthesising a gramicidin S analogue without Pro that retained the β-sheet structure. The analogues with the proline residues replaced azidoproline, benzyloxycarbamate derivatives, and succinylamide derivatives of the residue lead to severe loss of antimicrobial activity. This indicates the critical importance of both ring size and the β-turn residues L-Pro and D-Phe [83, 95]. Substitution of the Orn residues with neutral residues [92], Glu, or Gln [96] led to total loss of activity illustrating the importance of the positively charged L-Orn residues on activity. This is may be related to electrostatic interaction with anionic membrane lipids and environment.

On microorganisms other than *B. brevis,* the gramicidin S mechanism of action involves both the cell membrane and intracellular targets [78, 79, 80, 81, 82, 97, 98]. The mechanism of action of gramicidin S also includes effects on the producer, *B. brevis* [99, 100, 101]. It has been shown that gramicidin S rapidly adsorbs to *Escherichia coli* cells [98]. Upon adsorption, gramicidin S disturbs membrane integrity. The mechanism of distortion may differ between Gram-positive, Gram-negative, and eukaryotic cells [91, 81, 102]. It has been demonstrated that gramicidin S increases the permeability of both the outer and the cytoplasmic membranes of Gram-negative cells (*E. coli*) with the concomitant release of intracellular components. Divalent cations such as Mg^{2+} and Ca^{2+} are essential to the stability of the lipopolisaccharide (LPS) moiety of the outer membrane [102]. Gramicidin S may compete with these cations for binding to the outer membrane. It is tenable that such binding may result in the destabilisation of the polysaccharides thereby enabling a second molecule of gramicidin S to reach the cytoplasmic membrane. Interaction between gramicidin S and the membrane lipids would then lead to the disruption of the permeability barrier. It is interesting to note that LPS

binding affinity does not correlate with antibacterial activity [91]. Furthermore, gramicidin S has also been shown to interact with the monovalent cations Li^+, K^+, Na^+, Rb^+, and Cs^+ [103, 104] through interaction of the β-turn carbonyl groups.

Investigation of the interaction of gramicidin S with dipalmitoylphophatidylcholine (DPPC) and dimyristoylphosphatidylcholine (DMPC) model membranes, using differential scanning calorimetry (DSC), showed a decrease in the T_m of both membranes (1.5–5 °C for DPPC and 4–6 °C for DMPC). However, ΔH of chain melting trends were unaffected by the addition of gramicidin S in the case of DPPC, but lowered in the case of DMPC [105, 106, 107]. In contrast to these findings Prenner *et al.* [108] found a decrease in ΔH values. This indicates that gramicidin S induced membrane disruption is in part achieved through the facilitation of gel to liquid crystalline state transition. Findings of a FTIR study by Akinoglu and co-workers [109] support the work of Prenner *et al.* They found that gramicidin S destabilised a model DPPC membrane. These findings [105, 106, 107, 108] underscore the heated debate regarding gramicidin S mechanism of action in relation to membrane action. Pache *et al.* [97] found that gramicidin S had no effect on the mobility of 12-deoxylstearic acid in dipalmitoyl lecithin bilayers and concluded that gramicidin S interaction with membranes occurs at the polar head groups. However, Kiricsi *et al.* [110] found that gramicidin S restricts the segmental movement of spin labelled C14 acyl chain in DMPC at a peptide: lipid ration of 1:10. In addition, Prenner and co-workers [111] found that the addition of cholesterol to DMPC model membranes attenuated the action of the antimicrobial peptide.

Studies with ^{14}C-labled gramicidin S and gramicidin S analogues showed that the peptide adhered more readily to protoplasts derived from gramicidin S susceptible bacteria (such as *B. subtilis* and *S. aureus*) than to insensitive bacteria (such as *E. coli*) [81]. In both cases, peptide adhesion increased linearly with peptide concentration up to the minimum inhibitory concentration (MIC) where after the adhesion rate slowed. At the MIC, enough peptide was adsorbed onto the membrane to cover the cell surface [112]. The adhered peptide could not be removed from protoplasts by washing with aqueous salt solutions, but could largely be removed by the addition of phospholipids. This shows that, although interactions with the negatively charged head groups are essential for the initial peptide–membrane interaction, the molecule rapidly partition into the hydrophobic bilayer. Orlova and co-workers, working with gramicidin S resistant *S. aureus*, demonstrated the importance of this interaction [113]. They found that the resistant organisms differ from the wild type strains in the Gly/Ser ratio of the

peptidoglycan as well as the degree of amidation of the α-carboxyles of Glu in the muropeptide. The overall effect was a decrease in the net negative charge of the membrane. Wu *et al.* [114] demonstrated the peptide's ability to rapidly depolarise the inner membrane of a barrier defective strain of *E. coli*. Depolarisation occurred at concentration well below the MIC [114], indicating the formation of ion channels in the bacterial membrane. Katsu *et al.* [98] reported a good correlation between the MIC values and the ability to increase the permeability of the inner membrane to K^+. These findings, together with the conductance data, provide compelling evidence that the primary target of gramicidin S is the lipid bilayer of bacterial membranes.

Even though the lipid bilayer is thought to be the primary target of gramicidin S it has also been shown that the peptide interacts with and affects certain membrane proteins and intracellular components. Studies with protoplasts from *Micrococcus luteus* showed a marked decrease in respiratory chain function. At sub-lytic concentrations gramicidin S increased membrane permeability to respiratory chain substrates resulting in a decrease in the activity of several respiratory chain enzymes [112]. The activity of Ca^{2+}-ATPase from human red blood cells is also inhibited [82] – this inhibition is not the result of the inhibition of calmodulin as the stoichiometry involved showed that it is unlikely that gramicidin S interacts with the small number binding sites on the enzyme. Inhibition is more likely the result of increased membrane permeability. In contrast, gramicidin S increased the activity of the calcium/calmodium dependent guanylate cyclase from *Paramecium* [99] and particulate guanylate cyclase from rat lung [115]. Gramicidin S has also been shown to interact with certain membrane bound transport systems [100].

Gramicidin S mechanism of action also extends to the producer organism. Interaction does not inhibit vegetative growth of *B. brevis,* but delay spore outgrowth with up to eight hours [100, 101]. Outgrowth of gramicidin S negative mutants started at 80 minutes, as did a rapid increase in respiration that continued for up to 200 minutes. During this time, RNA biosynthesis started at 100 min and peaked at 180–190 minutes. Protein synthesis developed at 190 minutes and continued until 250 minutes. In contrast, wild-type spores showed no outgrowth before 250 minutes with negligible respiration. This delay in outgrowth may be connected with the inhibition of amino acid transporters rather than nucleotide transporters as measured by [^{14}C]uracil and [^{14}C]lysine uptake. Gramicidin S did not show any interference with [^{14}C]uracil uptake in vegetative cells [100]. This observation led to the hypothesis that

gramicidin S is not only an antimicrobial peptide but also a bacterial hormone.

1.2.3.2 Iturin A and C

The combination of the C_{14}–C_{17} β-amino fatty acid moiety with the polar peptide ring imparts an amphipatic character on the iturins, which promotes interaction with cell membranes. This amphipathic character causes these molecules to spontaneously aggregate into micelles in an aqueous environment [116]. Their surfactant nature leads to the formation of monolayers at the air/water interface thus lowering the surface tension of aqueous solutions. The decrease of the critical micellular concentration (CMC) of iturin A is inversely proportional to aliphatic chain length [117]. Substitution of the fatty acid moiety with β-Ala led to total loss of activity and illustrates the importance of the fatty acid in its activity [118].

Substitutions and deletions in the peptide sequence elucidated the relative importance of not only the individual amino acids, but also their importance in terms of conformation and spatial orientation of the molecule as a whole. This is illustrated by the loss of antifungal activity by the addition of a carboxyl group near the fatty acid moiety as found in the inactive natural analogue, iturin C. This iturin has a L-Asp in position 2 at the C-terminal end of the fatty acid [17, 119]. No further investigation on the mechanism of action of iturin C has been done since its initial isolation in 1968 because no antimicrobial activity was then observed [17, 24]. Modification of the two invariant α-amino acid residues, D-Tyr and L-Asn, through O-methylation or O-acetylation eradicates all activity against *S. cerevisiae* [120]. This modification also leads to loss of haemolytic activity probably because of interference with lipid interaction [121]. Substitutions in the region flanking the N-terminal seems to be part of the evolutionary design of these peptides as modifications can occur in this region without the same devastating effect on peptide function that occurs with modifications at the C-terminus.

Rautenbach *et al.* [122, 123] did extensive work on the metal ion selectivity of iturin A and N-terminally modified analogues using electrospray mass spectrometry. They found that the number of sodium ions bound were dependent on analogue chain length, which is probably due to the elimination of carbonyl oxygens at the N-terminus. The iturin A analogues exhibited a selectivity with respect to alkali metal ion binding with $Na^+ > K^+ > Rb^+$, which indicates a size limitation in the interaction with the binding cavity or cavities. Furthermore, of the cyclic peptides bound to single sodium ion, the cyclic 7-beta analogue (iturin A_2 with L-Asn_2 deletion) was in a higher abundance compared to the cyclic 8-beta analogue

(synthetic iturin A_2), indicating that a single cation binding site is probably situated inside the peptide ring [122]. Rautenbach *et al.* [123] also demonstrated the sequence specific stabilisation of iturin A and analogues by bound sodium. Mass spectrometric fragmentation data revealed that sodium interacted with peptide bond carbonyl oxygens in the β-turns of the iturin A analogue, and may be part of the stabilisation of the structure. They postulated that the peptide ring carboxyl oxygens in one of the β-turns chelate alkali metal ions. This chelation would result in a cationic environment required for the formation of iturin A dependent anion selective pores that were observed by other investigators [12, 124].

Iturin A exerts its effect on the cell membrane as well as on intracellular targets. Interaction with the cell membrane leads to a disruption of the permeability barrier and an initial leakage of K^+. This is followed by a release of proteins, nucleic acids and the release of vesicles, which contain membrane lipids and iturin A [125, 126, 127]. The recognition of membrane components such as lipids may be part of this mechanism and may account for target cell specificity. The presence of cholesterol, ergosterol, oleic acid, phosphatidylcholine (PC), phosphatidic acid, and petroselenic acid in the membrane of *S. cerevisiae* inhibit the action of the peptide on this organism [128, 129]. This may also explain the lytic action of iturin A on erythrocytes since erythrocyte membranes contain PC and cholesterol in its membrane. Similarly, the resistance of the producer, *B. subtilis*, may be explained by the absence of PC and sterols from the outer membrane leaflet [12].

This action, which is dependant on the fatty acid moiety, is thought to be the result of peptide aggregation in the membranes with resultant formation of pores of unknown size and structure [130, 131, 132]. The invariant Tyr plays a key role in membrane interaction and aggregation. A comparison between iturin A and another peptide of the same family, mycosubtilin, lends some insight into the mechanism of action of the former. Mycosubtilin, which is also a lipopeptide, differs from iturin A in residues seven and eight. The D-Asn_7 and L-Ser_8 are replaced by L-Ser_7 and D-Asn_8 [130, 131]. Aggregates formed in DMPC membranes contain only iturin A molecules while that of mycosubtilin contain both mycosubtilin and DMPC in a 1:2 ratio [131, 132]. The difference in the ability to interact with membrane lipids may account for the increased biological activity of mycosubtilin. Mycosubtilin interacts with cholesterol in a 1:2 ratio where as a 1:1 ratio is found with iturin A [132]. The immiscibility of the complexes coupled to the interaction with monovalent cations leads to the formation of ion selective pores [122, 133, 134, 135, 136]. This is demonstrated by the slow increase in

membrane conductance, which is independent of the membrane potential [12]. Membranes treated with iturin A are slightly anion selective [133, 135]. The ability to bind cations may cause iturin A to act as an ion carrier transferring cations across membranes [122, 130]. Besson *et al.* [137] and Rautenbach [138] showed the transition of iturin A from a possible random conformation to organised secondary structures in lipid membranes using circular dichroism. This may be of significant relevance to biological activity. These results have been supported by the work of Grau and co-workers [116 139]. Furthermore, it was also shown that iturin A molecules have a strong tendency to interact with each other. This interaction changes with increasing concentration from a micelle to another form of aggregate, probably a lamellar vesicle. Furthermore, it has been suggested that that iturin A might form an integrated bilayer, which is consistent with results obtained with molecules of comparable amphipathic structure such as lysophosphatidylcholine [116].

It has also been suggested that iturin A activates phospholipases in membrane vesicles of *S. cerevisiae*. At this stage it is unclear whether activation occurs because of direct interaction or indirectly through stereoselective interaction with phospholipids substrates [128]. Other interactions may also take place if the synergistic effect of surfactin on the action of iturin A is taken into account [88, 89].

Recent studies suggest that the biological activity of iturin A also extends to the producer organism, *B. subtilis*. Ahimou and co-workers [140] found that upon secretion the molecule adsorb unto the producer, thereby changing the cell surface hydrophobicity. This may facilitate bacterial colonisation through enhanced interaction with environmental surfaces [140]. Similar mechanisms of adhesion have been found for *Serratia marcescens* and *Serratia rubidaea* [141].

1.2.3.3 Surfactin

Unlike the other lipopeptides used in this study, surfactin exhibits true biosurfactant and foaming properties for which it is renowned and has been described as the most powerful biosurfactant known [24, 142]. This property is the result of a pronounced amphipatic character imparted on the molecule by the β-hydroxy fatty acid and Glu and Asp residues [35, 36]. The β-hydroxy fatty acid moiety allows interaction with lipid bilayers and the polar residues contribute the molecule's metal chelating properties [143]. This selective chelating effect can be explained in terms of the partial neutralisation of the two acidic residues. These

residues form an "ionic basket" which can easily stabilise monovalent and divalent cations [143]. As a result, surfactin can transport mono and divalent cations through an organic barrier [143]. The selective affinities for divalent cations can be explained by the partial neutralisation of the acidic residues by Na^+ and K^+ where as Ca^{2+} causes complete neutralisation [144]. Cation selectivity studies have shown ion selectivity with $K^+ > Rb^+ > Na^+ > Cs^+ = Li^+$ [145]. Binding affinity measurements shows that surfactin can discriminate between Ca^{2+} and Mg^{2+}. The best fitting cation is Ca^{2+}, which stabilises the surfactin conformation and serves as an assembly template for the micelliation process [44, 146]. Furthermore, the stable β-sheet conformation facilitates the stacking of surfactin in stable rod shape micelles with an aggregation number $n = 173$. In addition Osman and co-workers [146] showed that Ca^{2+} induces α-helical conformation in surfactin up to 0.3 mM and 0.5 mM for surfactin monomers and micelles respectively. Although the authors reported a α-helical conformation structure size of the molecule would probably not allow this conformation. Therefore, the structure observed was more likely a 3_{10}-helix. At higher concentrations Ca^{2+} β-sheets were observed [146, 147].

Morikawa and co-workers [148] further illustrated the importance of the Asp and Glu residues as well as environmental conditions. They found that methylation and amidation of the residues lead to a 20% increase in surfactant activity but water solubility was lost. In contrast, the addition of aminomethane sulfonic acid drastically decreased activity. Environmental pH was found to have a profound influence and higher peptide activity was recorded under alkaline conditions. Acidic conditions, on the other hand, drastically reduced surfactin activity. It is interesting to note that a mutation of the Asp residue to Asn (thereby forming lichenysin [20]) caused a marked increase in surfactant and ion chelating properties where as the Asn to Asp mutation of iturin A (thereby forming iturin C [17]) lead to complete loss of biological activity.

Surfactin, as the name denotes, has powerful surfactant properties (it lowers the surface tension of water from 72 mNm^{-1} to 27 mNm^{-1} at concentrations as low as 20 μM) that forms the basis of its mechanism of action [149]. Surfactin's cellular effect results from the disruption of membrane integrity [150]. The basis of this disruption is the ability to interact with phospholipids although interactions with cations have to be considered given the molecule's ionic nature. Maget-Dana *et al.* [151, 152] found that these interactions facilitate peptide penetration into the membrane. A recent study showed that solubilization of the

membrane at high peptide concentrations is in part responsible for biological activity [153]. Another part of the activity can be explained by the formation of cation selective "pores" at concentrations significantly below the surfactin/lipid ratio required for membrane solubilization [145]. Surfactin showed antibiotic action against bacteria, mycoplasma, and enveloped viruses [87, 154]. The latter function is of special interest in a pharmaceutical context as the HIV virus belongs to this class of viruses. In addition, surfactin can differentiate between mycoplasma and viruses [149]. Other biological activities include antitumoral agent, a hypocholesterolemic, fibrin clot inhibitor, and starfish oocyte inhibitor [24, 149, 155].

The synergism between iturin A and surfactin sparked interest in the field of biological control. It was shown that iturin A inhibited the growth of various plant pathogenic fungi at low dosages [12]. Surfactin, which can form mixed micelles with iturin A, considerably augments the latter peptide's antifungal activity [88, 68, 156]. Ahimou and co-workers also found that surfactin, like iturin A, adheres to the producer cell surface. Furthermore Kinsinger *et al.* showed that rapid surface motility in the presence of surfactin is dependent on extra-cellular K^+ concentration [157].

1.3 Peptide Applications

Emergence of multi-drug resistant micro-organisms accentuated the need for continued development of antimicrobial agents. Overexposure to antibiotics in medicine and agriculture led to the evolution of these resistant strains [158, 159, 160, 161]. Moreover, many of the synthetic pesticides and insecticides may become useless due to revised safety regulations and concern over non-target effects [162, 163, 164, 165]. The broad-spectrum of antimicrobial activity coupled with membrane specificity makes these secondary metabolites an attractive alternative to current antibiotics. The cyclic peptides described here are already in use or exhibit potential to be used as biological control. Unfortunately, a plethora of complications has limited the general use of these compounds.

Even though the primary aim of many of the investigations concerning these molecules has been directed at antimicrobial applications, these molecules also possess other biological activities. In addition to agricultural and medicinal potential, important industrial applications are associated with surfactin as it may prove to be a natural alternative to many synthetic

surfactants currently in use.

1.3.1 Gramicidin S

Gramicidin S has already been patented as a topical antimicrobial agent [166, 167], but the strong haemolytic character has prohibited systemic use of its antimicrobial action. [83]. Fortunately, the dissociation of haemolytic and antimicrobial activity through manipulation of ring size and amphipathicity has been demonstrated [83]. These developments may in future pave the way to analogues with systemic application. The possible use of gramicidin S as biological control agent in agriculture has also been demonstrated [168, 169, 170]. Even though gramicidin S shows potent antimicrobial activity, widespread use has been hampered by high production costs and adverse systemic side effects. At this stage, the most promising use of this peptide is in biological control. Gramicidin S producing bio-films has successfully been used to combat the corrosion of mild steel in nuclear power plants by inhibiting the growth of sulfate reducing bacteria [171].

1.3.2 The iturins

The iturin family has been investigated as alternative antifungal agents. A broad-spectrum antifungal activity makes this group of peptides promising candidates for agriculture, medicine, and food preservation. A recent study by Deleu *et al.* [172] showed that, in addition to biological activity, iturin A has surfactant properties with the ability to resist creaming-flocculation. This characteristic extends this peptide's potential applications to industry as well as bioremediation.

Unfortunately, as with gramicidin S, large-scale use of the iturins has been hampered by a variety of factors. These include high production cost and peptide delivery to the target. Chemical syntheses of these compounds are not a viable production method due to the difficulty and high cost of synthesis and purification. However, high production costs may be counteracted by lower susceptibility to proteolytic degradation that in turn lowers the required dosage. The resistance to proteolytic degradation is imparted on the molecule through the inclusion of D-amino acids and β-amino fatty acid as well as the cyclic structure. Crude iturin A was used in clinical trials as topical treatment for dermatomycoses in both animals and

humans and was shown to have great potential because of a broad-spectrum of activity, low toxicity and low allergenic effect [173]. The adverse environmental effects and mammalian toxicity of many synthetic fungicides has drawn renewed attention to natural alternatives [174]. The iturins provide another alternative biological control agent whether used in purified form or as a product of the producing organisms [175].

The co-producer of iturin A and surfactin, *B. subtilis* RB-14 effectively inhibited damping-off of tomato seedlings caused by *Rhisoctonia solani* [176]. Brown fruit rot (caused by *Monolinia fructicola*) of stone fruits was controlled by *B. subtilis* B-3 [177]. One field study showed a marked reduction of mycoflora on stored feed grains at iturin A concentrations as low as 50–100 ppm [178].

1.3.3 Surfactin

Although experiments have shown that surfactin possesses a broad range of biological activities, the primary focus was the industrial applications of surfactin especially in relation to surfactant characteristics [149]. These characteristics may find applications in diverse industrial fields such as food formulation, cosmetics, road construction, pesticides, detergents, enhanced oil recovery, and bioremediation [179, 180]. Surfactin has successfully been used *in situ* for volatile organic compounds (VOC) contaminated soil remediation [181]. The viability of heavy metal extraction from soil using surfactin needs to be determined as other biological substances are far more effective [182]. Surfactin is preferred to the synthetic surfactants because of the bio-degradability of the natural product. Unfortunately, surfactin is unable to compete with chemically synthesised products due to poor strain yield, expensive growth media, and complicated purification processes [75, 183]. The biological application of surfactin is at this stage limited to biological control when secreted together with iturin A [168]. In this regard it is interesting to note that surfactin possesses insecticide activity against *Drosophila melanogaster* where as iturin is ineffective [184]. It possesses activity against bacteria and mycoplasma, but not in the same range as gramicidin S [85, 185]. Furthermore surfactin has been shown to selectively inhibit growth of cyanobacteria [186]. Bacteriostatic activity on *Micrococcus luteus* has been demonstrated when the organism was cultured in minimal medium [185]. Systemic applications such an antitumoral and antiviral agent are hampered not only by production costs, but also by its high haemolytic activity. Surfactin,

along with other bio-surfactants, have been shown to inhibit colonisation and bio-film formation of pathogenic bacteria on medical equipment and have successfully been used as adjuvant for the generation of monoclonal antibodies [42]. Further medical interest in surfactin was stimulated when it was shown that surfactin enhanced intratracheal delivery of insulin in rat lung [187] and that [Val_7] surfactin enhances the activation plasminogen [188].

1.4 References

1. Bu'lock J.D. (1961) *Adv. Appl. Microbiol.*, **3**, 293–342
2. Katz E. (1977) *Bacteriol. Rev.*, **41**, 449–474
3. Schaeffer P. (1969) *Bacteriol. Rev.*, **33**, 48–71
4. Sonenshein A. L., Hoch, J. A., Losick R. (eds.) (1993) Bacillus subtilis and other gram-positive bacteria biochemistry, physiology and molecular genetics, American Society for Microbiology, U.S.A.
5. Rinaldi A. C.(2002) *Curr. Opin. Chem Biol.*, **6**:799–804
6. Rautenbach M. & Hastings J. W. (1999) CHIMICA OGGI/*chemistry today,* November/December 1999, 81 –89
7. Dubos R. J. (1939) *J. Exp. Med.*, **70**, 1
8. Sarges R. & Witkop B (1964) *J. Am. Chem. Soc.*, **86**, 1862
9. Sarges R. & Witkop B (1965) *J. Am. Chem. Soc.*, **87**, 2011-219
10. Sarges R. & Witkop B (1965) *J. Am. Chem. Soc.*, **87**, 2020-2026
11. Sarges R. & Witkop B (1965) *J. Am. Chem. Soc.*, **87**, 2027-2034
12. Maget-Dana R. & Peypoux F. (1994) *Toxicology,* **87**, 151 –174
13. Peypoux F., Guinand M., Michel G., Delcambe L., Das B. C., Varenne P., Lederer E. (1973) *Tetrahedron* **29**, 3455 –3459
14. Delcambe L. (1965) *Bull. Soc. Chem. Belges*, **74**, 315 –328
15. Nagai U., Besson F., Peypoux F., (1979) *Tetrahedron Lett.* **25**, 2359 –2360
16. Winkelmann G., Allgaier H., Maget-Dana R., Thimon L., Peypoux F. Ptak M. (1992) *Biochimie,* **74**, 1047 –1051
17. Lupp R., Jung G. (1983) *J. Antibiotics* **36**, 1451 –1457
18. Peypoux F., Besson F., Michel G., Delcambe L., Das B. C. (1978) *Tetrahedron,* **34**, 1147 –1152
19. Yakimov M. M., Timmis K. N., Wray W., Fredrickson H. L. (1995) Appl Environ. Microbiol.**61**, 1706 –1713
20. Yakimov M. M., Timmis K. N., Wray W., Fredrickson H. L. (1996) *Biotechnol. Appl. Biochem.* **23**, 13 –18
21. Yakimov M. M., Abraham W-R., Meyer H., Giuliano L, Golyshin P. N., (1999) *Biochim et Biophys Acta*, **1438**, 273 –280

22. Trischman J. A., Jensen P. R., Fenical W. (1994) *Tetrahedron Lett.*, **35,** 5571 –5574

23. Batrakov S. G., Rodionova T. A., Esipov S. E., Polyakov N. B., Sheichenko V. I., Shekhovstova N. V., Lukin S. M., Panikov N. S., Nikolaev Y. A. (2003) *Biochim et Biophys. Acta*, **1634**, 107 –115

24. Naruse N., Tenmyo O., Kobaru S., Kamei H., Miyaki T., Konishi M., Oki T. (1990) *J. Antibiotic (Tokyo)* **43**, 80 –82

25. Arima K., Kakinuma A., Tamura G. (1968) Biochem. Biophys Res Commun. **31**, 488 –494

26. Gause G.F., & Brazhnikova M.G. (1944) *Nature (London)* **154**, 703

27. Battersby A. R. & Craig L. C. (1951) *J. Am. Chem. Soc.*, **73**, 1887 –1888

28. Hodgekin D. C., & Oughton B. M. (1957) *Biochem. J.* **65**, 752 –756

29. Stern A., Gibbons W. A., Craig L. C. (1968) *Proc. Natl. Acad. Sci. U.S.A* **61**, 734 – 741

30. Rae I. D. & Scherage H. A. (1978) *Biochem. Biophys. Res. Comm.*, **81**, 481 –485

31. Jones R. C., Sikakana C. T., Hehir S., Kuo M-C, Gibbons W. A. (1978) *Biophys. J.*, **24**, 815 –832

32. Marion D., Genest M., Caile A., Peypoux F., Michel G., Ptak M. (1986) *Biopolymers* **25**, 153–170

33. Kakinuma A., Hori M., Isono M., Tamura G., Arima K. (1969) *Agric Biol Chem.* **33**, 991–997

34. Garbay-Jaureguiberry C., Roques B. P., Delcambe L., Peypoux F., Michel M. (1978) *FEBS Lett.* **93**, 151 –156

35. Bonmatin J. M., Labbé H., Ptak M. (1994) *Biopolymers* **34**, 975 –986

36. Kakinuma A., Sugino H., Isono M., Tamura G., Arima K. (1969) *Agric Biol Chem.* **33**, 973–976

37. Kakinuma A., Sugino H., Isono M., Tamura G., Arima K. (1969) *Agric Biol Chem.* **33**, 971–972

38. Besson F., Tenoux I., Hourdou M.L., Michel G., (1992) Biochim Biophys Acta, 1123, 51-8

39. Kanatomo S., Nagai S., Ohki K., Yasuda Y. (1995) *Yakugaku Zasshi*, **115**, 756-64

40. Baumgart F., Kluge B., Ulrich C., Vater J., Ziessow D. (1991) *Biochem. Biophys. Res. Commun.*, **177**, 998 –1005

41. Peypoux F., Bonmatin J.M., Labbé H., Das B.C., Ptak M., Michel G (1991) *Eur. J. Biochem.*, **202**, 101-6

42. Peypoux F., Bonmatin J.M., Labbé H., Grangemard I., Das B.C., Ptak, M., Wallach J., Michel, G. (1994) *Eur J Biochem*, **224**, 89-96

43. Singh P. & Cameotra S. (2004) *TRENDS in Biotechnology*, **22**, 142 –146

44. Ferré G., Besson F., Buchet R. (1997) *Spectrochemica Acta Part A.*, 53, 632 –635

45. Ishigami Y., Osman M., Nakahara H., Sano Y., Ishiguro R., Matsumoto M. (1995) *Colloids. Surf. B.*, **4**, 341 –348

46. Kleinkauf H., & von Dohren M. (1990) *Eur. J. Biochem.* **192**, 1 –15

47. Stein T., Vater J., Kruft V., Otto A., Wittman-Liebold B., Franke P., Panico M., McDowell R., Morris H. R. (1996) *J. Biol. Chem.* **271**, 15428 –15435

48. Kohli R. M., Trauger J. W., Schwarzer D., Marahiel M. A., Walsh C. T. (2001) *Biochemistry*, **40**, 7099 –7108

49. Lipmann F. (1973) *Accounts. Chem. Res.* 6, 361 –367

50. Kurahashi K. (1974) *Annu. Rev. Biochem.* **43**, 445 –459

51. Laland S. G. & Zimmer T. L., (1973) *Essays Biochem.*, **9**, 31 –57

52. Krause M. & Marahiel, M. A., (1988) *J. Bacteriol.* **171**, 4669 –467 .

53. Krätzsmar J., Krause M., Marahiel M. A. (1989) *J. Bacteriol.,* **171**, 5422 –54

54. Hori K., Yanamoto Y., Minetoki T., Kurotsu T., Kanda M., Miura S., Okamura K., Furuyama J., Saito Y., (1989) *J .Biochem.*, **106**, 639 –6

55. Marahiel, M. A., Krause M., von Döhren H., Kleinkauf H., (1985) *J. Bacteriol.,* **162**, 1120 –11

56. Komura S. & Kurahashi K. (1985) *J. Biochem.*, **97**, 1409 –1417

57. Turgay K., Krause M., Marahiel M. H. (1992) *Mol. Microbiol.* **6**, 529 –546

58. Demain A. L. (1972) *J. Appl. Chem. Microbiol.*, **22**, 345 –362

59. Demain A. L. & Agathos S. N. (1986) *Can. J. Microbiol.*, **35**, 208 –214

60. Vandamme E. J. & Demain A. L. (1976) *Antimicrob. Agents Chemo.* **10**, 265 –273

61. Feignier C., Besson F., Michel M. (1996) *FEMS Microbiol. Lett.* **136**, 117 –122

62. Kluge B., Vater J., Salnikov J., Eckhart K. (1988) *FEBS Lett.* **231**, 107 –110

63. Ulrich C., Kluge B., Palacz Z., Vater J. (1991) *Biochemistry* **30**, 650 –650

64. Menkause M., Ulrich C., Kluge B., Vater J. (1993) *J. Biol. Chem.* **268**, 7678 –7684

65. Cosmina P., Rodriguez F., de Ferra F., Grandi G., Perego M., Venema G., van Sinderen D., (1993) *Mol. Microbiol.*, **8**, 821 –831

66. Nakano M. M., Magnusson R., Myers A., Curry J., Grosamn A. D., Zuber P. (1991) *J. Bacteriol.,* **173**, 1770 –1778

67. Vollenbroich D., Metha N., Zuber P., Vater J., Kamp R. M. (1994) *J. Bacteriol.,* **176**, 395 –400

68. Walsh C. T., Gehring A. M., Weinreb P. H., Quadri L. E., Flugal R. S. (1997) *Curr. Opin. Chem Biol.,* **1**, 309 –315

69. Kearns D. B., Chu F., Rudner R., Losick R., (2004) *Mol. Microbiol.*, **52**, 357 –359

70. Cooper D. G, MacDonald C. R, Duff S. F. B., Kosaric N. (1981) *J. Appl. Environ. Microbiol.*, **42**, 408 –412

71. Lin S. C., Carswell K. S., Sharma M. M., Georgiou G. (1994) *J. Appl. Microbiol. Biotechnol.,* **41**, 281 –285

72. Sheppard J. D. & Cooper D. G. (1991) *Appl. Microbiol Biotechnol.,* **35**, 72 –76

73. Wei Y. & Chu I. (1998) *Enzyme Microb. Technol.*, **22**, 724 –728

74. Nakano M. M., Marahiel M. A., Zuber P., (1988) *J. Bacteriol,.* **171**, 5662 –5668

75. Kim H. S., Yoon B. D., Lee C. H., Oh H. M., Katsugari T., Tani Y., (1997) *J. Ferment. Bioen.*, **84**, 41 –46

76. de Roubin M. R., Mulligan C. N., Gibbs B. F. (1989) *Can. J. Microbiol.*, **35**, 854 –859

77. Davies D. A., Lynch H. C., Varley J. (1999) *Enzyme and Microbial Technology*, **25**, 322 –329

78. Danders W. & Marahiel M. A. (1981) *FEMS Microbiol. Lett.,* **10**, 277 –283

79. Marahiel M. A., Danders W., Krause M., Kraepelin G., Kleinkauf H. (1979) *Eur. J. Biochem.,* **99**, 49 –55

80. Ristow H., Pschorn J., Hansen, Winkel U. (1979) *Nature (London),* **280**, 165 –167

81. Yonezawa H., Kaneda M., Tominag N., Hihashi S., Izumiya N. (1981) *J. Biochem.,* **90**, 1087 –1091

82. Iglesias R. O. & Rega A. F. (1987) *Biochim. Biophys. Acta,* **905**, 383 –389

83. Kondejewski L. H., Farmer S. W., Wishart D. S., Hancock R. E. W., Hodges R. S. (1996) *J. Biol. Chem.,* **271**, 25261 –25268

84. Prenner E. J., Lewis R. N. A. H., McElhaney R. N. (1999) *Biochim. Biophys. Acta*, **1462**, 201 –221

85. Béven L. & Wróblewski H. (1997) *Res. Microbiol.*, **148**, 163 –175

86. Johnson E. A. & Burdon K. L. (1946) *J. Baceriol.,* **51**, 591

87. Tsukagoshi N., Tamura G., Arima K. (1970) *Biochim. Biophys. Acta,* **196**, 204 –210

88. Ohno A., Ano T., Shoda M. (1995) *J. Ferment. Bioeng.*, **80**, 517 –519

89. Maget-Dana R., Thimon L., Peypoux F. Ptak M. (1992) *Biochimie,* **74**, 1047 –1051

90. Setsuko A., Nishikawa H., Takiguchi H., Lee S., Sugihara G. (1993) *Biochim Biophys Acta,* **1147**, 42–49

91. Jelokhani-Niaraki M., Kondejewski L. H., Farmer S. W., Hancock R. E. W., Kay C. M., Hodges R. S. (2000) *Biochem. J.,* **349**, 747 –755

92. Ovchinikov Y. V. & Ivanov V.T. (1975) *Tetrahedron* **31**, 2177 –2209

93. McInnes C., Kondejewski L. H., Hodges R. S, Sykes B. D. (2000) *J. Biol. Chem.*, **275**, 14287 –14294

94. Gibbs A. C., Bjorndahl T. C., Hodges R. S., Wishart D. S. (2002) *J. Am. Chem. Soc.*, **124**, 1203 –1213

95. Grotenbreg G. M., Spalburg E., de Neeling A. J., van der Marel G. A., Overkleeft H. S., van Boom J. H., M. Overhand (2003) *Bioorg. Med. Chem.,* **11**, 2835–2841

96. Tamaki M., Akabori S., Muramatsu I. (1996) *J. Peptide Protein Res.,* **47**, 369 –375

97. Pache W., Chapman D., Hillaby R. (1972) *Biochim. Biophys. Acta,* **255**, 358 –364

98. Katsu T., Kobayashi, H., Fujita, Y. (1986) *Biochim. Biophys. Acta,* **860**, 608 –619

99. Azuma T. & Demain A. L. (1996) *J. Indust. Microbiol.,* **17**, 55 –61

100. Seddon B. & Nandi S. (1978) *Biochem Soc. Trans.,* **6**, 412 –413

101. Nandi S. & Seddon B. (1978) *Biochem. Soc. Trans.,* **6**, 409 –411

102. Lugtenberg, B. & Van Alpen L. (1983) *Biochim. Biophys. Acta,* **737**, 51 –115

103. Gross D. S. & Williams E. R. (1996) *J. Am. Chem. Soc.,* **118**, 202 –204

104. Pankiewicz R., Gurzkowa A., Brzezinski B., Zundel G., Bartl F. (2002) *Journal of Molecular Structure*, **xx**, 1 –8

105. Wu E. S., Jacobson K., Szoka F., Portis A., (1978) *Biochemistry,* **17**, 5543 –550

106. Datema K. P., Pauls K. P., Bloom M. (1986) *Biochemistry,* **25**, 3796 –3803

107. Susi H., Sampugna J., Hampson J., Ward J. S. (1979) *Biochemistry,* **27**, 297 –301

108. Prenner E.J., Lewis R. N. A. H., Kondejewski L. H., Hodges R. S., McElhaney R. N. (1999) *Biochim. Biophys. Acta,* **1417**, 211 –223

109. Akinoglu B. G., Gheith M., Severcan F. (2001) *Journal of Molecular structure*, **565 – 566**, 281 –285

110. Kiricsi M., Horváth L. I., Dux I., Páli T. (2001) *Journal of Molecular structure*, **563 – 564**, 469 –475

111. Prenner E.J., Lewis R. N. A. H., Jelokhani-Niaraki M., Hodges R. S., McElhaney R. N. (2001) *Biochim. Biophys. Acta,* **1510,** 83 –92

112. Prenner E. J., Lewis R. N. A. H., McElhaney R. N. (1999) *Biochim. Biophys Acta,* **1462**, 201 –221

113. Orlova T. I., Bulgakova V. G., Polin A. N. (2003) *Antibiot. Khimoter.*, **48**, 13 -17

114. Wu M., Maier E., Benz R., Hancock R. E. W. (1999) *Biochemistry,* **38**, 7235 –7242

115. LAD P. J. & White A. A. (1979) *Biochim. Biophys Acta,* **570,** 198 –209

116. Grau A., Gómez-Fernández J. C., Peypoux F, Ortiz A., (2001) *Peptides*, **22**, 1 –5

117. Thimon L., Peypoux F., Maget-Dana R., Michel G. (1992) *J. Am. Oil. Chem Soc.,* **62**, 92 –93

118. Bland J. M., Lax A., Klich M. In: *Peptides* 1990: Proceedings of the Twenty-First European Peptide Symposium (Eds. Giralt E., Andreu D.,) ESCOM, Leiden, IL, pp 426 –427

119. Quentin M. J., Besson F., Peypoux F., Michel G. (1982) *Biochim. Biophys. Acta,* **684**, 207 –211

120. Besson F., Peypoux F., Quentin M. J, Michel G. (1984) *J. Antibiotics,* **37**, 172 –177

121. Besson F., Peypoux F., Michel G., Delcambe L. (1972) *J. Antibiotics,* **32**, 828 –833

122. Rautenbach M., Swart P., van der Merwe M. J. (2000) *Bioorg. Med. Chem.*, **8**, 2539 – 2548

123. Rautenbach M., Swart P., van der Merwe M. J. (2001) *J. Am. Mass Spectrom.*, **12**, 505 –516

124. Maget-Dana R., Ptak M., Peypoux F., Michel G (1992) *J. Colloid. Interface Sci.*, **149**, 174 –183

125. Thimon L., Peypoux F., Wallach J., Michel J. (1995) *FEMS Microbiol. Lett.,* **128**, 101 –106

126. Thimon L., Peypoux F., Exbrayat J. M., Michel G. (1994) *Cytobios,* **79**, 69 –83

127. Latoud C., Peypoux F., Michel G. (1987) *J. Antibiotics,* **40**, 1588 –1599

128. Maget-Dana R., Harnois I., Ptak M. (1989) *Biochim. Biophys. Acta,* **981**, 309 –314

129. Latoud C., Peypoux F., Michel G. (1990) *Can. J. Microbiol.*, **36**, 384 –389

130. Harnois I., Maget-Dana R., Ptak, M. (1988) *J. Colloid. Interface Sci.,* **123**, 85 –91

131. Maget-Dana R., Harnois I., Ptak, M. (1989) *Biochim. Biophys. Acta,* **981**, 309 –314

132. Maget-Dana R., Ptak M., Peypoux F., Michel G. (1987) *Biochim. Biophys. Acta,* **898**, 1 –5

133. Maget-Dana R., Ptak M., Peypoux F., Michel G. (1985) *Biochim. Biophys. Acta,* **815**, 405 –409

134. Maget-Dana R., Heitz F., Ptak M., Peypoux F., Guinand M. (1985) *Biochim. Biophys. Res. Commun.,* **129**, 965 –971

135. Maget-Dana R., & Ptak M. (1985) *Biochim. Biophys. Acta,* **1023**, 34 –40

136. Klumpp S., Jung G., Schultz J. E. (1984) *Biochim. Biophys. Acta,* **800**, 145 –151

137. Besson F., Raimbault C., Hourdou M. L., Buchet R. (1996) *Spectrochemica Acta Part A*, **52**, 793 –803

138. Rautenbach M., unpublished results

139. Grau A., Ortiz A., de Godos A., Gómez-Fernández J. C., (2000) *Archives of Biochemistry and Biophysics*, **377**, 315 –323

140. Ahimou F., Jacques P., Deleu M., (2000) *Enzyme and Microbial Technology*, **27**, 749 –754

141. Matsuyama T. & Nakagawa Y. (1996) *Colloids and Surfaces B: Biointerfaces*, **7** 207 – 214

142. Razafindralambo H., Paquot M., Popineau Y., Deleu M., Hbid C., Jacques P., Thonart P., (1998) *J. Agric. Food Chem.*, **46**, 911 –916

143. Timon L., Peypoux F., Wallach J., Michel J. (1993) *Colloids Surf. B.* **1**:57 –62

144. Maget-Dana R. & Ptak M. (1992) *J. Colloid. Interface Sci.,* **153**, 285 –291

145. Sheppard J.D., Jumarie C., Cooper D.G., Laprade R., (1991) *Biochim Biophys Acta*, **1064**, 13-23

146. Osman M., Høiland H., Holmson H., Ishigami Y. (1998) *J. Peptide Sci.,* **4**, 449 –458

147. Vass E., Besson F., Majer Z, Volpon L., Hollósi M. (2001) *Biochem. Biophys. Res. Commun.*, **282**, 361 –367

148. Morikawa M., Hirate Y., Imanaka T., (2000) *Biochim. Biophys. Acta*, **1488**, 211 –218

149. Peypoux F., Bonmatin J. M., Wallach J. (1999) *Appl Microbiol Biotechnol.,* **51**, 553 – 563

150. Bernheimer, A. W. & Avigad L. S. (1970) *J. Gen. Microbiol.,* **6**, 31 –36

151. Maget-Dana R. & Ptak M. (1995) *Biophys. J.,* **68**, 1937 –1943

152. Deleu M, Paquot M, Jacques P, Thonart P, Adriaensen Y, Dufrène Y. F. (1999) *Biophys. J.,* **77**, 2304 –2310

153. Carrillo, C, Teruel, J.A., Aranda, F.J., Ortiz, A. (2003) Biochim Biophys Acta, 1611, 91 –97

154. Vollenbroich D., Özel M., Vater J., Kamp R. M., Pauli G. (1997) *Biologicals,* **25**, 289 –297

155. Toroya, T, Maoka T., Tsuji H., Kobayashi M. (1995) *Appl. Environ. Microbiol.,* **61**, 1799 –1804

156. Thimon L., Peypoux F., Maget-Dana R., Roux B., Michel G. (1992) *Biotechnol. Appl. Biochem.*, **16**, 144 –151

157. Kinsinger R. F., Shirk M. C., Fall R. (2003) *J. Bacteriol.* 185, **5627-5631**

158. Neu H. C. (1992) *Science,* **256**, 1064 –1072

159. Amábile-Cuevas C. F., Cádenas-Garcia M., Ludgar, (1995) *Am. Scientist,* **83**, 320 – 329

160. DeMuri G. P., Hostetter M. K. (1995) *Paediatric Clinics of North America,* **42**, 665 – 685

161. Russell P. E. (1995) *J. Agric. Sci.*, **124**, 317 –323

162. Duke, S. O., Menn J. J., Plimmer J. R. (eds) (1993) Pest control with enhanced environmental safety, 1 –13, American Chemical Society, Washington DC

163. Felton G. W. & Dahlman D. L. (1984) *J. Econ. Entomol.*, 77, 847 –850

164. Dernoeden P. H. & McIntosh M. S. (1991) *Agron. J.*, **83**, 322 –326

165. Elmholt S. (1991) *Microb. Ecol.*, **22**, 99 –108

166. Bourinbaiar Aldar S, (1999) Method of treating herpes virus infections with spermostatic gramicidin - Administering effective amount of gramicidin for therapy and prevention, Metatron Inc, US 6001808

167. Bourinbaiar Aldar S, (1996) Gramicidin as a spermicide against sexual transmission of HIV, Metatron Inc, US 5552382

168. Singer S., Van Fleet A. L., Viel J. J., Genevese E. E. (1997) *J. Ind. Microbiol.Biotechnol.*, **18**, 226-231

169. Bapat S. & Shah A. K. (2000) *Can. J. Microbiol.*, **46**, 125 –32

170. Edwards S. G. & Seddon B. (2001) *J. Appl. Microbiol.*, **91**, 652 –659

171. Zuo R., Örnek D., Syrett B. C., Green R. M., Hsu C.-H., Mansfield F. B., Wood T. K. (2004) *Appl. Microbiol. Biotechnol.*, **64**, 275 –283

172. Deleu M., Razafindralambo H., Popineau Y., Jacques P., Thonart P, Paquot M., (1999) *Colloids Surfaces A: Physiochem. Eng. Aspects*, **152**, 3 –10

173. Blocquiaux S. & Delcambe L. (1956) *Arch. Belg. Derm. Symp.,* **12**, 224 –227

174. Clairbois J. P. & Delcambe L. (1958) *Arch. Belg. Derm. Symp.,* **14**, 63 –82

175. Besson F., Peypoux F., Michel M., Delcambe M (1978) *J. Antibiotics,* **31**, 248 –288

176. Asako O. & Shoda M. (1996) *App. Environ. Microbiol.*, **62**, 4081 –4085

177. Pusey P. L. & Wison C. L (1989) *Pestic. Sci.*, **27**, 133 –140

178. Klich M. A., Arthur K. S., Lax A. R., Bland J. M. (1994) *Mycopathologia*, **127**, 123 – 127

179. Georgiou G., Lin S-C., Sharma M. M. (1992) *Biotechnology*, **10**, 60 –65

180. Desai J. D. & Banat (1997) *Microbiol. Mol. Biol. Rev.*, **61**, 47 –64

181. Mulligan C. N., Yong, R. N., Gibbs B.F. (2001) *Engineering Geology*, **60**, 371 -380

182. Mulligan C. N., Yong, R. N., Gibbs B.F. (2001) *Journal of Hazardous Materials,* **85**, 311 -125

183. Davis D.A., Lynch H.C., Varley J. (2001) *Enzyme and Microbial Technology,* **28**, 346–354

184. Deleu A. L. K., Arnaud M., Paquot M., Thornart P., Gasper C. H., Haubruge E. (2002) *Meded Rijksuniv Gebt Fak Landbouwkd Toegep Biol Wet.*, **67**, 647 –655

185. Vlok N. M. & Rautenbach M., unpublished result

186. Joung A., C., Y., Jeon J. J. W., Kim H. S., Yoon B. D., Oh H. M. (2003) *Biotechnol. Lett.*, **25**, 1137 –1142

187. Okumura K., Iwakawa S., Yoshida T., Seki T., Komada F. (1992) *International Journal of Pharmaceutics*, **88**, 63 –73

188. Kikuchi T. & Hasumi K. (2002) *Biochim. et Biophys. Acta*, **1596**, 234 –245

Chapter 2

Syntheses, purification and analyses of peptides

2.1 Introduction

All the peptides used in his study, gramicidin S, iturin A and surfactin could be commercially obtained, except for iturin C. Solid phase peptide synthesis was used to first synthesise the linear analogues of iturin C (8-Beta$_c$) and iturin A (8-Beta). Although one of the aims was to synthesise iturin C, it also presented the opportunity to investigate the importance of structure and cyclisation in interaction with gramicidin S. Therefore, the linear iturin analogues 8-Beta$_c$ and 8- Beta were purified and analysed for use in this investigation (Chapter 6).

Peptide analogues of natural occurring peptides have successfully been used to elucidate the structural characteristics required for antimicrobial action. Analogues of gramicidin S have been used to investigate the importance of peptide sequence, and ring size [1, 2, 3, 4, 5, 6]. Similarly, analogues of surfactin have been employed to evaluate the importance of the acidic residues and fatty acid chain length [7, 8, 9]. Using iturin analogues, the importance of fatty acid chain length, the invariant L-Tyr and L-Asn residues as well as the influence of peptide chain length on metal ion chelation [10, 11,12, 13] were revealed.

2.1.1 Peptide synthesis

The history of solid phase peptide synthesis (SPPS) dates back to 1959 with the pioneering work of R.B. Merrifield. The success of the Merrifield protocol was demonstrated by the first solid phase synthesis of a biological peptide, bradykinin (1964) [14] and the first active enzyme, ribonuclease A (1969) [15].

Solid phase peptide synthesis involves four steps: 1) the immobilisation of the first amino acid to a functionalised insoluble matrix, 2) elongation of the peptide chain through the sequential addition of activated amino acids which are protected against side-chain reaction with labile protection groups, 3) the removal of excess reagents and by products trough filtration and 4) termination of the synthesis through the release of the crude peptide from the solid support

followed by purification. All current synthesis protocols proceeds from the C-terminal amino acid to the N-terminal amino acid. Synthesis in the C→N direction dictates the activation of the α-carboxyl group (to assist peptide bond formation) of the unbound amino acid as well as the reversible protection of the α-amino group (to limit polymerisation). The first step in SPPS involves the coupling of the first amino acid (C-terminal amino acid) to the solid support *via* ester formation with a functionalised linker. A two-dimensional protection scheme is employed in SPPS, the first involve a "semi-permanent" protection of the α-amino group of the incoming amino acid and the second a "permanent" protection of the functional side-chains of the bonded amino acid in the formed peptide chain. Successful SPPS depends not only on a successful coupling step, but also on the conditions under which the respective protection groups are removed. During the synthesis procedure, conditions are carefully controlled to ensure that deprotection of the α-amino group occurs at the appropriate step during the synthesis, while keeping all other protection groups intact. After completion of the synthesis, conditions are altered allowing the liberation of the peptide from the solid support and the removal of the remaining protection groups.

The original SPPS protocol, as devised by Merrifield, α-amino group protection was provided by the acid-labile N^{α}-tertiary-butyloxycarbonyl (tBoc) group. This group was cleaved from the amino acid using trifluoroacetic acid (TFA) [16]. Side-chain protection was conferred by ether, ester, and urethane derivatives based on benzyl alcohol, which could only be cleaved with hydrofluoric acid (HF) in the presence of carbonium ions [16] Several problems were associated with this protocol such as premature release of the peptide, trifluoroacetylation, as well as side reactions during HF cleavage [16]. In addition, the resin cleavage procedure required Teflon® coated equipment and the use and neutralisation of a strong acid (TFA) during each coupling step.

The problems experienced with the Merrifield protocol led to the development of N^{9}-fluoroenylmethyloxycarbonyl (Fmoc) protection scheme by Atherton, Sheppard, and Dryland (reviewed in [16, 17, 18]). This method of synthesis is based on the protection of the α-amino group with the base-labile Fmoc group [19], which can easily be removed through a β-elimination mechanism. The elimination of this group is initiated by secondary amines such as piperidine, which also scavenges the formed dibenzofulvene intermediate thus preventing re-addition to the peptide chain [16]. Side-chain protection in this protocol is conferred by tertiary butanol-based ether, ester, and urethane derivatives, which can be cleaved with TFA

with the concomitant release of the peptide chain from the solid phase. The developers of this method also introduced the use of a rigid solid support in the form of functionalised dimethylacrylamide cross-linked within Kieselguhr. The use of such a rigid solid support enabled the development of continuous flow synthesis [20].

Since peptide bond formation does not occur spontaneously, it follows that the process is mediated through the activation of the group/groups of involved in bond formation. The Merrifield protocol requires the activation of the α-carboxyl group, which are achieved through various methods. These methods include the use of carbodiimides to form anhydrides, active esters of the amino acids, phosphonium-based *in situ* activation agents such as benzotriazol-1-yl-oxy-tris-dimethylaminophosphonium hexafluorophosphate (BOP) [16, 17, 18] or its less toxic analogue benzotriazol-1-yl-oxy-tris-pyrrolidinophosphonium hexafluorophosphate (PyBOP®) [18, 20] and aminium/uranium salts as *in situ* activation agents such as O-(benzotriazol-1-yl)-1,1,3,3 tetramethyl uronium hexafluorophosphate (HBTU) [21].

The active amino acid esters employed in peptide synthesis are p-nitrophenyl [16], 3,4-dihydro-4-oxo-1,2,3-benzotriazin-3-yl (DhBt) [18] and pentafluorophenyl (Pfp) [16, 18] esters. These esters are generally used with 1-hydroxy-benzotriazole (HOBt) as acylation catalyst. The reactivity of the active esters was found to be lower than the symmetrical anhydrides, but the addition of HOBt greatly increased the reactivity and thus the reaction rate of the esters [22]. Both Dhbt and Pfp esters are suitable for peptide synthesis system that employs a polar, aprotic solvent such as N'N'-dimethylformamide (DMF).

Activation of the α-carboxyl group can also be accomplished through the formation of a active anhydride. Carbodiimides such as dicyclohexylcarbodiimide (DCC) and *N',N'*-diisopropylcarbodiimide (DIPCDI) are commonly used for this form of *in situ* activation.

The other general method of activation used in the syntheses required the use in situ activation agents such as of PyBOP® in the reaction mixture. Addition of PyBOP® to the reaction mixture, in the presence of a base (such as diisopropylethyl amine) creates highly active oxybenzotriazolyl esters [16]. Such coupling reagents rely on the formation of oxybenzotriazolyl esters for amino acid activation. This form of activation eliminates the time consuming process of symmetrical anhydride preparation and offers a cost effective alternative to active esters.

With most coupling methods, the use of HOBt as trapping" agent is recommended, because it leads to the formation of the racemisation-resistant oxybenzotriazolyl esters[18].

2.1.2 Peptide cyclisation

Cyclic peptides, of the "head-to-tail" variety, offer a variety of attractive characteristics, not found in linear peptides, for drug development. The absence of ionisable termini makes them resistant to *in vivo* degradation, resulting in higher bioavailability. Furthermore, cyclisation reduces conformational flexibility thereby enhancing receptor selectivity. Unfortunately, peptide cyclisation is not as straight forward as linear peptide synthesis and depends on a variety of factors. Peptide cyclisation has been reviewed extensively in literature [23, 24] and will be discussed in the broadest terms only. The synthesis of cyclic peptides from linear precursors can be performed in both solution phase and on solid phase.

Although solution phase cyclisation utilises the same coupling reagents as SPPS, another dimension to peptide bond formation is introduced, namely solubility and conformational variation in different solvents [24]. Kurome and co-workers [24] used a variety of solvents during the synthesis of auraobasidin and found a final product yield of 45% was obtained in dichloromethane (DCM), whereas the use of DMF did not result in cyclisation. This difference in product yield can be attributed to the difference in conformation of the linear precursor in the solvents.

Success has been achieved with all conventional activators activators, but recent reports suggest that uronium/aminium salts are more efficient at achieving cyclisation [24]. Contradictory to these findings, recent reports suggested that uranium-type reagents with tetramethyluronium moieties are involved in end-capping of the α-amino group involved in cyclisation [23]

Other strategies of involve cyclisation on solid supports and enzyme-catalysed cyclisation. Solid support cyclisation strategies involve the coupling of the C-terminal residue to the resin *via* the amino acid side chain, cleavage upon cyclisation ("cyclitive cleavage") [23, 24], and enzyme-catalysed cyclisation [25]. The coupling of the C-terminal amino acid side chain to the resin is most commonly used method, but the emergence of specialised linkers for "cyclitive" cleavage is pushing this method to the fore. Enzymes that are involved in the cyclisation of natural cyclic peptides can also be used to cylicise the linear precursor. The

use of enzyme-catalysed cyclisation is at this stage considered "cutting edge" [25] (reviewed in [23]).

2.1.4 Separation and analyses

After synthesis of a peptide, it is necessary to purify the peptide and confirm its chemical integrity and purity. A variety of separation and analytical techniques are available to the modern peptide chemist. Techniques in general use are chromatography and mass spectrometry. Other physical techniques such as circular dichroism, infrared spectrometry, and nuclear genetic resonance spectrometry are also used for structural analyses.

High performance liquid chromatography (HPLC) offers the advantage of being both a separation and an analytical tool. In this study, HPLC was used for both purification and separation. HPLC was first introduced between 1967 and 1969. This form of liquid chromatography revolutionised the field of separation science by offering the same quality of separation with greatly reduced analysis separation times. All types of chromatography are based on the selective partitioning of solutes between a mobile and a stationary phase. The separation and analytical reverse phase chromatography HPLC used in this study, is based on differences in hydrophobicity. A solvent gradient with decreasing polarity allows the analytes to desorb from the hydrophobic packing material in increasing order of hydrophobic character. This allows the more polar peptide synthesis by-products to elute first, followed by the synthesised peptide and more hydrophobic contaminants.

The development of "soft ionisation" techniques (reviewed in [26]) extended the use of mass spectrometry to large biomolecules, and especially peptides and proteins. Mass spectrometry, therefore, became a very important tool to evaluate the purity and chemical integrity of synthetic peptides. A variety of ionisation techniques such as matrix assisted laser desorption/ionisation (MALDI), electrospray ionisation (ES) atmospheric pressure chemical ionisation (APCI), and atmospheric pressure photo ionisation (APPI) are particularly suited to the analysis of bio-molecules.

The ionisation source utilised on all the analyses in this study was an ES source. Electrospray ionisation is based on the formation of highly charged droplets in a strong electric field. The ions created are liberated through desolvation by heat, vacuum, and dry gas. Ions can be generated through several mechanisms such as electron ejection, electron transfer, transfer

of a charged molecule from a condensed phase to the gas phase, protonation and deprotonation, as well as cationisation.

The ions are subsequently passed through a mass filter/analyser and are separated according to the mass to charge (*m/z*) ratios before being detected by either an electron multiplier or a scintillation counter. Two mass analysers were used in this study, the one a quadrupole and the other a time-of-flight analyser (TOF). A quadrupole analyser filters ions by passing them through four electromagnetic staves arranged perpendicular to one another. The radio frequency of the magnetic field generated are manipulated that only molecules with a certain *m/z* have stable trajectory through the analyser [27]. TOF-MS is based on the acceleration of gas-phase ions through an electric field into a field-free drift region. The constant acceleration voltage gives all ions the same kinetic energy, and the ions are propelled through the field-free drift region based on their specific mass-to-charge ratios. Smaller ions will move faster than larger ions for mass separation and the time needed to travel the length of the drift region can be related to the mass of the ion [28, 29] – hence the "time-of-flight".

In addition to the use of a mass spectrometer for analyte detection, it was also used for peptide identification through tandem mass spectrometry (MS/MS). Tandem mass spectrometry, also known as collisionally induced dissociation or collision activated dissociation, involves the decomposition/fragmentation of a selected molecular ion through the collision of the ion with a neutral gas. The ion is selected in the first mass analyser/filter before being passed into the fragmentation cell containing the collision gas. The product ions are subsequently analysed by the second mass analyser. The fragmentation of the peptides generally occurs at the peptide bond [30, 31, 32], but this may vary according to peptide sequence [33, 34] and protonation sites [30, 35, 36]. Cyclic peptides in general undergo ring opening at a proline residue [30, 33, 34]. The nomenclature used in describing fragmentation product ions from linear peptides were originally devised by Roepstorff and Fohlman [37] and later revised by Biemann [38] (*Figure 1*). An alternative nomenclature for cyclic peptides have been proposed by Ngoka and Gross [39] and adapted by Williams and Brodbelt [40]. According to the Roepstorff & Fohlman nomenclature, the scission at a peptide bond at the N-terminal side of the peptide is denoted as b_n with n the number of the peptide bond. Therefore, scission of the first peptide bond, between the first and the second residues, will create a b_1 fragment. Similarly, a scission at a C-terminal peptide bond is denoted y_m with m being the peptide bond as counted from the C-terminus. For a four residue peptide the scission of the peptide bond between residue four and three will result in a y_1 fragment (*Figure 1*). Scission of the bonds flanking the peptide

bond from the N-terminus are denoted a (i.e. resulting in decarboxylation of the preceding residue), and c (i.e. resulting in deamination of the following residue). Similarly scission of the bonds flanking the C- terminal peptide bond results in the formation of x (i.e. resulting in decarboxylation of the residue following the peptide bond) and z (i.e. resulting in deamination of the residue preceding the peptide bond) fragments. The system devised by Ngoka and Gross takes into account the more complicated nature of cyclic peptide fragmentation and allows for the unambiguous assignment of fragments – especially were repeat amino acid residues are involved. Instead of this nomenclature system, we opted to use the revised system of Biemann. This decision was based on the presence of a Pro residue(s) in two of the cyclic peptides in this study, which favours ring opening at the amino side of this residue. Therefore, the Pro residues of gramicidin S and iturin A were taken as the N-terminal residue of the linear peptide formed after ring opening. The lactone bond of surfactin is also the preferential site for ring opening for surfactin leaving its β-hydroxy fatty acid as N-terminal residue.

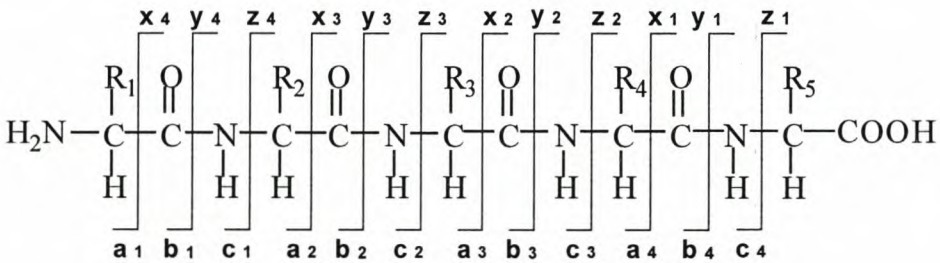

Peptide backbone product ions

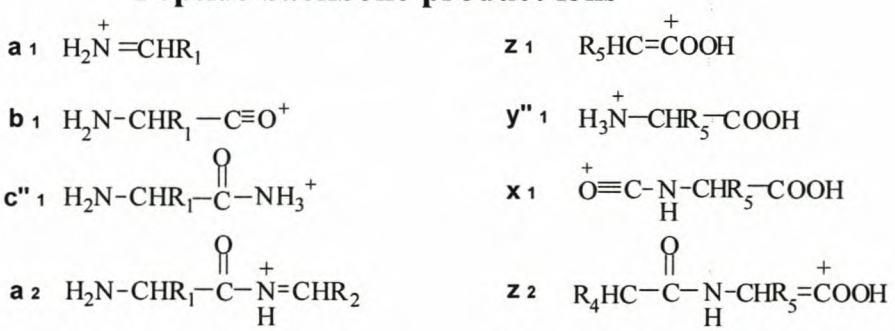

Figure 1 Peptide backbone product ions generated during tandem mass spectrometry [37, 38]. Figure reproduced with permission from M. Rautenbach [17].

2.1.5 Peptides in this investigation

Iturin A and surfactin are commercially available as lipopeptide mixtures from bacterial extracts. Gramicidin S, of which no known variations exist, could also be commercially obtained. These three peptides or peptide mixtures are of particular interest in the investigation, and most of the work of this thesis focussed on them (see Table 1 for their primary structures). As all these compounds are prepared from bacterial extracts, variations may exist in batch composition. In order to ensure comparability between our experiments, these products were analysed by analytical high performance liquid chromatography (HPLC) and electrospray ionisation mass spectrometry (ESMS) to ascertain their purity and composition.

The composition and yield of bio-synthetically obtained surfactin is greatly dependent on the nutrients supplied in the producer culture [41]. As a result, three main surfactin variants are produced named surfactin A, B, and C with residue 7 as Leu, Ile and Val respectively and fatty acid composition $C_{14\text{-}15}$. In addition surfactin variants have been isolated with Val_3, mutated to Ala, as well as the fatty acid chain C_{13} and C_{16} (see Chapter 1 for structures). This natural variation in surfactin composition necessitated the evaluation of surfactin composition of commercially obtained surfactin.

The group of compounds, collectively known as iturin A, consists of three compounds with the same primary structure, but varying fatty acid chain length [42, 43]. In addition, iturin A is co-produced with surfactin and mycosubtilin in some *B. subtilis* strains [44, 45, 46]. The ability of *B. subtilis* to co-produce compounds as well as the influence of nutrition on extract composition dictated the need to verify the commercial product composition.

Iturin C was not commercially available, so this necessitated its synthesis. Linear analogues of iturin C_2 (8-$Beta_c$) and iturin A_2 (8-Beta) with the fatty acid moiety as β-aminotetradecanoic acid (β-NC_{14}) were synthesised (Table 1). Iturin A_2 contains a lipid moiety, β-D-amino tetradecanoic acid (β-NC_{14}), but only the highly insoluble HCl salt of a racemic β-NC_{14} preparation was available to us [17]. Previously solubility problems were experienced with the synthesis of the Fmoc-derivative of the β-NC_{14} [17], therefore the tBoc derivative was used. The use of tBoc-βNC_{14} limited the inclusion of the residue at the N-terminal of the final coupling reaction. The use of a racemic mixture of β-NC_{14} in the

synthesis would therefore result in a racemic mixture of lipopeptide products. The cyclic peptide iturin A_2 was previously prepared through the cyclisation of 8-Beta [17]. A similar approach was followed in the synthesis iturin C_2, namely cyclic 8-$Beta_c$. The synthetic products were then purified by semi-preparative HPLC and analysed by analytical HPLC and ESMS.

Table 1 Primary structures of the commercial peptides and the iturin analogues synthesised in this study. The "N-terminal" of the cyclic peptides is as expected during ring-opening under mass spectrometry conditions. The "–" before the N-terminal and after the C-terminal residue denotes a cyclic structure. Possible variations in the lipid moieties are: $^{\$}$ *n*-,*i*-, *a*-C_{13-16}, $^{\#}$*n*-, *i*-, *a*-C_{14-16}. (Abbreviations: β-OHC = β-hydroxy fatty acid; β-NC_{14} = racemic β-aminotertadecanoyl; other amino acids are abbreviated by the standard 3-letter abbreviation including the D- or L-configuration).

	amino acid residue N→ C										
Peptide	**1**	**2**	**2**	**4**	**5**	**6**	**7**	**8**	**9**	**10**	**M_r**
Gramicidin S [47]	–L-Pro	L-Val	L-Orn	L-Leu	D-Phe	L-Pro	L-Val	L-Orn	L-Leu	D-Phe–	1141.2
Surfactin [48]	–βOHC	L-Glu	L-Leu	D-Leu	L-Val/ Ala	L-Asp	D-Leu	L-Leu/ Ile/ Val			1021.8*
Iturin A [49,50,51]	–L-Pro	D-Asn	L-Ser	D-β-$NC^{\#}$	L-Asn	D-Tyr	D-Asn	L-Gln–			1042.2
Iturin C [49]	–L-Pro	D-Asn	L-Ser	D-β-$NC^{\#}$	L-Asp	D-Tyr	D-Asn	L-Gln–			1043.2
8-Beta [17]	D/L-β-NC_{14}	L-Asn	D-Tyr	D-Asn	L-Gln–	D-Asn	L-Ser	L-Gln			1060.2
8-$Beta_c$	D/L-β-NC_{14}	L-Asp	D-Tyr	D-Asn	L-Gln–	D-Asn	L-Ser	L-Gln			1061.2

* M_r calculated using L-Val_5 and L-Leu/Ile_8

2.2 Materials

N, N'-dimethylformamide (DMF, 99%), diethyl ether, piridine, chloroform (>99%), glacial acetic acid, ethanol (>99.8%), butan-1-ol (99.5%), dichloromethane (DCM), phenol, potassium cyanide (KCN), *di*-phosphorous-pentoxide, 2',7'-dichlorofluorescein, ninhydrin, aluminium oxide 90, molecular sieve (0.3 nm pore size) and Kieselgel 60-F254 were from Merck (Darmstadt, Germany). Potassium hydroxide, anhydrous sodium sulphate, and self-

indicating silica gel were from Saarchem (Krugersdorp, South Africa). Ethyl acetate and 2-methyl-butan-2-ol (t-amyl alcohol; 98%) were from BDH Chemicals (Poole, UK). Fluka Chemicals (Buchs, Switzerland) supplied 1-fluoro-2,4,-dinitrobenzene, N, N'-diisopropylethyl amine (DIPEA) and CaH_2. Gramicidin S, trifluoroacetic acid (TFA, >98% and 99.5%) and piperidine (98%) were from Sigma (St Louis, USA). Romill Ltd (Cambridge, UK) supplied the acetonitrile (ACN) (HPLC-grade, UV cut-off 190 nm) and methanol (HPLC-grade, UV cut-of 205 nm). Nova-Pak® C18 (5 µm particle size, 60 Å pore size, 150 mm X 3.9mm) reverse phase analytical column, 0.45 micron HVLP membrane filters were from Waters-Millipore (Milford, USA). Macherey-Nagel supplied the Polygosil packing material (C_{18}, 60 °A, irregular particle size, 250mm X 10mm) packing material for the semi-preparative HPLC column. Analytical grade water was prepared by filtering water from a reverse osmoses plant through a Millipore Milli Q® water purification system. The purified 8-Beta reference peptide was kindly donated by Dr. M Rautenbach, University of Stellenbosch.

Fmoc-D-Asn(trt)OH, Fmoc-L-Pro(OH), Fmoc- D-Tyr(tBu)OH and Fmoc-L-Asn-OPfp were from Advanced Chemtech (Kentucky, USA). Calbiochem-NovaBiochem (La Jolla, USA) supplied benztriazol-1-yl-oxy-tris-pyrrolidinophosphonium hexafluorophosphate (PyBOP®), 1-hydroxy-benzotriazole (HOBt) and Fmoc-Gln-OPfp. The Fmoc-L-Asp(otBu) and Fmoc-L-Ser(tBu)-Pepsyn KA-resin (0.09 meq/g) and diisopropylcarbodiimide (DIPCIDI) were supplied by Milligen-Millipore (Milford USA). Fluka Chemicals (Buchs, Switzerland) supplied 2-(BOC-oxyimino)-2-phenylacetonitrile (BOC-ON). The HCl salt of β-aminotetradecanoic (β-NC_{14}) acid was donated by Dr. R. Levitt, formerly from Fine Chemicals, South Africa.

2.3 Methods

2.3.1 Preparation of solvents and reagents

2.3.1.1 Distillation and testing of N, N'-dimethylformamide

DMF is the primary solvent for Fmoc synthesis method and may contain impurities such as secondary amines and H_2O. The presence of these impurities will lead to the loss of the Fmoc and active ester groups. Reaction of water with DMF leads to the formation of dimethylamine and formic acid. Distilled, high purity DMF was used during the synthesis to avoid side

reaction with the amines, water, and other impurities. Before distillation, the DMF was placed on a rotary shaker with 10–20 g/L dry potassium hydroxide pellets to remove residual water. Volatile impurities such as secondary amines were removed by fractional distillation under reduced pressure (4 –7 mm Hg vacuum) with a dry nitrogen bleed. The high boiling point of DMF (163°C at atmospheric pressure) necessitated distillation under vacuum to avoid solvent decomposition at high temperature. The first 10% of the distillate was discarded and the constant boiling fraction collected (45°C at 10 mm Hg, [14]). Distilled DMF was stored in dark glass bottles at room temperature. Only DMF that passed Sanger's test for amines (see below) were used within 24 hours of distillation. The distillation procedure was done according to Rautenbach [17].

2.3.1.2 Sanger's test for amines

Because of the liability of the Fmoc group in the presence of secondary amines, all DMF was tested before use with Sanger's test for amines [52]. The test was carried out by mixing equal volumes of 1-fluoro-2, 4-dinitrobenzene (1 mg/mL FDNB in 95% ethanol) and DMF and leaving the mixture for 30 minutes in the dark at room temperature. The absorbance was measured at 381 nm, and 0.5 mg/mL FDNB was used as blank. The blank was only accepted if the absorbance was 0.20±0.01 absorption units. Suitably pure DMF had an absorbance of 0.02 to 0.07 absorbance units above the blank.

Sanger's test for amines was also performed on the DMF used in the final washing steps to ensure the complete removal of piperidine used in the deblocking steps of the synthesis protocol. A sample was taken from the final DMF wash and mixed with equal volume Sanger's reagent and determined spectrophotometricly at 381 nm without prior incubation. Synthesis continued if a zero reading was obtained.

2.3.1.3 Distillation of piperidine and pyridine

Quality control of piperidine and pyridine is essential for the same reasons as DMF quality control. Fractional distillation over 10–20 g/L potassium hydroxide with nitrogen bleed at atmospheric pressure was used to purify the solvents. The first 10% of the distillate was discarded and the constant boiling fraction (104°C for piperidine and 108°C for pyridine) was collected and stored in dark bottles [53].

2.3.1.4 Distillation of N'N-diisopropylethylamine

Distillation of N'N-diisopropylethylamine (DIPEA) was performed over ninhydrin (1-2 g/L) under nitrogen flow, and the fraction boiling above 116 °C was collected. The first distillate was the redistilled over KOH and under nitrogen flow. The constant boiling fraction at 127 °C was collected, aliquoted, and stored under nitrogen in airtight 4 mL vials at –10°C [20].

2.3.1.5 Distillation of Dichloromethane (DCM) (adapted from [54])

Dichloromethane was pre-dried over activated (dried at 100 °C for 72 hours) molecular sieve for 48 hours. Trace amounts of H_2O were subsequently removed by treating the DCM with CaH_2 (5g/L). The distillation of DCM was performed over CaH_2 The constant boiling fraction was collected at 40 °C after a small run-off was discarded.

2.3.1.6 Preparation of N^{β}-t-butyloxycarbonyl-β-aminotetradecanoic acid

N^{β}-t-butyloxycarbonyl-β-aminotetradecanoic acid was synthesised according to Rautenbach [17] (original method adapted from [55]). The HCl-salt of β-aminotetradecanoic acid (1.05 g, 3.75 mmole) was suspended in 5 mL DMF. TEA (2 mL) was added to the suspension while stirring at 50°C in an oil-bath. A 1.2 fold excess (1.16 g; 4.6 mmole) of 2-tertiary-butyloxycarbonyl-2-oxyimino-2-phenylacetonitrile (BOC-ON) was dissolved in 1.5 mL DMF and added drop-wise to the suspension. The resulting yellow suspension was stirred for a further two hours until clear. The reaction mixture was evaporated under vacuum to oil at 45°C. Diethyl ether (25 mL; filtered through activated aluminium oxide) was used to dissolve the oil and extracted twice with 5 mL saturated citric acid (59.2% m/m at 20°C) to remove residual BOC-ON and β-aminotetradecanoic acid. The aqueous fractions were combined and extracted twice with 5 mL diethyl ether. The combined diethyl ether fractions were washed twice with 25 mL water and dried twice with anhydrous sodium sulphate. The diethyl ether was evaporated under vacuum and the resultant oil dissolved in 10 mL heated acetonitrile (40°C). The solution was cooled in an ice bathed and left overnight at 4°C. The resultant crystalline product was filtered and washed with chilled acetonitrile and dried overnight under vacuum at room temperature.

Thin layer chromatography was performed on aluminium backed Kieselguhr 60-F_{254} and developed in chloroform:methanol:acetic acid (85:10:5). [16]. Plates were carefully air-dried and visualised under UV-light (254 nm) before being sprayed with 0.025% 2',7'-

dichlorofluoroscein in 95% ethanol. The sprayed plates were developed at 110°C for 5 minutes and visualised under UV-light. The plates were then sprayed with 0.2% ninhydrin in 95% and developed at 110°C for 5 minutes to detect residual amino groups.

2.3.1.7 Quality control and Kaiser test

All the amino acid derivatives used were tested before synthesis. This involved the determination of melting points and the Kaiser test for free primary amino groups [56]. The Kaiser test were performed by dissolving 5 mg of derivative in 100 µL DMF and adding 100 µL of each Kaiser solutions. Colours were evaluated after 5 minutes in an 80°C water bath by comparison to a standardised colour chart [57]. Only amino acid derivatives with the correct melting points and negative Kaiser tests were used in syntheses.

Three reagents are required for the Kaiser test: (1) 500 mg ninhydrin in 10 mL 95% ethanol; (2) 40 g phenol in 10 mL 95% ethanol; and (3) 2 mL 0.001 M KCN solution diluted to 100 mL with distilled pyridine. A 100 µL of each solution were added to 5 mg of the amino acid derivative and the. The mixture was heated in a water bath for 5 minutes at 80°C.

2.3.2 Peptide syntheses

2.3.2.1 Syntheses of linear peptides

Glassware used during peptide synthesis and removal of the completed peptide from the resin, was first rinsed three times with 60% ethanol/water and the three times with deionised water. After drying the glassware were pyrolysed at 650 °C for 90 minutes. Alternatively, the glassware were treated with chromic acid (5mg/mL potassium dichromate in H_2SO_4), washed, and dried before use. All dry reagents were desiccated for at least 30 minutes under vacuum in a desiccator containing self-indicating silica gel and *di*-phosphorous pentoxide before use.

The peptides were synthesised at room temperature using the Fmoc-polyamide principle using a shake-flask bench procedure according to Rautenbach [17]. The peptides were synthesised on commercially available Pepsyn-KA-resin (0.09 milli-equivalent per gram dry resin), with Fmoc-L-Ser(tBu) already attached. The resin was swollen before the synthesis in high purity DMF (20 mL/gram) for 30 minutes. The masses of the derivatives needed for peptide elongation were calculated from the resin capacity. A three times molar excess of Fmoc-

amino acids, HOBt (catalyst and "trapping" agent), and PyBOP (*in situ* activator), as well as a six fold molar excess of N,N'-diisopropylethyl amine (DIPEA) were used for coupling Fmoc-D-Asn(Trt)OH, Fmoc-L-Pro-OH, Fmoc-D-Tyr(tBu)OH, Fmoc-L-Asp(OtBu)-OH residues and the β-NC_{14} fatty acid moiety. The dry reagents were dissolved in minimum volume of DMF not exceeding 1.5 mL. The Fmoc pentafluoro esters derivatives of L-Asn (Fmoc-L-Asn-OPfp) and L-Gln (Fmoc-L-Gln-OPfp) were coupled using a three times molar excess of amino acid derivative and HOBt. The coupling reaction times varied from 60 to 90 minutes or until completion of the reaction as determined with the Kaiser test [56]. Four drops of each Kaiser solution were added to ether washed and dried resin sample taken during the synthesis. A Kaiser positive test was detected when the primary amino groups on the peptide chain and the reaction changed colour. The colour varied with the derivative coupled and the sequence of amino acids. Colours ranging from deep blue, orange and brown were detected. In a Kaiser negative test the beads remained a cream-yellow colour and the reaction mixture yellow. Resin samples were taken at the expected end of the coupling step. If this test was positive, the coupling time were extended until a negative test was obtained. Another resin sample was taken at the end of the deblocking step and had to be positive before the synthesis proceeded further.

Analytical Fmoc test was performed by deblocking a small analytically weight amount of resin (typically 10 mg). The resin was washed with ether and dried under vacuum before weighing. Piperidine (20% piperidine/DMF) was added to the resin (200 µL/µmole expected Fmoc-groups) and allowed to react for 30 minutes at room temperature. The characteristic UV absorbance of the liberated Fmoc-fulvene groups [18, 19] was measured at 290 nm after 50 times dilution of deblocking mixture with DMF. Coupling efficiency was calculated from the following equation [17]:

$$\%\text{Coupling efficinecy of the coupling step} = \frac{(\text{dilution} * A_{290} + 0.9975)}{0.2848}$$

Light path = 1 cm; resin capacity = 0.1 mmoles/1000 mg

After completion of a coupling step, as determined by negative Kaiser test, the resin was thoroughly washed with DMF to remove all traces of the reaction mixture. Piperidine (20% in DMF) was added to the resin to remove the Fmoc-group of the previously coupled amino acid. The reaction was allowed to proceed for 30 minutes after which the liberation of the

Fmoc-group was monitored at 290 nm and the deblocked α-amino group on the resin with the Kaiser test. The piperidine was washed from the resin with DMF until the DMF used in the washing process tested negative with Sanger's test.

The different peptides were synthesised up to the hexapeptide unit D-Tyr-D-Asn-L-Gln-L-Pro-D-Asn-L-Ser and split into three batches. The β-amino acid residue was coupled to one batch to produce 7-Beta (not used in the is study). L-Asn-βNC_{14} and L-Asp-βNC_{14} were coupled to the remaining batches to form 8-Beta (linear iturin A) and 8-$Beta_c$ (linear iturin C) respectively.

2.3.2.2 Removal of completed peptides from the resin

The resin was washed after the final coupling reaction and DMF, t-amyl alcohol, acetic acid, and again with t-amyl alcohol, and finally with peroxide free diethyl ether before being dried under vacuum. The peptides were cleaved from the resin by treating the resin for three hours with six bed-volumes 95% TFA and 5% phenol as scavenger [17]. After cleavage, the resin was removed by filtration and washed with one bed-volume 95 % TFA, two bed-volumes methanol and the mixture evaporated under vacuum using a Buchi Rotavapor at 45°C. The resin was then washed with four-bed volumes 50% acetonitrile/water that was added to the oily residue obtained with the first evaporation. The acetonitrile was evaporated as above and the peptide re-suspended in 50% acetonitrile and lyophilised.

2.3.2.3 Cyclisation of the peptides (adapted from [17])

Cyclisation using PyBOP®: The linear analogue (8-$Beta_c$) was either dissolved in DMF (15 μmole in 3 mL) and diluted ten fold in DCM or dissolved in DCM (30 mL) and then titrated with DMF to a clear solution. The peptide solution was then cooled to 0°C in an ice bath before PyBop®, HOBt (30 μmole each) and DIPEA (60 μmole) in 0.5mL DCM was added while stirring. The reaction mixture was stirred at room temperature (≈ 23 °C) for three days before a sample was taken and additional PyBOP® was added. This mixture was left to react for a further seven days at room temperature while continuously stirred. The reaction mixture was dried under N_2 stream before being dissolved in minimal volume 50% ACN/water and lyophilised.

Cyclisation using DIPCDI: As previous attempts at cyclisation using PyBOP were unsuccessful, the activated anhydride approach was investigated. A small quantity of 8-$Beta_c$

(1.5 μM) was dissolved in DCM (4 mL) and titrated with DMF until clear. The coupling reagent 263 μL (1.2 times molar excess) was dissolved in 4 mL DCM. The peptide solution was added drop wise to the DIPCDI solution over a period of 60 minutes, while stirring over ice. The mixture was left to react at room temperature for three days. The reaction was quenched by adding 2 times molar excess glacial acetic acid (192.6 μL) to the reaction mixture 30 minutes before removing the excess solvent under N_2 stream. The resultant residue was stored at –20 °C before HPLC purification.

2.3.3 Purification of the lipopeptides

2.3.3.1 Purification through self assembly (adapted from [58])

The lipopeptides were dissolved in minimum volume of 50% ACN/water and left to self-assemble (self-associate/aggregate) for seven days. The pellet and supernatant was separated through centrifugation and the pellet dissolved in 50% ACN/water and lyophilised.

2.3.3.2 High Performance liquid chromatography (HPLC)

The synthesised peptides were purified after self-assembly by semi-preparative HPLC [17]. The lyophilised pellets containing peptide were dissolved (1.5 mg/mL) in 50% ACN/water and centrifuged for 10 minutes at 1000 g to remove any particulate. The peptide solution was subsequently purified on a C_{18} Polygosil column (irregular particle size, 60 °A pore size, 25 mm X 10 mm). The chromatographic system comprised of two Waters 510 pumps, Waters Model 440 detector and a WISP 712 auto-sampler. The system was regulated by a MAXIMA software control system. A linear gradient at a flow rate of 3 mL/min was generated over 13 minutes from 70% eluant A (0.1% TFA in water) to 100% eluant B (10% eluant A and 90% ACN). The separation was monitored at 254 nm. Samples were lyophilised before further analyses were performed.

2.3.4 Analyses of peptides

2.3.4.1 Analytical HPLC

All peptides were analysed for purity on a C_{18} Nova-Pak® column (5 micron particle size, 60

°A pore size, 150 mm X 3.9 mm) using the same solvents and gradient program as for the semi-preparative HPLC, except that the flow rate was 1.0 mL/minute (Table 2.2).

2.3.4.2 Electrospray mass spectrometry

A Waters Q-TOF Ultima mass spectrometer, fitted with electrospray ionisation sources, was used for ESMS analyses of sample. Sample analyses and collisionally induced dissociation (CID) were performed in positive mode.

All the samples were prepared in 50% acetonitrile/water at 2 mg/mL (or 20 μM). Samples were dissolved immediately before analysis and 10 μL injected into the ESMS through a Rheodyne injector valve at 50 μL/analysis with 50% acetonitrile as carrier solvent. A capillary voltage of 3.2 kV was applied with ionisation source temperature at 80 °C. The cone voltage for the analyses was set at 40 or 60V. Data was collected in continuum mode through *m/z* = 100–2000 with a scan time of 1s and inter-scan time of 0.1s in the Waters Q-TOF Ultima mass spectrometer. Combining the scans across the elution peak and subtracting the background produced representative scans.

Collisionally induced dissociation was performed on the Q-TOF Ultima mass spectrometer with a collision gas pressure of 11 psi argon gas in the fragmentation cell with collision energy of 35 eV. Data acquisition was in the positive mode through the m/z = 200 –1400 at a scan time of 1s and inter-scan time of 0.1s with. The sum of an average of 150 scans was used to compile the mass spectra.

2.4 Results and Discussion

2.4.1 Analyses of commercially obtained peptides

2.4.1.1 Gramicidin S

Analytical HPLC was performed on the gramicidin S from Sigma to ascertain purity. The sample used throughout this study was found to be >99% pure. A single 254 nm absorbing fraction in the gramicidin S preparation eluted at 13:30 minutes as shown in *Figure 2*.

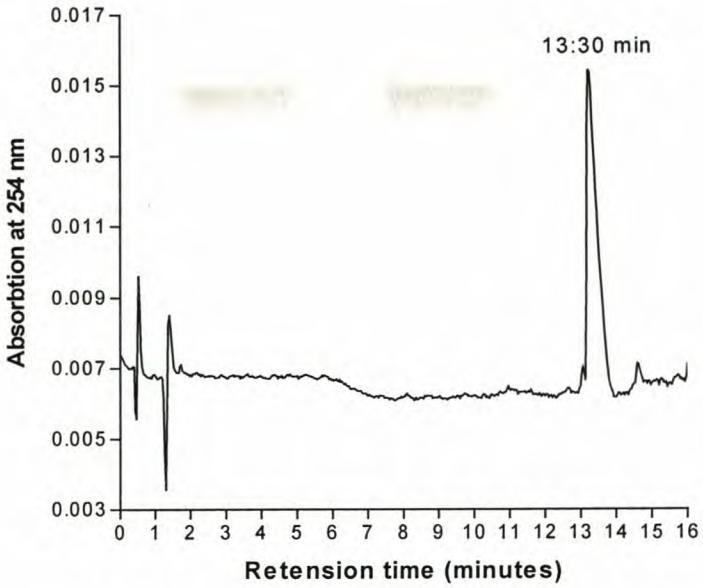

Figure 2 Analytical HPLC chromatogram of gramicidin S using a Nova-Pak C_{18} column. A linear gradient generated over 13 minutes with eluant A 0.1% TFA in water and eluant B 10% eluant A and 90% ACN. The fraction eluting at Rt = 13:30 minutes was evaluated with ESMS.

ESMS analysis of the gramicidin S (*Figure 3A*) also showed that the peptide is of high purity. Singly (*m/z* = 1141.24, expected *m/z* = 1141.70) and doubly charged molecular ions were detected with *m/z* of 570.72 (expected *m/z* = 571.35). Expected *m/z*-values for all the peptides were calculated from the mono-isotopic mass of the constituent amino acid residues [59]. In addition, two isotope species were also detected at 1142.28 and 1143.36, with a doubly charged isotopes at *m/z* = 572.16. Three other species were detected with *m/z* of 1183.38, 1155.40, and 1127.38. The specie with *m/z* of 1183.38 corresponds to an acetonitrile adduct of gramicidin S and the other two signals to M_r (gramicidin S) ±14. These may be unknown contaminants or may correspond to Leu_5/Leu_{10} mutated to either Val (*m/z* = 1127.38; expected *m/z* = 1127.44) or Val_3/Val_8 mutated to Leu (*m/z* = 1155.40; expected *m/z* = 1155.49), although no mutations on the gramicidin S structure have been reported. A trace signal was also detected at *m/z* = 881.34, which is the b8 fragment ion of gramicidin S. Tandem mass spectrometry (MS/MS) was performed (*Figure 3*B) on the molecular ion with *m/z* = 1141.2. Fragment assignment was done according to the nomenclature devised by Roepstorff and Fohlman [37] and revised by Biemann [38]. The major fragments detected were species with *m/z*-values of 881.58 (b_8), 831.49 (y_7), 666.84 (y_6), 571.34 ($[M+2H]^{2+}$ or b_5), 457.28 (b_9/y_5) and 311.20 (b_3). In addition a series of isotope signals (marked with *, *Figure 3*B) were detected with *m/z*-values of 1027.64, 1028.65, and 1029.66. These species could not be assigned to fragments generated with ring opening at Pro residue. However,

this series of species do correspond to the molecular ion with either of the Orn residues excised (see Addendum A for fragment analysis).

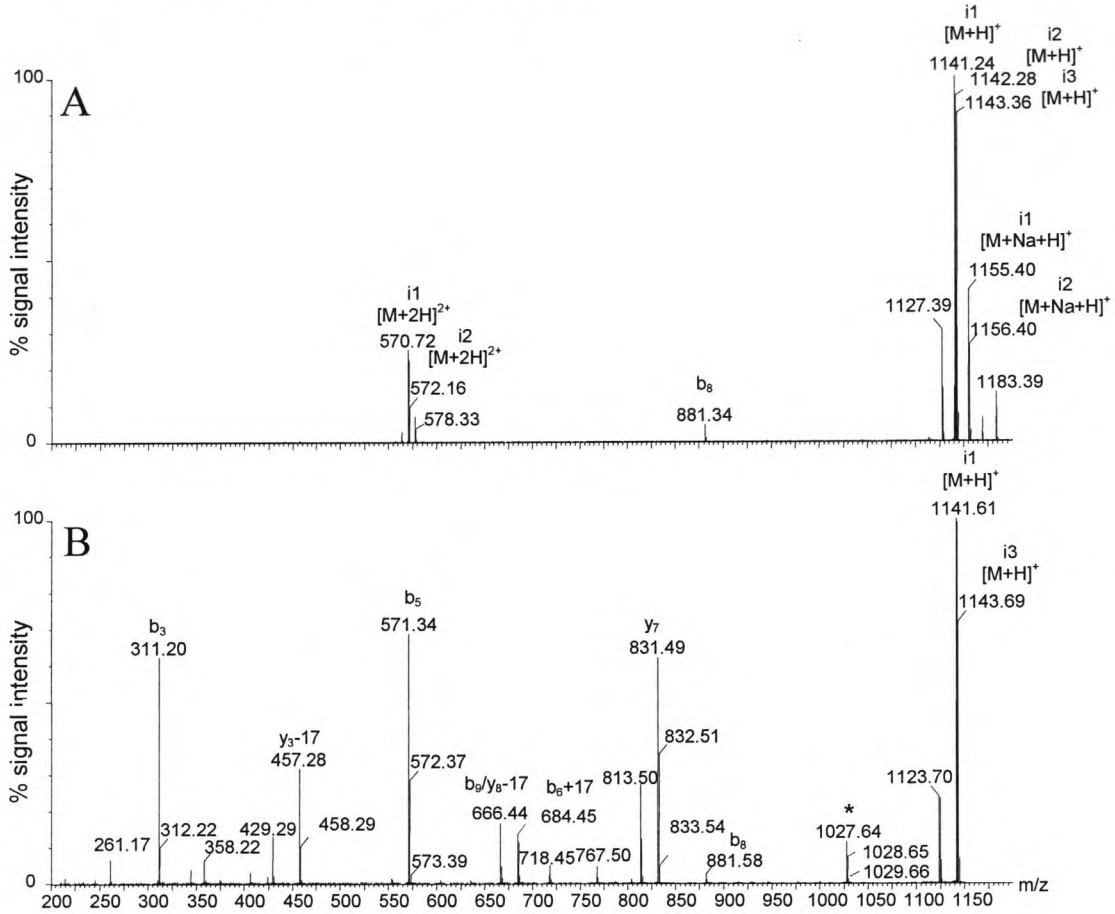

Figure 3 ESMS and CID spectra of gramicidin S. Positive mode ESMS spectrum (A) isotope variations are indicated by i1, i2 and i3 corresponding to *m/z* ratio's with 1 amu higher than the M_r calculated from mono-isotopic residue mass. Spectrum B shows the results of CID of the molecular ion with *m/z* =1141.24, which rendered fragments previously reported in literature. The unknown fragments are denoted with "*". (Also see Addendum A)

2.4.1.2 Surfactin

Analytical HPLC of surfactin supplied by Sigma (*Figure 4*) showed that at least three peptides were present in the commercially product (Fraction I-III). The fractions were distributed as follows: I = 19.4%, II = 45.7% and III = 31.7%. Closer inspection of the chromatogram showed that fraction II consisted of two fractions with the minor fraction comprising 2.2% of the total.

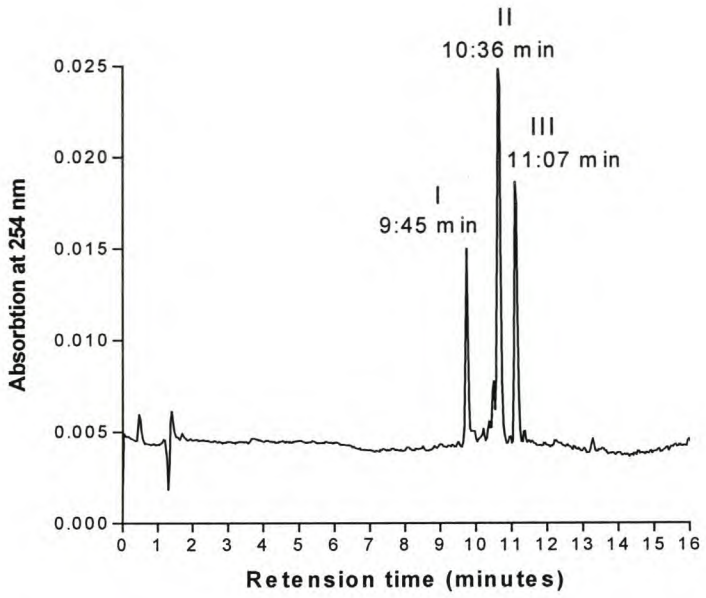

Figure 4 Analytical HPLC chromatogram of surfactin (Sigma). The same analysis conditions were used as for gramicidin S (*Figure 3*).

ESMS of this surfactin sample revealed the molecular species corresponding to the *m/z* ratio of five known forms of surfactin (*m/z* = 994.92, calculated *m/z* = 994.85; 1008.91, calculated 1008.80; 1022.90, calculated 1022.83; 1036.94; calculated 1036.85), as well as the Ca^{2+} adduct of the molecular ion with *m/z* = 1022.83 (*m/z* =1062.72) (*Figure 5*A). The limited amount of this specific batch of surfactin did not allow for the separation of sufficient amounts of surfactin to identify each in the three HPLC fractions (*Figure 4*). However, fragmentation analyses showed that surfactin variants with C_{13}–C_{15} fatty acids were present (see below). As a C_{18} reverse phase purification system was used, it is conceivable that the surfactins were partitioned according to fatty acid chain length. Since the peptides elute in increasing order of hydrophobicity, it is likely that fraction I (Rt = 9:46 min) contains surfactin variants with fatty chain length C_{13}, fraction II (Rt = 10:36 min) the C_{14} variants, and fraction III (Rt = 11:07 min) the C_{15} variants. A similar pattern was observed for iturin A (see below). Interestingly, the surfactins eluted later than the iturin variants, with the possible C_{13} fraction eluting at the same time as the iturin C_{15} fraction. This indicated that, in this case, hydrophobicity might not be the sole determining factor in retention time with our solvent system containing TFA as modifying agent.

The molecular ions present that corresponds to known surfactin variants were analysed with MS/MS (*Figure 5*B) and the results obtained for the molecular ion with *m/z* = 1022.90, corresponded to previously obtained results for this surfactin variant [60, 61]. The major fragments detected that corresponded to published results were *m/z* = 685.19 (y_6), 442.09

(y_4 or b_6/y_6), 335.9 (b_2) and 228 (a_1) (see addendum B for explanation of fragmentation pattern). From the fragmentation data, the composition of this specie was calculated as Leu/Ile$_7$, C_{14}-surfactin. The other variants identified were Ala$_4$, C_{15}-surfactin (*m/z* = 994.92), Leu/Ile$_7$, C_{13}-surfactin (*m/z* =994.92); Val$_7$ C_{14}-surfactin (*m/z* = 1008.91), Leu/Ile$_7$, C_{13}-surfactin, (*m/z* = 1008.91); Leu/Ile, C_{14}-surfactin (m/z = 1022.90); Leu/Ile$_7$,C_{15}-surfactin (*m/z* = 1036.90) (see Addendum B for fragment assignment and analysis).

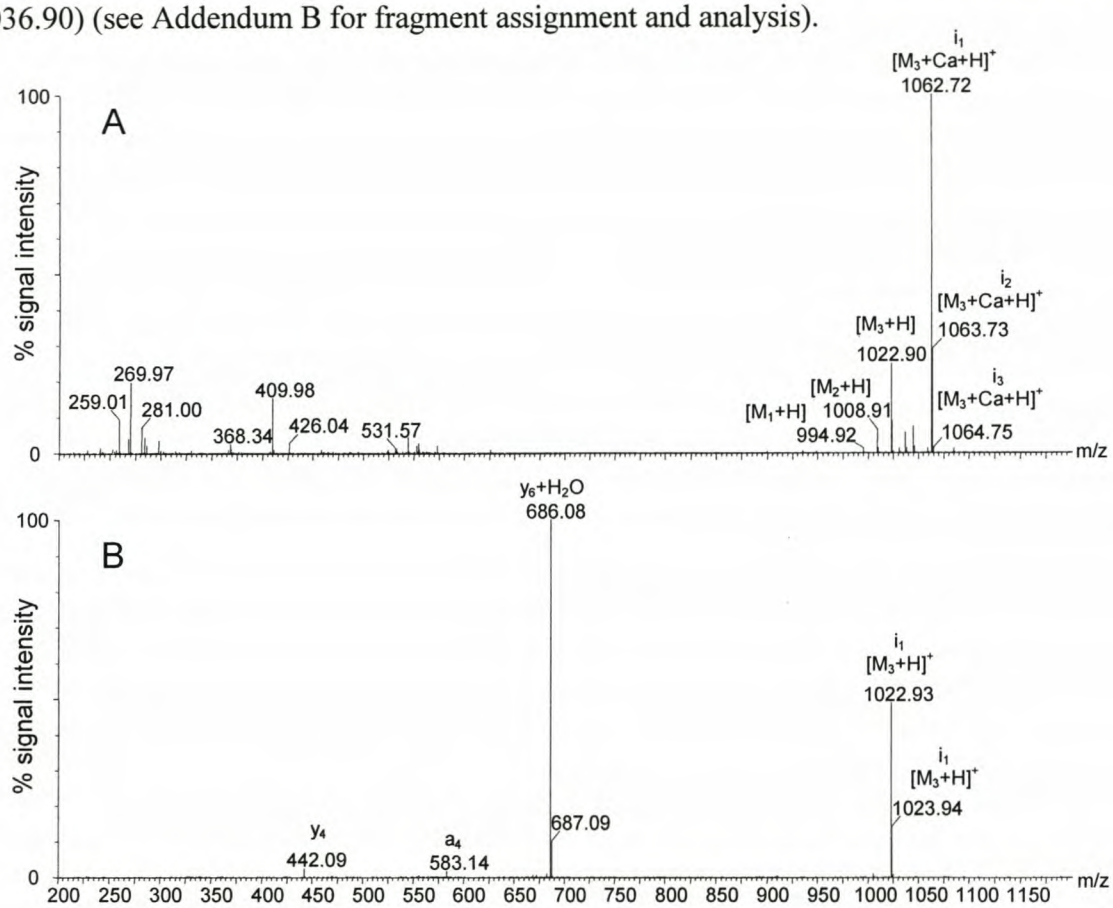

Figure 5 ESMS and CID spectra of spectra of surfactin. The positive mode ESMS spectrum (A) shows the three variants with *m/z* = 994.92, 1008.91, and 1022.90 denoted as M_{1-4} with isotope variations denoted by i. The CID spectrum of surfactin with *m/z* = 1022.90, generated with tandem mass spectrometry, is given in (B) (also see Addendum B)

2.4.1.3 Iturin A

HPLC of the commercially obtained extract of iturin A revealed six 254 nm absorbing fractions (*Figure 6*). Two major fractions, Fraction I and II eluted at 9:18 minutes and 9:48 minutes, followed by two minor fractions (Fraction III and IV) at 10:30 minutes and 11:12 minutes. Two more minor fractions, which eluted between 12 and 13 minutes, were not further analysed. Analysis of the eluate revealed that fraction II may consist of two or more compounds that co-eluted. Fractions I-IV were collected and subjected to ESMS-TOF

MS/MS for identification. The distribution of the iturin fractions were as follows: I = 51.1%, II = 31.1 %, III = 6.4% and IV = 5.0%.

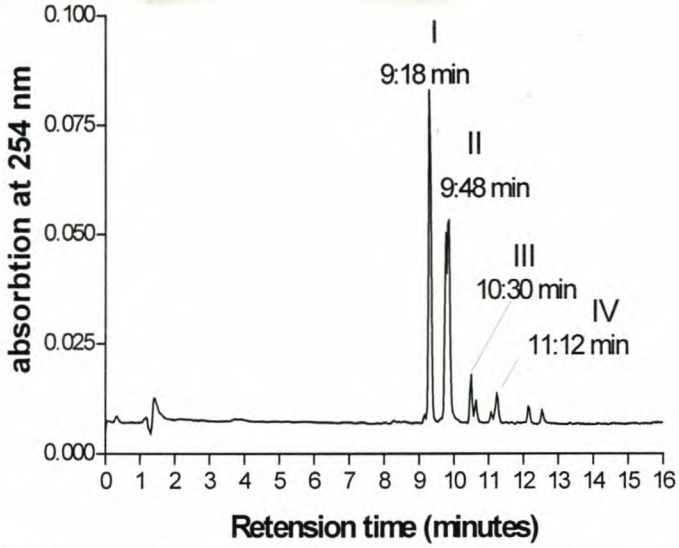

Figure 6 Analytical HPLC chromatogram of iturin A from Sigma. Analyses conditions as for surfactin were used for gramicidin S (*Figure 2*).

The ESMS analysis of the iturin A sample showed the mixture contained singly charged compounds with *m/z*-values of 1043.75, 1057.76, 1071.71, as well as a molecular ion with *m/z* of 1079.71 that corresponds to the sodium adduct of 1057.75 (*Figure 7*A). In addition, doubly charged molecular ions were detected for aforementioned species with *m/z*-values of 523.4, 535.01, 541.99 and trace amounts of a specie with m/z = 572.08, which is possibly y"5+Na-H. The iturin A variants separated with HPLC as follows: fraction I contained the molecular ion with *m/z* of 1043.75, corresponding to iturin A_2, fraction II the molecular ion with *m/z* of 1057.32 corresponding to iturin A with a C_{15} β-amino fatty acid residue, fraction III the molecular ion with *m/z* =1071.32 corresponding to iturin A_L with a C_{16} β-amino fatty acid residue and fraction IV the molecular ion with *m/z* of 1085.41, which was attributed to the related peptide mycosubtilin [42, 62].

Fraction I was subjected to TOF-MS/MS and the fragmentation products detected of the molecular ion with *m/z* =1043.32 corresponded to previously published results obtained for iturin A_2 [63]. The major fragments detected (*Figure 7*B) corresponded to published results [63] and have *m/z* values of 832.38 (y_6), 801.33 (b_6), 638.09 (b_5), 523.6 (b_4), 407.72 (y_3), and 229.54 (b_3) (see Addendum C for fragment assignment and full fragment analysis). The other fractions were not fragmented as the differences correspond to variation in the fatty acid moiety. It must be noted that fraction IV were only present in trace amounts and were not further analysed.

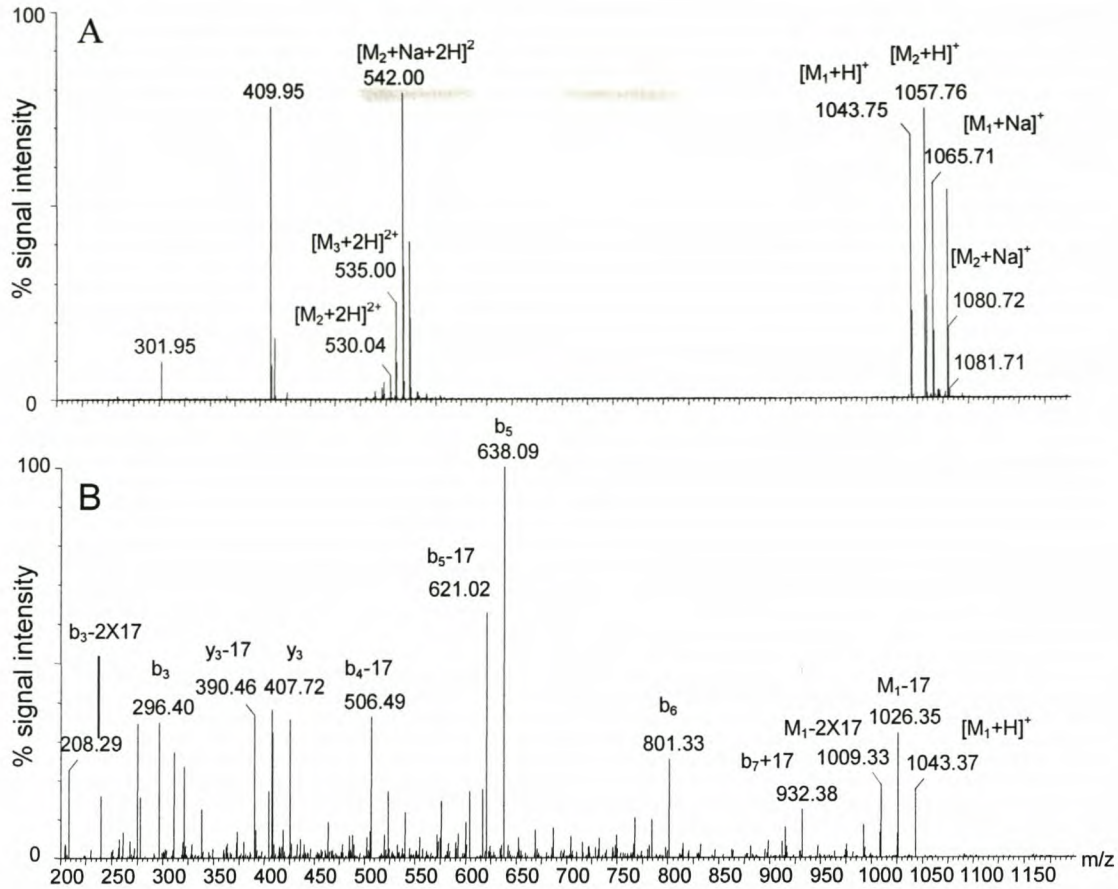

Figure 7 ESMS and CID spectra of iturin A. The ESMS spectrum (A) shows the three iturin A variants, iturin A_2, iturin A C_{15} and iturin A_L denoted as M_{1-3}. The CID spectrum of iturin A_2 (m/z = 1043.75) generated with tandem mass spectrometry is given in (B) (also see Addendum C).

2.4.2 Preparation of two synthetic linear iturin analogues

Iturin C was not commercially available, therefore it was necessary to synthesise this peptide. However, as the cyclic iturin C_2 is synthesised from a linear intermediate (8-$Beta_c$), the syntheses presented the opportunity to investigate the structural properties required for peptide-peptide interaction with the intermediate. Iturin A was commercially available, so we only synthesised the iturin A_2 linear analogue, 8-Beta. Previously, it was shown that 8-Beta shares a number of functional characteristics with iturin A_2, such as preferential binding to sodium and aggregation [12,17]. Furthermore, it was shown through molecular modelling techniques that the 8-Beta retains at least one of the β-turns present in the peptide backbone structure [17].

2.4.2.1 Synthesis of t-BOC-βNC$_{14}$

The HCl salt of the β-aminotetradecanoic acid used in this study was not protected at either the carboxylic acid or at the β-amino group. In addition, the β-NC$_{14}$ was a racemic mixture and would therefore result in an optically impure synthesis product (see later on). Protection of this residue was imperative to limit polymerisation during the synthesis. Previous reports [17] indicated that N-terminal protection of this residue is 1) extremely difficult and 2) the resultant product has a very low solubility in DMF and it would difficult to attain the required molar excess. Therefore, the amino terminus was protected with a tBOC group. Synthesises of the t-BOC-β-NC$_{14}$ moiety of the lipopeptides were evaluated with thin layer chromatography. A single spot (R_f = 0.7) for the product was detected with 2',7'-dichlorofluoroscein reagent and no visible BOC-ON or β-NC$_{14}$ contamination was detected. The product showed a negative Kaiser test and a melting point of 56–58°C (56–58°C expected, [17, 55]). Both the quality control results correlated to previous reports [17, 55].

2.4.2.2 Peptide syntheses

A benefit of using the Fmoc-based peptide synthesis protocol is that the synthesis can be spectrophotometrically followed because of the inherent UV-absobtion of the Fmoc group. We monitored the removal of the Fmoc group throughout the syntheses in order to attain the coupling efficiency. The average coupling efficiency of 97.4±3.8% was acceptable. However, analysing the coupling efficiency of each residue revealed the problematic couplings occurred with the some of the acid amide residues (*Figure 8*). The substantial decrease in the detected Fmoc fulvene, from that of Ser Asn, was expected, as a substantial amount of resin was lost because of solid support fining and difficulties experienced with the transfer of the resin from the reaction vial to the sintered funnel. After the initial loss, the absorption values remained within the expected 10% error margin of the analysis for the coupling of Asn$_4$, Pro$_6$, and Asn$_7$. The Tyr$_3$ value was too high, but still within the 10% analytical error of the Fmoc-analysis. However, the values observed for Gln$_5$ and Asp$_2$ were marginally below the 10% margin at 87% each with Asn$_2$ at 88%. This indicated that incomplete coupling might have occurred at those points. The synthesis resulted in crude mass yields of 120% for both 8-Beta and 8-Beta$_c$ indicating that a substantial amount of scavengers/side protection groups were present.

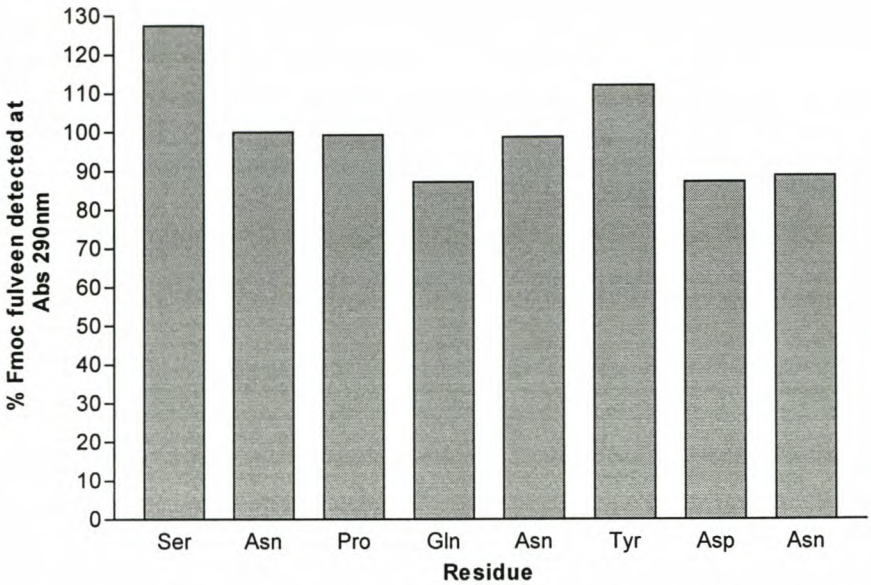

Figure 8 Absorption values detected from deblocking reactions during the synthesis of 8-Beta$_c$ (Asp as final amino acid with Fmoc group) and 8-Beta (Asn as terminal amino acid with Fmoc group).

2.4.2.3 Purification of peptides

Naidoo [58] successfully purified a bola-amphiphilic compound (i.e. a molecule with two hydrophilic moieties connected by a hydrophobic linker) from crude product mixtures by self-assembly to form large insoluble complexes. The same procedure was followed for the crude lipopeptide preparations, because of their known aggregation character [17]. The HPLC analysis of the supernatants and pellets showed that several contaminants were removed for both the crude lipopeptide mixtures (*Figure 9A* and *9B*). The peptide fractions with Rt =9:39/9.45 minutes for 8-Beta and 9:33/9.38 minutes for 8-Beta$_c$ were found, as expected, in the pellet.

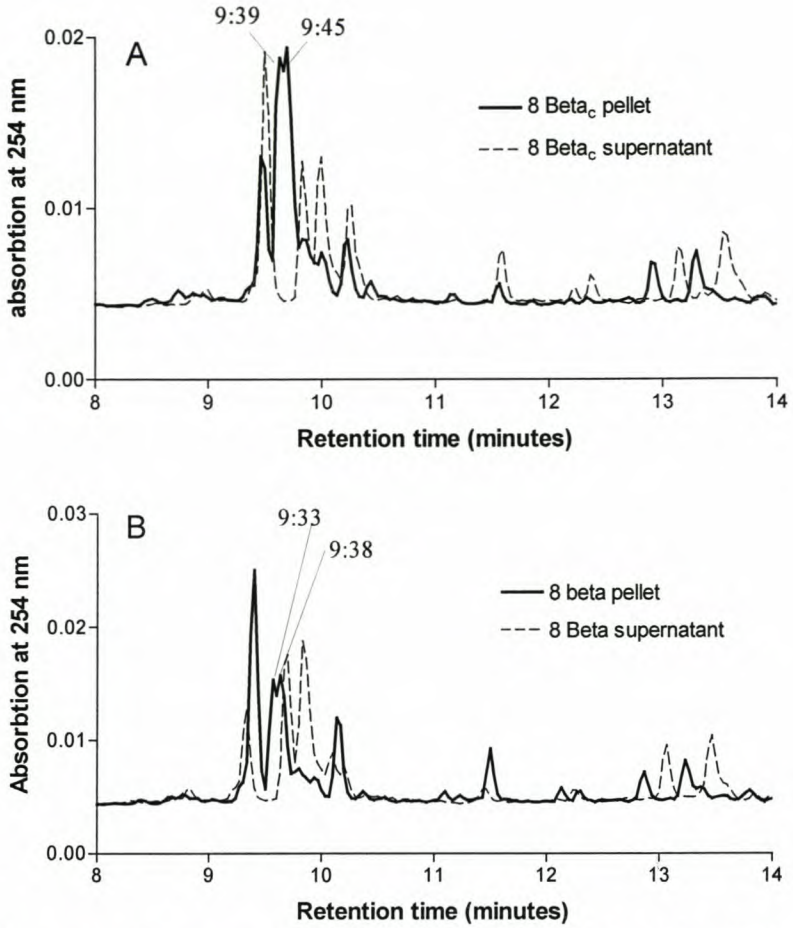

Figure 9 Chromatograms recorded with a Waters analytical C_{18} HPLC column of the supernatant and pellet of 8-Beta (A) and 8-Beta$_c$ (B) after self-assembly

The mass spectra of the purified fractions (*Figure 10*A and B) showed molecular ions with *m/z* values of 1062.08 and 1061.02, corresponding to 8-Beta$_c$ and 8-Beta respectively. In addition to the molecular ions, sodiated peptides (*m/z* = 1085.08 and 1084.02) and the dehydrated peptides, 1045.07/1043.53 were also detected. Trace amount of tritylated peptide (*m/z* = 1304.65 and 1303.65) as well as free trityl (m/z = 243.1) were detected. Furthermore, the spectrum (*Figure 10*A and B; and the CID spectrum (see later on *Figure 16*A and B and Addendum D) indicated that peptides with the correct amino acid sequence were synthesised. Therefore, the principles of SPPS were successfully applied.

The expected peptide fragments were detected with *m/z* 317.35 (y"$_3$ calculated *m/z* = 317.3) and *m/z* = 746.82/745.76 (b_5+H) for both peptides (former *m/z* value corresponds to 8-Beta and latter to 8-Beta$_c$, the same sequence is maintained for the rest of this discussion). In addition, fragments were detected that did not form under the CID conditions used (see later on Addendum D). The fragments were attributed to: a hydrated a_7+H fragment *m/z* = 949.16/948.02 (calculated at *m/z* = 948.97 and 947.97); b_7+H fragment with *m/z* of

820.98/ 819.84 (calculated at *m/z* = 820.98 and 819.68); and a_7-CO+H fragment with *m/z* of 899.94/998.90 (calculated at *m/z* = 900.2 and 899.2). In addition to the native peptide fragments, a sodiated peptide fragment, b_7+Na-CO-17, was also detected with *m/z* of 934.95/933.68 (calculated at 934.97and 933.97). All the fragments detected correlated with previously obtained results [13, 17]

Self-assembly process resulted in concentrating low molecular weight species and the tritylated peptides (*m/z* = 1305.35 for 8-Beta$_c$ and 1304.36 for 8-Beta), in the supernatant as the Trt signal intensity (*m/z* = 243.3 increased in supernatant spectra (results not shown). As sufficient time was allowed for deprotection and liberation of the peptides, this is likely the result of the trityl group re-attaching to an Asn. The reattachment of Trt to Cys has been documented and it is possible that a similar reaction might have occurred [64].

The mass spectra show that this method is a feasible method of purification given that sufficient difference in self-assembly character exists between the compound of interest and the contaminants.

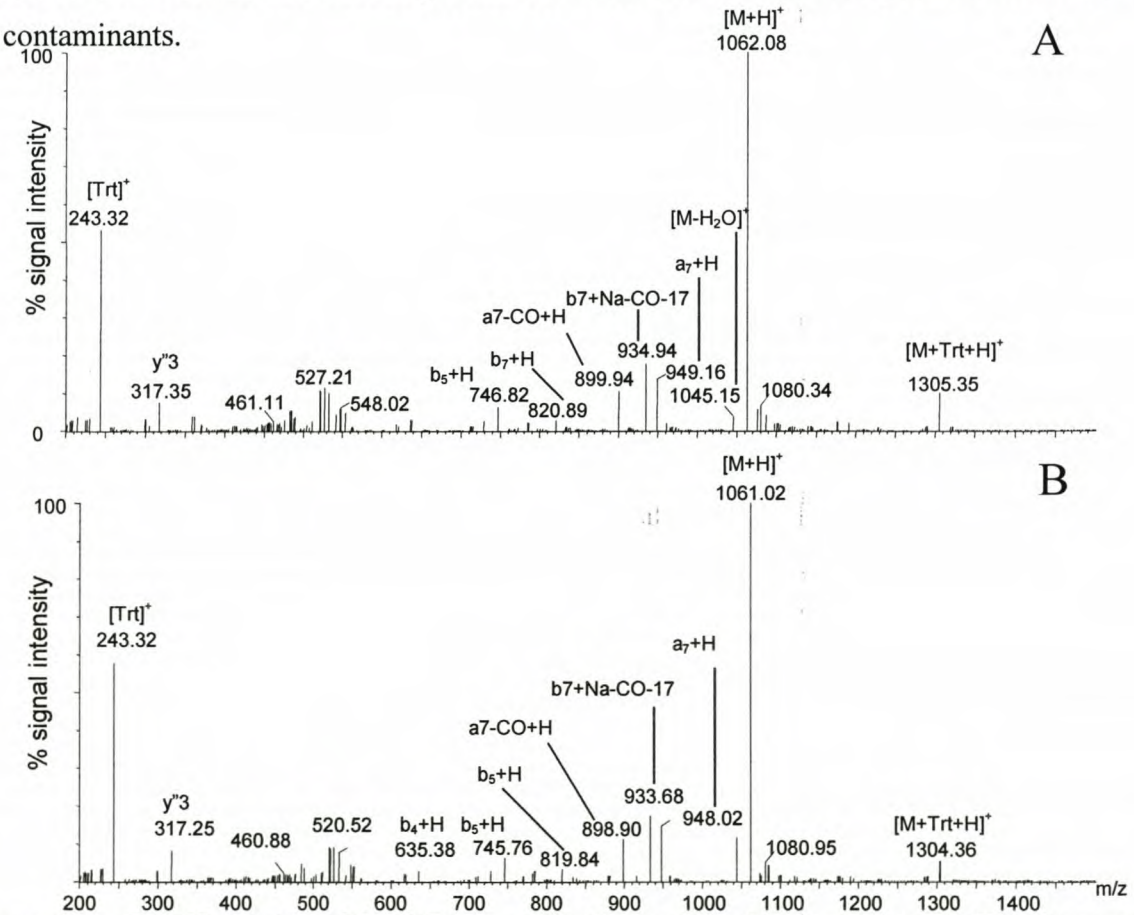

Figure 10 ESMS spectra of the 8-Beta$_c$ pellet (A), and the 8-Beta pellet (B). The fragments are identified according to the nomenclature devised by Roepstorff and Fohlman as revised by Biemann [37, 38].

The self-assembled products of 8-Beta and 8-Beta$_c$ were further purified by semi-preparative HPLC. Two fractions (Fraction I and II) were collected during purification (*Figure 11*A and B) of each of the linear analogues. The first two fractions eluted at Rt = 8:48 and 9:21 for 8-Beta$_c$ and 8:36 and 9:19 for 8-Beta. It is interesting to note that the 8-Beta$_c$ fractions had longer retention times than the 8-Beta fractions even though 8-Beta$_c$ is more polar than 8-Beta. The longer retention time of 8-Beta$_c$ relative to 8-Beta seemed anomalous to the amphipatic character. Increased solvent interaction, as apposed to hydrophobic interaction, was expected resulting in a shorter rather than longer retention time. However, because TFA is added as modifying agent in the solvents, the mode of separation may also depend on ion-paring interactions.

The last fraction collected contained a fraction with strong UV absorbance at 254 nm that did not correlate to the small amount of dry mass collected. It is likely that this fraction comprised of cleavage by-products. The final yield of 8-Beta$_c$, as determined by mass, from semi-preparative HPLC was 34% for fraction I, 22% for fraction II and 30% for the rest of the absorbing fractions collected, giving a final yield of 56% for purified 8-Beta$_c$. Purification of 8-Beta yielded 30% for fraction I, 20% for fraction II and 30% for the rest of the collected absorbing fractions, giving a final yield of 50% of purified 8-Beta.

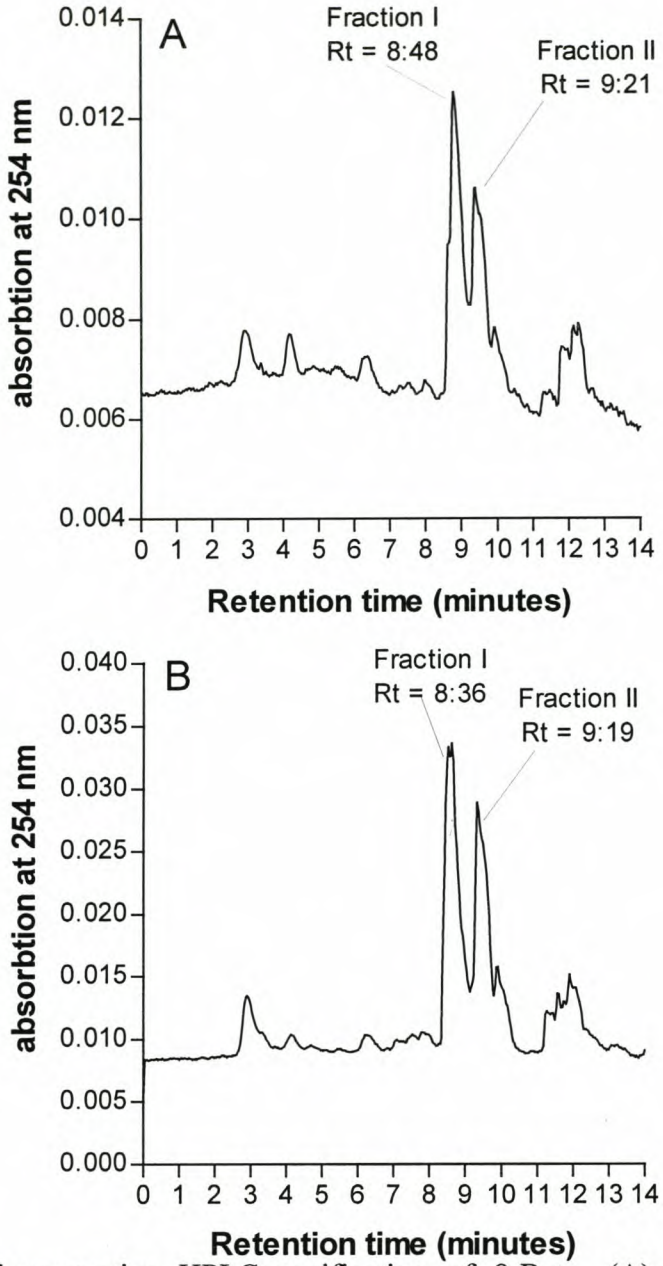

Figure 11 Semi-preparative HPLC purification of 8-Beta$_c$ (A) and 8-Beta (B) from synthesis pellets. A C_{18} Polygosil column (irregular particle size, 60 °A pore size, 25 mm X 10 mm) was used with a linear gradient over 13 minutes from 30% eluant A (0.1% TFA in water) to 100% eluant B (10% eluant A and 90% ACN). All the eluting fractions other than Fractions I and II were combined as fraction III.

ESMS analysis indicated (*Figure 12*A and B) successful purifications of 8-Beta$_c$ and 8-Beta from the synthesis products. Fraction I collected during HPLC purification of 8-Beta$_c$ showed in addition to the singly charged molecular ion of 8-Beta$_c$ (*m/z* of 1062.52 with isotope signals at 1063.53 and 1064.53), the presence of both the singly charged (*m/z* of 1085.52) and doubly charged (*m/z* of 542.76) ions of the sodiated peptide. The expected fragmentation products (y''_3+H; *m/z* =318.00, b_5; *m/z* = 746.82; denoted F in *Figure 12*B) (see Addendum D for

fragment analysis) were also present. ESMS analysis showed that fraction II also contained a molecular ion with the correct *m/z* ratio of the synthesis product (result not shown). This is consistent with the racemic products obtained from the use of the racemic $\beta NC1_4$ moiety [17]. In addition to the synthesis product, fraction II collected during 8-Beta purification also contained trace amounts of tritylated peptide as well as trityl.

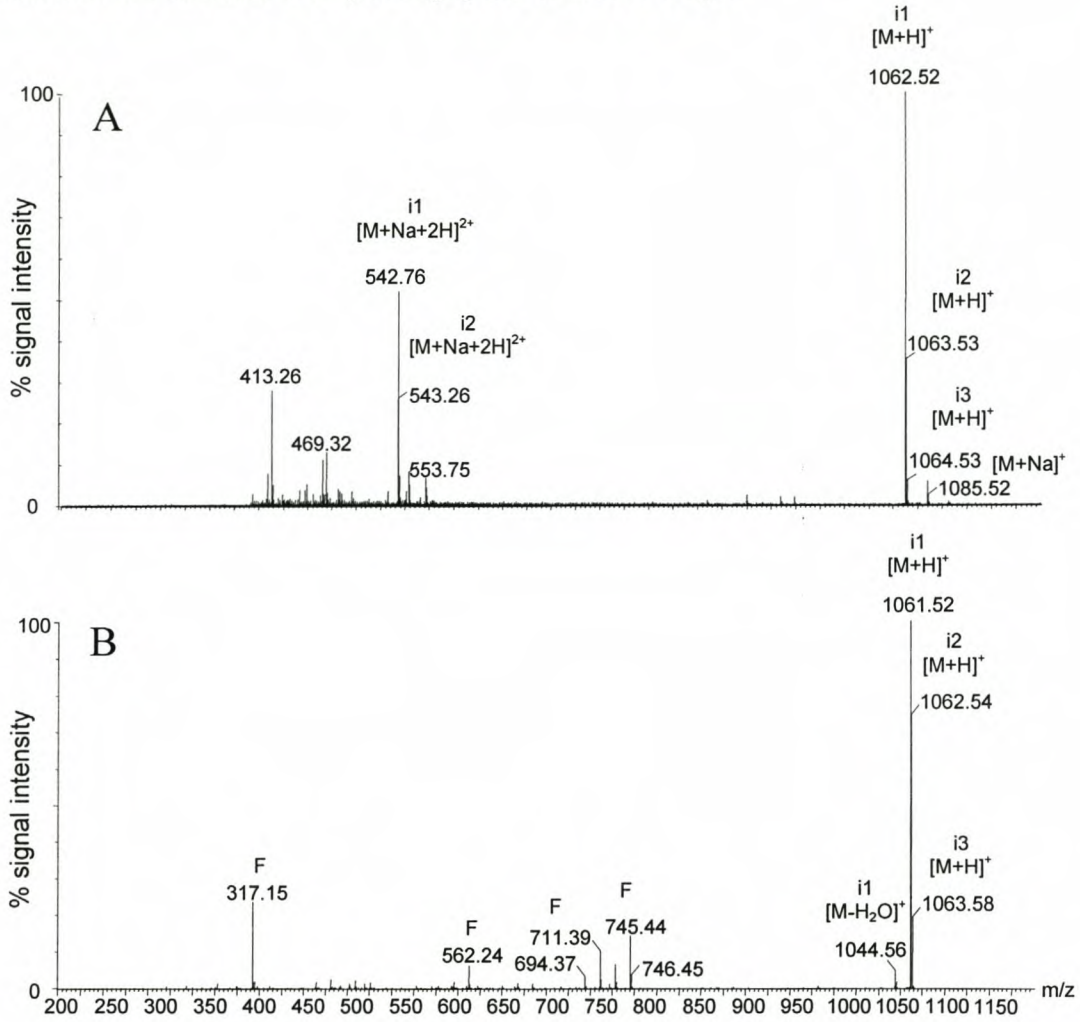

Figure 12 ESMS-TOF spectra of fractions I collected during the purification of 8-Beta$_c$ (A) and 8-Beta (B). The peptide backbone fragments are denoted F and isotopes as i1-3

2.4.2.4 Analysis of the purified linear iturin analogues

Analytical HPLC of the linear analogues showed that the two purified synthetic peptides were of high purity, but of racemic nature. The purity was calculated from the HPLC profile at 254 nm as 92.6% for 8-Beta$_c$ (8-Beta$_c$ I accounting for 41.6% and 8-Beta$_c$ II for 51%) and 95.5%

for 8-Beta (8-Beta I accounting for 42.5% and 8-Beta II for 53% of the sample.

HPLC retention times were comparable to previously obtained results (*Figure 13*A and B) [17]. The retention times for 8-Beta enantiomers were 8:42 min and 8:52 min respectively (*Figure 13*B) (*viz*. 8:52 min and 9:02 min as found by Rautenbach [17]). As this is, to the best of our knowledge, the first synthesis of 8-Beta$_c$, as no reference could be found for comparison. However, given the similarities between the peptides, as well as the use of a racemic β-NC_{14} mixture, results comparable to 8-Beta were expected. The results (*Figure 13*B) show that the two peptides eluted at 8:48 min and 8:57 min respectively. The peptides were collected and subjected to ESMS and both fractions rendered molecular ions with an *m/z*-value of 1062.36, which support the assumption the two fractions are 8-Beta$_c$ enantiomers.

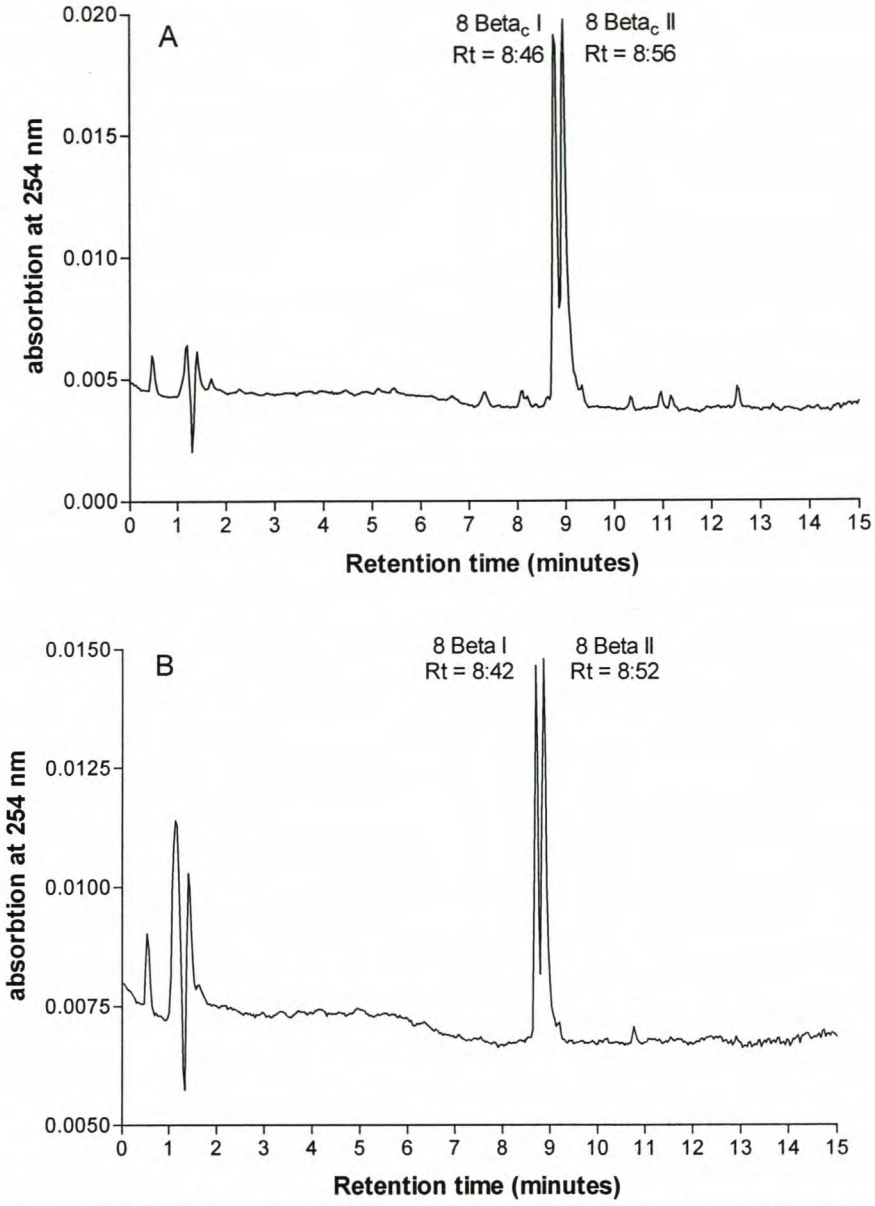

Figure 13 Analytical HPLC chromatograms of 8-Beta$_c$ (A) and 8-Beta (B) using a Nova-Pak C_{18} column. A linear gradient generated over 13 minutes with eluant A 0.1% TFA in water and eluant B 10% eluant A and 90% ACN. The enantiomers are labelled I and II as used by Rautenbach [17]

The integrity fidelity of the intended synthesis products was determined with TOF-MS/MS. Although no reference to the linear analogue of iturin C could be found in literature, its identification was done by comparing the fragmentation spectrum of the analogue (*Figure 14*A) with 8-Beta donated by M. Rautenbach. Similarly, the synthesised 8-Beta (*Figure 14*B) was compared to the donated peptide. The fragmentation spectrum of 8-Beta in this synthesis showed identical fragments to that of the previously characterised 8-Beta (results not shown). We found the expected major fragments with *m/z*-values of 747.00 (b_5+H), 712.98 (b_5+H-34), 636.07 (b_4+H_2O), 389.99 (b_5y_6) 317.99 (y_3"), 278.96 (b_4y_6/b_3y_7) (*Figure 14*A and B,

Addendum D). The N-terminal fragments of 8-Beta$_c$ were detected at 1 amu higher than the 8-Beta fragments, which is consistent with the Asn_2 to Asp_2 mutation.

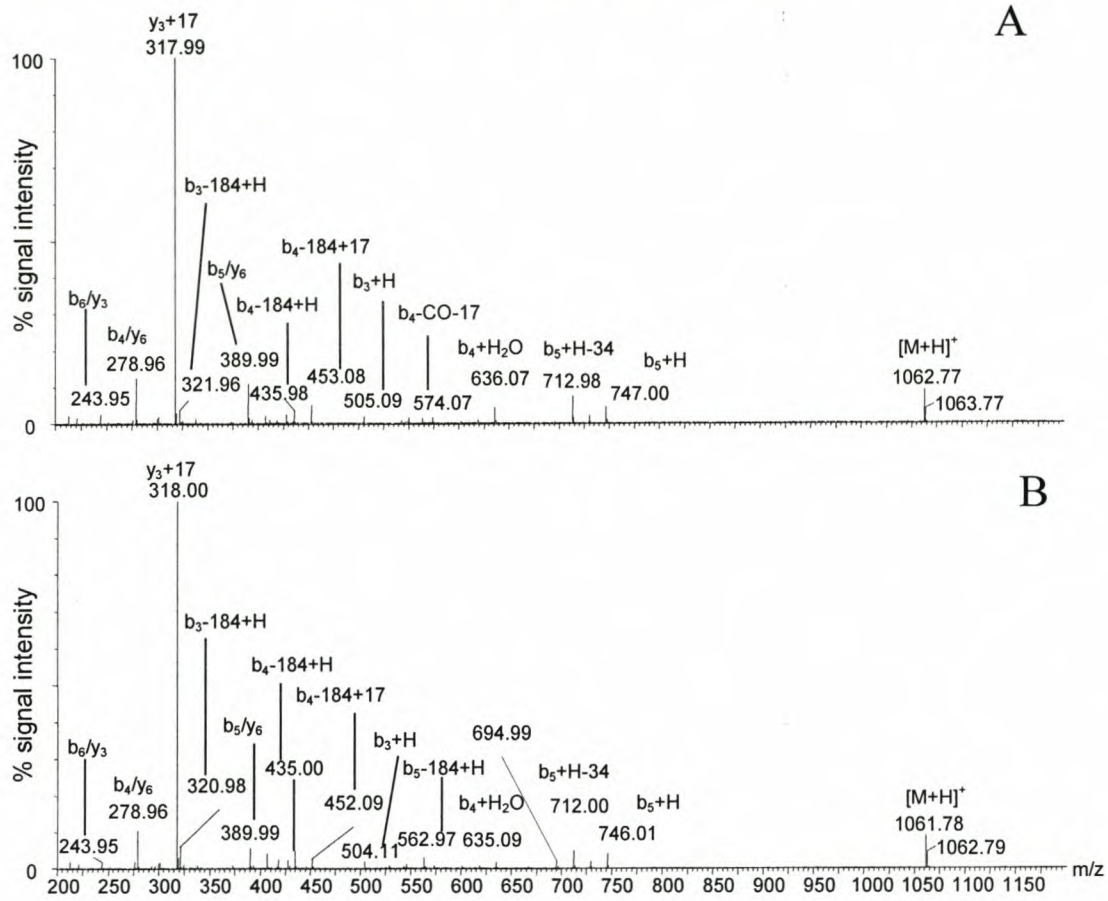

Figure 14 CID mass spectra of 8-Beta$_c$ (A) and 8-Beta (B). The product ions observed for 8-Beta correlates with previously published results [13, 17]. The product ion identified as b_4/y_6 may also be b_3/y_7. The ion with *m/z* of 694.99 may be a b_5-$2NH_3$-OH fragment.

2.4.3 Preliminary studies into the preparation of iturin C

The cyclisation methods used in this study were previously employed in the synthesis of iturin A_2, which yielded 48% cyclisation efficiency, with approximately a 50:50 distribution of the two enantiomers [17]. The procedure, using PyBOP as activation agent, was utilised in the cyclisation of 8-Beta$_c$. Unfortunately, the same decree of success was not achieved with this cyclisation. Initially, no cyclisation occurred when the peptide was dissolved in DMF before being diluted in DCM. This result is consistent with other reports [17, 24] and is related to the conformation of the peptide backbone and/or backbone solvation in this solvent.

A subsequent attempt at cyclisation was performed and the cyclisation product (m/z = 1042.7) was detected after three days, with ESMS in the negative mode (*Figure 15*A). In addition to the cyclic peptide, the linear analogue (m/z = 1060.55) and a peptide dimer (m/z = 1051.82) were also detected. Because linear peptide remained in the reaction, the reaction was allowed to proceed for a further seven days. The similarities in hydrophobicity of the resultant two cyclic peptides and the linear analogues would have resulted in a difficult separation. Therefore, an extended reaction time was allowed in an attempt to obtain a reaction mixture that contains either cyclic product or dimer/polymers to facilitate purification. Analysis of the reaction mixture after 10 days showed that trace amounts of the linear analogue and the cyclic product were still present, but that the dominant dimer signal was replaced by a ion at m/z = 1012.28 (*Figure 15*B), indicating polymerisation. Neither the cyclic product, nor the polymers could be detected with negative mode ESMS, and the spectrum were recorded in the positive mode. Similar results were obtained with DIPCDI as activation agent. Due to the complexity of this synthesis (see conclusions below), as well as financial and time constrictions, we decided to pursue the synthesis of iturin C in a future investigation.

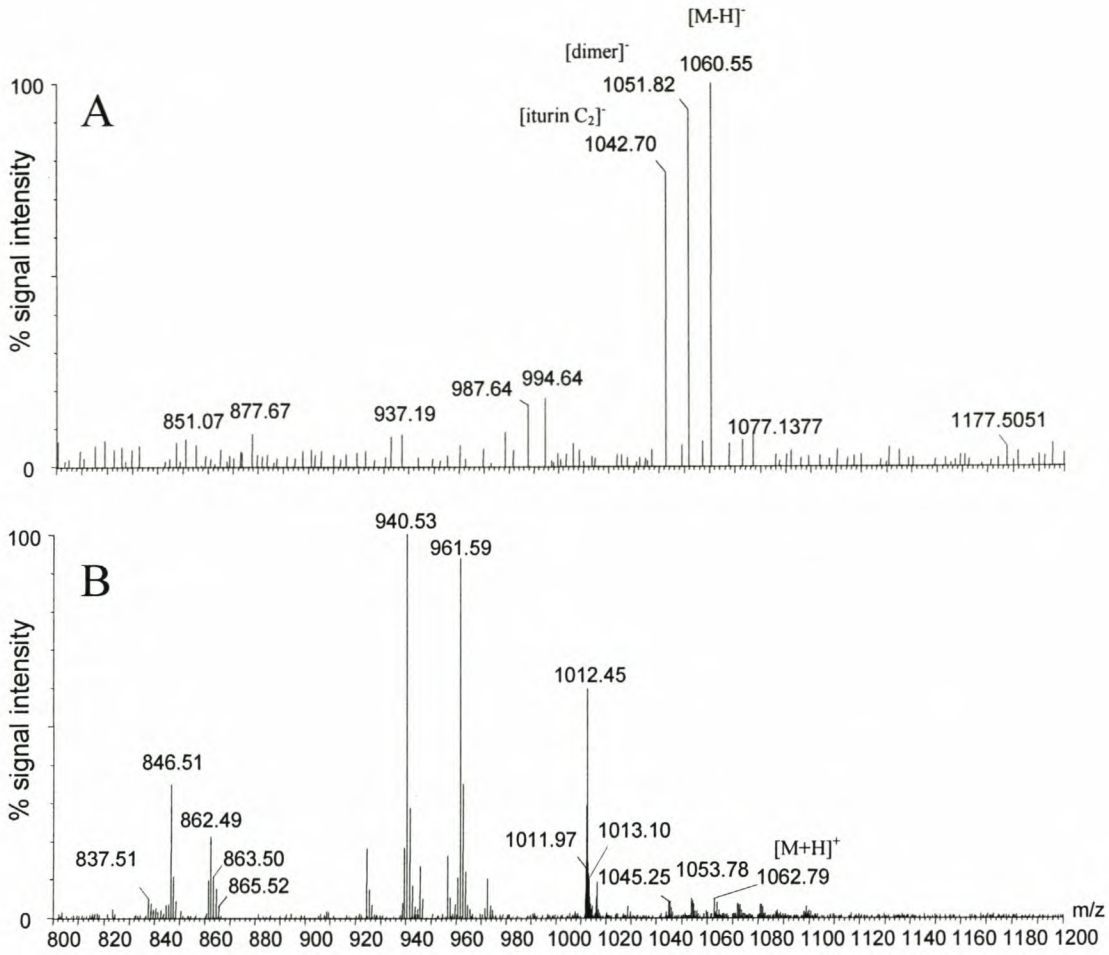

Figure 17 Mass spectrum of the reaction mixture using PyBOP® after three days (A) and 10 days. The spectrum after three days were recorded in the negative mode and shows 8-Beta$_c$ ([M-H]$^-$), a dimmer ([dimmer]$^-$), and iturin C_2 ([iturin C_2]-. The spectrum after 10 days was recorded in the positive mode.

2.5 Conclusions

Although the commercially obtained peptides were bought from reputable companies, the analysis shows that considerable variation exists from supplier to supplier and also between batches obtained from the same supplier (i.e. surfactin obtained from Sigma at different times differed in the number of surfactin variants present (data not shown as the latter was not used in this study). It is therefore important to ascertain the composition of the product before use – especially if analytical studies are planned. The commercial surfactin were determined as 99.6% pure using HPLC, which met the manufacturers specification of >98% and the sample was found to be of high enough purity for use is our investigation. The iturin sample however, contained only 89% iturin A according to our HPLC analysis, whereas the supplier indicated

that the sample is approximately 97% pure. Fraction IV (refer to *Figure 6*) comprised 4.9% of the sample and an MS analysis showed that component of this fraction is likely to be mycosubtilin.

Successful syntheses and purification of both 8-Beta$_c$ and 8-Beta were accomplished. The majority of the contaminants in the crude peptide mixtures could easily be removed from the synthesis mixture by using a novel purification *via* self-assembly/aggregation. The remainder of the contaminants were successfully removed from both the peptide preparations with preparative HPLC. The final HPLC analyses showed that both the peptides were indeed of high purity with >92% purity for 8-Beta$_c$ and >95% for 8-Beta.

The low peptide yields can be attributed, in part, to the mass of the synthesis contaminants in the crude mass, as well as to peptide lost the incomplete deprotection of the tritylated acid amide. It is known that the deprotection Trt protected N-terminal Asn proceeds very slowly and therefore four hours of cleavage is recommended [18]. Since the Asn residues are not terminal residues, therefore the three hours allowed for cleavage and deprotection should have been sufficient. Therefore, it appears that the trityl group reattached to the peptides [64]. In addition, losses in peptide material could be due to peptides sticking to plastic-ware used in preparation. Rautenbach [17] previously found that up to 30% loss could occur due to this problem. Peptides were centrifuged in Eppendorf tubes to remove undissolved particulate before HPLC purification.

The problems experienced with the cyclisation of 8-Beta$_c$ to form iturin C illustrates the need for the development of a different cyclisation strategy, other than the one successfully employed during the synthesis of iturin A_2 by Rautenbach [17]. The low level of cyclisation, regardless of the reagents used, indicated that cyclisation in this instance is not only a function of solvent and reagents, but may also be greatly influenced by peptide conformation. Our results illustrated that a one-size-fits-all approach is not always effective, even when working with related peptides, and that the strategy should be tailor-made for each peptide. The only difference between iturin C and iturin A is the Asn to Asp mutation at position two. It is conceivable that the charge repulsion, due to the β-carboxyl group of the Asp in the unprotected peptide leads, to either low concentration of activated precursor or a sterically unfavourable conformation for peptide bond formation. Given the high degree of polymerisation it appears that sufficient activation, possibly of both the α- and β-carboxyl groups, was achieved and that the latter scenario seems the more likely. However, the use of

an unprotected precursor did add a complicating factor to the synthesis of the cyclic peptide. As most activating agents cannot discriminate between the α-carboxyl group of the terminal Ser residue and the β-carboxyl group of the Asp residue, accessibility of this side-chain introduced another site for polymerisation. Clearly, a different approach to the synthesis of this peptide is required. A more suitable approach may be the synthesis and use of a protected precursor or a solid support strategy. Both approaches would require unique and expensive solid phase peptide synthesis resins. Alternatively a linear analogue with Pro residue as C-terminal residue can be employed (this would limit racemisation [23] and shift the Asp residue to the centre of the molecule).

The research that is reported in the following chapters depended on high purity peptides. This is especially true for mass spectrometric analyses (Chapters 5 and 6), which requires not only high purity but also peptides of known composition. To this end, the composition of the commercial peptides was conclusively established. Some difficulties were experienced in the synthesis of the linear analogues, but final analysis showed that the synthetic peptides were of suitable purity for use in this investigation.

2.6 References

1. Kondejewski L. H., Farmer S. W., Wishart D. S., Hancock R. E. W., Hodges R. S. (1996) *J. Biol. Chem.,* **271**, 25261 –25268

2. Setsuko A., Nishikawa H., Takiguchi H., Lee S., Sugihara G. (1993) *Biochim Biophys Acta,* **1147**, 42–49

3. Jelokhani-Niaraki M., Kondejewski L. H., Farmer S. W., Hancock R. E. W., Kay C. M., Hodges R. S. (2000) *Biochem. J.,* **349**, 747 –755

4. Ovchinikov Y. V. & Ivanov V.T. (1975) *Tetrahedron* **31**, 2177 –2209

5. McInnes C., Kondejewski L. H., Hodges R. S, Sykes B. D. (2000) *J. Biol. Chem.*, **275**, 14287 –14294

6. Gibbs A. C., Bjorndahl T. C., Hodges R. S., Wishart D. S. (2002) *J. Am. Chem. Soc.*, **124**, 1203 –1213

7. Timon L., Peypoux F., Wallach J., Michel J. (1993) *Colloids Surf. B.* **1**:57 –62

8. Osman M., Høiland H., Holmson H., Ishigami Y. (1998) *J. Peptide Sci.,* **4**, 449 – 458

9. Morikawa M., Hirate Y., Imanaka T., (2000) *Biochim. Biophys. Acta*, **1488**, 211 –218

10. Bland J. M., Lax A., Klich M. In: *Peptides* 1990: Proceedings of the Twenty-First European Peptide Symposium (Eds. Giralt E., Andreu D.,) ESCOM, Leiden, IL, pp 426 –427

11. Besson F., Peypoux F., Quentin M. J, Michel G. (1984) *J. Antibiotics,* **37**, 172 – 177

12. Rautenbach M., Swart P., van der Merwe M. J. (2000) *Bioorg. Med. Chem.*, **8**, 2539 –2548

13. Rautenbach M., Swart P., van der Merwe M. J. (2001) *J. Am. Mass Spectrom.*, **12**, 505 –516

14. Merrifield R. B. (1964) *Biochemistry*, **3**, 501 –502

15. Merrifield R. B. (1969) *Science*, **150**, 178 –185

16. Bodansky M. & Bodansky A. (1984) The practice of peptide synthesis (Eds. Hafner K., Rees C. W., Trost B. M., Lehn J., Von Ragné Schleyer P., Zahradnik R.), Springer Verlag, Berlin

17. Rautenbach M. (1999) The synthesis and characterisation of analogues of the antimicrobial peptide iturin A_2, Ph.D. – Thesis (Biochemistry) University of Stellenbosch, pp. 2.11 –2.12

18. Gloor A. P., Hoare S. M., Lawless K., Steinauer R. A., White P., Yong C. W. (1994) NovaBiochem 94/95 Catalogue and Peptide synthesis handbook, pp. S1 – S42

19. Carpino L. A. & Han G. Y. (1972) *J. Org. Chem.*, **37**, 3404 –3406

20. Atherton R. C. & Sheppard (1989) Solid Phase Peptide Synthesis: A practical approach, In: The practical approach series (Series Eds. Rickwood D., Hames B. D.), IRL Press, Oxford University Press, Oxford

21. Knorr R, Trzeciak, A., Bannawarth W., Gillessen, D. (1989). *Tetrahedron Lett.*, **30**, 1927 –1930

22. Atherton E., Cameron L. R., Sheppard R. C., (1988) *Tetrahedron*, **44**, 843 –857

23. Davies J. S. (2003) *J. Pep. Sci.*, **9**, 471 –501

24. Li P., Roller P. P., Xu J. (2002) *Current Organic Chemistry*, **6**, 411 –440

25. Wu X, Bu X, Wong KM, Yan W, Guo Z (2003) *Org. Lett.*;**5**, 1749-52

26. Daniel M. J., Fries D. S., Rajagopalan S., Wendt S., Zenobi R., (2002) *Int. J. Mass Spectrom.*, **216**, 1 –27

27. Watson D. G., Atsriku C., Oliveira E. J. (2003) *Analytica Chemica Acta*, **492**, 17 –47

28. Guilhaus M. (1995) *Journal of Mass Spectrometry*, **30**, 1519 –1532

29. Boesl U., Bäβmann C., Käsmeier R. (2001) Int. J. Mass Spectrom., 206, 231 – 244

30. Vékey K. (1995) *Mass Spectrometry Reviews*, **14**, 195 –225

31. Loo J. P., Edmonds C. G., Smith R. D. (1990) *Science*, **248**, 201 –204

32. Tang X-J. & Boyd R. K, (1992) *Rapid Communications In Mass Spectrometry*, **6**, 651 –657

33. Gaskell S. J. & Reilly M. H. (1988) *Rapid Communications in Mass Spectrometry*, **2**, 188 –191

34. Schilling B., Wang W., McMurray J. S., Medzihradszky K. F. (1999) *Rapid Communications In Mass Spectrometry*, **13**, 2174 –2179

35. Tomer K. B., Crow F. W., Gross M. L. (1984) *Anal. Chem.*, **56**, 880 –886

36. Gonzalez J., Besada V., Garay H., Reyes O., Pardon G. (1996) *J. Mass Spectrom.*, **31**, 150 –158

37. Roepstorff P. & Fohlman J. J. (1984) *Biomed. Env. Mass Spectrom.*, **11**, 601

38. Bieman K. (1988) *Biomed. Env. Mass Spectrom.*, **16**, 99 –111

39. Ngoka L. C. M. & Gross M. L. A. A. (1999) *J. Am. Soc. Mass Spectrom.*, **10**, 360 –363

40. Williams S. M. & Brodbelt J. S. (2004) *J. Am. Soc. Mass Spectrom.*, **15**, 1039 – 1054

41. Peypoux F., Bonmatin J. M., Wallach J. (1999) *Appl Microbiol Biotechnol.*, **51**, 553 –563

42. Maget-Dana R. & Peypoux F. (1994) *Toxicology,* **87**, 151 –174

43. Winkelmann G., Allgaier H., Maget-Dana R., Thimon L., Peypoux F. Ptak M. (1992) *Biochimie,* **74**, 1047 –1051

44. Ohno A., Ano T., Shoda M. (1995) *J. Ferment. Bioeng.*, **80**, 517 –519

45. Maget-Dana R., Thimon L., Peypoux F. Ptak M. (1992) *Biochimie,* **74**, 1047 – 1051

46. Peypoux F., Michel G., Delcambe L. (1976) *Can. J. Biochem.*, **63**, 391 –398

47. Battersby A. R. & Craig L. C. (1951) *J. Am. Chem. Soc.*, **73**, 1887 –1888

48. Kakinuma A., Sugino H., Isono M., Tamura G., Arima K. (1969) *Agric Biol Chem.* **33**, 973–976

49. Maget-Dana R. & Peypoux F. (1994) *Toxicology,* **87**, 151 –174

50. Winkelmann G., Allgaier H., Lupp R., Jung G. (1983) *J. Antibiotics* **36**, 1451 – 1457

51. Peypoux F., Besson F., Michel G., Delcambe L., Das B. C. (1978) *Tetrahedron,* **34**, 1147 –1152

52. Steward J. M. & Young J. D. (1984) Solid phase synthesis, 2nd edition, Pierce Chem. Co. Rockford, Illinois, pp 69 –70

53. Gait M. J. (Ed) (1984) Oligonucleotide synthesis, In: A Practical Approach Series (Series Eds. Rickwood D., Hames B. D.) IRL Press, Washington D. C., p. 99

54. Furniss B. S., Hannaford A. J., Smith P. W. G., Tatchell A. R. (1989) Vogel's Text Book of Practical Organic Chemistry 5th edition, Longman Scientific & Technical, London, p399

55. Levitt R. R. (1986) The synthesis of a novel octapeptidolipid antibiotic, Ph. D. Thesis (Biochemistry), Univeristy of Stellenbosch, pp 28 –31

56. Kaiser E., Colescott R. L., Bossinger C. D., Cook P. I. (1970) *Anal. Biochem.*, **34**, 595 –598

57. Rautenbach M. (1999) Biopep Laboratory Manual

58. Naidoo V. B. (2004) The supramolecular chemistry of novel synthetic biomacromolecular assemblies, Ph. D. Thesis (Chemistry), University of Stellenbosch, pp 3-7

59. Data for the Calculation of the Molecular Masses of Peptides and Proteins for use in Mass Spectrometry, Fisons Plc, Suffolk, UK

60. Yakimov M. M., Abraham W-R., Meyer H., Giuliano L, Golyshin P. N., (1999) *Biochim et Biophys Acta*, **1438**, 273 –280

61. Ishigami Y., Osman M., Nakahara H., Sano Y., Ishiguro R., Matsumoto M. (1995)
Colloids. Surf. B., **4**, 341 –348

62. Peypoux F., Michel G., Delcambe L. (1976) *Can. J. Biochem.* **63**, 391 –398

63. Cho S-J., Lee S. K., Cha B. J., Kim Y. H., Shin K-S. (2003) *FEMS Microbiol Lett.,* **223**, 47 –51

64. King D. S.. Fields C. G., Fields G. B. (1990) *Int. J. Peptide Protein Res.*, **36**, 255 –266

Addendum A

M/z observed	Proposed fragment	Calculate m/z	Sequence
1141.4	M+H	1141.46	PVOLFPVOLF
881.58	b_8	881.13	PVOLFPVO
831.49	y_7	831.06	LFPVOLP
813.50	y_7-H_2O	813.06	LFPVOLP
718.45	y_6	717.90	FPVOLF
684.45	b_6+17	684.84	PVOLFP
666.44	b_9/y_8-17	666.89	LFPVOL
571.34	b_5	570.73	PVOLF
457.28	y_3-17	456.61	VOLP
429.29	y_3-CO-17	428.61	VOLP
311.2	b_3+H	311.39	PVO
261.17	y_2 + H	261.33	FP
197.16	b_2+H	197.25	PV

Addendum B

M/z observed	Proposed fragment	Calculate m/z	Sequence
1022.93	M+	1022.33	β-OHC_{14}ELLVDLL
686.08[1]	y_6+H_2O	684.85	LLVDLL
583.14	a_4+H	582.78	β-OHC_{14}ELL
470.13	x_4+H	469.63	VDLL
452.13	b3-17	452.63	β-OHC_{14}EL
442.09[2]	y_4+H or b_6/y_6	441.54	VDLL
361.07	y_3+H_2O	359.40	DLL
339.08	b_2-17	339.46	β-OHC_{14}E
329.05[3]	b_6y_5	328.34	LVD
246.03	b_1+H_2O	246.35	β-OHC_{14}
228.01[4]	b_1	228.35	β-OHC_{14}

[1]Fragmentation of *m/z* =994 resulted in three product ions with *m/z* = 686.08, 672.1 and 658.09 coresponding to [Leu/Ile_7]surfactin, [Val_7]sufactin and [Ala_4]surfactin respectively. Collisionaly induced dissociation of *m/z* = 1008 rendered product ions with *m/z* = 686.09 and 672.09 corresponding to [Leu/Ile_7]surfactin, [Val_7]sufactin repsectively. Surfatin with *m/z* = 1022 and 1036 rendered only this specific product ion.

[2]Fragmentation of *m/z* =994 resulted in three product ions with *m/z* = 442.10, 428.08 and 414.10 coresponding to [Leu/Ile_7]surfactin, [Val_7]sufactin and [Ala_4]surfactin. Collisionaly induced dissociation of *m/z* = 1008 rendered product ions with m/z = 442.1 and 428.09 corresponding to [Leu/Ile_7]surfactin, [Val_7]sufactin repsectively .Surfatin with m/z = 1022 and 1036 rendered only this specific product ion.

[3]Fragmentation of *m/z* =994 resulted in two product ions with *m/z* = 329.05 and 311.06 coresponding to [Leu/Ile_7]surfactin or [Val_7]sufactin and [Ala_4]surfactin respectively.

[4]Fragmentation of *m/z* =994 and m/z = 1008 resulted in three product ions with *m/z* = 211.30, 428.00 and 242.00 coresponding to surfactins with fatty chain length of C_{13} – C15. Collisionaly induced dissociation of *m/z* = 1022 and 1036 rendered product ions with m/z = 428.00 and 442.00 corresponding to C_{14}[Leu/Ile_7]surfactin and C15[Leu/Ile_7]surfactin repsectively

Addendum C

M/z observed	Proposed fragment	Calculate m/z	Sequence
1043.37	M+H	1043.2	PNSβNC$_{14}$-NYNQ
1026.35	M-17	1026.2	PNSβNC$_{14}$-NYNQ
1009.33	M-2X17	1010.04	PNSβNC$_{14}$-NYNQ
932.38	b_7 +17	931.91	PNSβNC$_{14}$NYN
801.33	b_6	800.81	PNSβNC$_{14}$NY
638.09	b_5	637.74	PNSβNC$_{14}$N
621.02	b_5-17	620.74	PNSβNC$_{14}$N
506.49	b_4-17	506.64	PNSβNC$_{14}$
407.72	y_3	406.29	YNQ
390.46	y_3-17	389.29	YNQ
296.40	b_3	298.32	PNS
208.29	y_2-2X17	208.23	NQ

Addendum D

Productions identified after CID of 8 Beta. The reference peptide 8 Beta II rendered the same fragments. Al the fragments detected for 8Beta were detected for 8 $Beta_c$ at 1 amu greater than 8 Beta.

M/z observed	Proposed fragment	Calculate m/z	Sequence
1061.78	M+H	1061.2	β-NC_{14}NYNQPNS
1044.79	M-H_2O	1044.2	β-NC_{14}NYNQPNS
746.01	b_5+H	745.9	β-NC_{14}NYNQ
729.01	b_5-17+H	728.9	β-NC_{14}NYNQ
712.00	b5-2 X 17+H	712.8	β-NC_{14}NYNQ
635.09	b_4+H_2O	634.8	β-NC_{14}NYN
618.07	b_4+H	617.8	β-NC_{14}NYN
601.07	b_4-17+H	600.8	β-NC_{14}NYN
573.09	b_4-CO-17	573.8	β-NC_{14}NYN
562.97	b_5-184+H	562.9	NYNQ
550.09	b_4/y_6+CO+H	549.32	DYNQ
545.96	b_5+OH-184+H	545.9	NYNQ
504.11	b_3+H	503.7	β-NC_{14}NY
452.09	b_4+17-184	451.8	NYN
435.00	b_4-184+H	434.8	NYN
417.98	b_4-17-184+H	417.8	NYN
389.99	b_5y_6-17+H	389.3	YNQ
324.08	b_7y_4-NH_3+H	324.3	QPN
320.98	b_3-184+H	320.7	NY
318.00	y_3+17	317.28	PNS
300.98	y_3"-2 X 17	300.28	PNS
278.96	b_4y_6/b_3y_7	278.28	YN/NY
243.95	b_6/y_3	244.24	QP
220.93	y2	220.2	NS
212.93	b_7y_3	212.2	PN

Chapter 3

Development of two novel antifungal testing methodologies

Abstract

A number of antimicrobial peptides with antifungal activity are produced by *Bacillus* strains, for example, iturin A and surfactin by *Bacillus subtilis.* The well-known gramicidin S, a cyclic decapeptide produced by *Brevibacillus brevis,* has a broad-spectrum antimicrobial and cytotoxic activity, but the antifungal activity of this peptide on post-harvest pathogens of stone fruit and grape has not yet been fully established. The aim in this study was to develop a sensitive analytical assay to determine the effect of gramicidin S on a group of post harvest pathogens using *Penicillium* cf. *corylophilium* as model organism. Since most agar-based antifungal assays are qualitative with only limited sampling capacities, we developed assays in 96-well microtiter plates, one broth assay for *P. corylophilium* and the other an adapted agar-based assay. Our broth assay correlates light dispersion at 620 nm with fungal growth and yields repeatable results within 24 hours. Since both the test organism and the peptide are added in solution, many of the inadequacies of conventional agar-based radial diffusion assays are eliminated. The agar-based assay is also performed in a microtiter plate and offers a high sampling rate and a relatively short assay time of 16 hours.

3.1 Introduction

The discovery of antibiotics and antimicrobial peptides ushered in an era with vast possibilities and new challenges. One of these challenges is to accurately assess the antimicrobial potency of newly discovered and synthesised molecules. Gramicidin S was the peptide of choice because of its broad-spectrum antimicrobial activity [1, 2]. Although extensive research has been done on gramicidin S as biological control agent, no reference could be found to the test organism *Penicillium corylophilium* or other plant pathogenic fungi. This presented a unique opportunity, not only in terms of assay development, but also in terms of establishing the inhibition parameters of gramicidin S on these types of phytopathogens.

Gramicidin S is a cyclic amphipatic decapeptide that consists of two pentapeptides, D-Phe-Pro-Val-Orn-Leu, linked between D-Phe and Leu [3]. It is active against gram-positive and gram-negative bacteria, as well as exhibiting broad-spectrum antifungal activity. Association of gramicidin S with cell membranes leads to the release of phospholipids, followed by a disruption of the permeability barrier and cell lyses [3, 4, 5, 6].

Because of their clinical importance, a great number of assays have been developed for pathogenic bacteria and yeast and consequently guidelines were laid down for the selection of clinical testing systems [7, 8]. The standardised testing systems include the agar radial diffusion assay [9, 10, 11], broth macro- and microdilution assays [12, 13, 14] and the micro-gel diffusion assay [15]. Unfortunately, one area of assay development has been lagging – the assessment of antifungal activity of antimicrobial peptides on fungi that is not of clinical importance. Even though these organisms do not directly influence human quality of life, they do have serious implications for food production and preservation. The determination of antifungal peptide activity is wrought with complications that include peptide inactivation by agar [16], and oxygen diffusion through the growth medium [13]. We have developed a standardised antifungal testing methodology with 1 μM, for the assessment of antifungal activity of gramicidin S on fungi that approximates natural growth conditions. This assay was standardised by comparison with an adapted methodology developed by Broekaert *et al.* [13]. The assay was adapted to a relative growth system measuring inhibition in terms of total fungal growth possible under assay conditions instead of biomass determinations. Furthermore, this methodology allows peptide-membrane interaction in the aqueous phase after which the growth medium is rapidly absorbed by the underlying agar. The assay is performed in 96-well microtiter plates. The advantages of using a microtiter-based system are, amongst others, an increased sampling rate and the small amounts of antibiotic used in the assay. A previous study showed the relationship between light dispersion and fungal growth as measured by biomass [13]. The use of biomass determinations, although highly accurate, is cumbersome and time consuming. By using the aforementioned relationship, we have developed an assay in terms of total growth possible under assay conditions, i.e. inhibition values are expressed relative to reference growth (well with fungi without peptide). The criteria set for these assays were 1) incubation time should not exceed 24 hours; 2) growth during this period should allow for the needed sensitivity; and 3) as the peptides used are active in micromolar concentrations, the assay must reflect activity in the same concentration

range. The assay methodology presented here offer fast, analytical quantification of antifungal activity with the added advantage of visualisation if required.

3.2 Materials

The Plant Pathology Department, University of Stellenbosch, Stellenbosch donated *Penicillium* cf. *corylophilium*. Gramicidin S was from Sigma (St Louis, USA). Casein was supplied by BDH laboratory supplies (Poole, England). The microtiter plates (Nunc-Immuno™ Maxisorp) were from Nalge NUNC (Roskilde, Denmark) Dulbecco's phosphate buffered saline (PBS) was prepared as previously described [17] from KCL, NaCl, KH_2PO_4 and NA_2HPO_4 which were supplied by Capital Enterprises (Hillcrest, RSA), Saarchem (Midrand, RSA) and Merck (Midrand, RSA) respectively. Potato dextrose broth (PDB) was from Difco Laboratories (Detroit, USA). Chemically pure agar was from Saarchem (Krugersdorp, South Africa). Tween 80 was supplied by Fluka Chemie (GmbH). Analytical quality water was prepared by passing water from a reverse osmoses plant through a Millipore (Milford, USA) Milli Q® water purification system.

3.3 Methods

2.3.1 Growth and harvesting of fungi

P. corylophilium was grown at 25 °C on potato dextrose agar (PDA). Spores were harvested from 14-day-old cultures with 10 mL sterile analytical water containing 10 µL/L Tween 80 and filtered through a double layer of gauze before being diluted.

3.3.2 Microdilution broth antifungal assay

Microtiter plates were blocked with 0.5% casein in Dulbeco's PBS for 1 hour, sterilised, and dried under UV-light for a further 4 hours. Normal procedures to ensure sterility were followed during the rest of the assays. After counting, spores were diluted with PDB to final spore concentrations of 60 X 10^3, 45 X 10^3 and 30 X 10^3 spores/well. Of the suspensions, 80

μL were added to each well of the microtiter plates except for columns A and H, which were reserved respectively as growth controls and sterility controls. The wells that served as growth controls received 20 μL analytical water and the remaining wells received 20 μL of peptide dissolved in analytical water. All wells contained a final volume of 100 μL. No less than eight determinations were done per concentration value. Test substances were added to the wells before spore germination (approximately 4 hours after harvesting). All light dispersion measurements were done at 620 nm with a Titertek Multiscan Plus Mk II (Flow Laboratories). Measurements were taken at 3-hour intervals up to and including 24 hours.

3.3.3 Microagar antifungal assay

All equipment, media, and materials were treated as described above. The plates were prepared as for the microdilution broth antifungal assay and 90 μL of 1.5% sterile PDA added to each well. Reverse pipetting was used to add the PDA at 70° C to the wells [15]. The plates were subsequently dried under UV light for another 60 minutes. Spore suspensions (40 μL) were then added to the wells to a final spore concentration of 5000 spores/well in PDB. Gramicidin S was added to the wells in 20 μL volumes to yield a concentration range of 1.7–21.8 μM. The final volume in each well was 150 μL. The plate layout was as described under microdilution broth assay. Light dispersion at 620 nm was determined at 2-hour intervals starting at 15 hours and ending at 24 hours. Results were visualised by incubating the plate for 72 hours.

3.3.4 Data analysis

Relative growth in each well in the broth assay was calculated in terms of the light dispersion per well divided by the mean light dispersion of the wells containing growth medium, spores, and acetonitrile. Subtracting the relative growth calculated from 1 and multiplying the value by 100 rendered percentage inhibition. The IC_{50} was calculated from the x-value halfway between the top and bottom plateau. Auto-initial values with no fixed constants, as well as stricter criteria for convergence values, were used to determine the various slopes. Statistical analyses of data also performed with GraphPad Prism included 95% confidence levels, Students t-test, correlation coefficients, and the absolute sum of squares, and standard error

μL were added to each well of the microtiter plates except for columns A and H, which were reserved respectively as growth controls and sterility controls. The wells that served as growth controls received 20 μL analytical water and the remaining wells received 20 μL of peptide dissolved in analytical water. All wells contained a final volume of 100 μL. No less than eight determinations were done per concentration value. Test substances were added to the wells before spore germination (approximately 4 hours after harvesting). All light dispersion measurements were done at 620 nm with a Titertek Multiscan Plus Mk II (Flow Laboratories). Measurements were taken at 3-hour intervals up to and including 24 hours.

3.3.3 Microagar antifungal assay

All equipment, media, and materials were treated as described above. The plates were prepared as for the microdilution broth antifungal assay and 90 μL of 1.5% sterile PDA added to each well. Reverse pipetting was used to add the PDA at 70° C to the wells [15]. The plates were subsequently dried under UV light for another 60 minutes. Spore suspensions (40 μL) were then added to the wells to a final spore concentration of 5000 spores/well in PDB. Gramicidin S was added to the wells in 20 μL volumes to yield a concentration range of 1.7–21.8 μM. The final volume in each well was 150 μL. The plate layout was as described under microdilution broth assay. Light dispersion at 620 nm was determined at 2-hour intervals starting at 15 hours and ending at 24 hours. Results were visualised by incubating the plate for 72 hours.

3.3.4 Data analysis

Relative growth in each well in the broth assay was calculated in terms of the light dispersion per well divided by the mean light dispersion of the wells containing growth medium, spores, and acetonitrile. Subtracting the relative growth calculated from 1 and multiplying the value by 100 rendered percentage inhibition. The IC_{50} was calculated from the x-value halfway between the top and bottom plateau. Auto-initial values with no fixed constants, as well as stricter criteria for convergence values, were used to determine the various slopes. Statistical analyses of data also performed with GraphPad Prism included 95% confidence levels, Students t-test, correlation coefficients, and the absolute sum of squares, and standard error

of the mean. Three-dimensional graphs were generated using G N U P L O T, MS-Windows v3.7, 1999, Williams T, Kelley C

3.4 Results and discussion

The need for high throughput, but sensitive antifungal assays, prompted the development of these methodologies. *P. corylophilium* was the organism of choice because of the ease with which it is cultured. Since some fungi do not culture well in liquid medium, we anticipated the need for an assay methodology that will allow quantitive evaluation of antimicrobial agents on these organisms.

3.4.1 Microdilution broth antifungal assay

Microdilution broth assays for antimicrobial testing have extensively been discussed [9, 18, 14]. From these discussions it has been proposed that the Amsterdam method [9] should be used as standard testing methodology. The ease of operation of the Broekaert methodology however makes it a likely candidate for fungal susceptibility testing. Therefore, we decided to adapt this methodology to be an even more user-friendly testing system and use it as a control for our new testing method. Spore dilution experiments were performed to determine the optimal spore concentration for *P. corylophilium* in the broth assay. The results indicate that, for our purposes, a spore concentration of 45 X 10^3 spores/well yielded optimum results. Spore concentrations of 60 X 10^3 spore/well resulted in rapid growth, but with a loss in sensitivity. The assays with 30 X 10^3 spores/well on the other hand led to assay times beyond 24 hours – a time period which exceeds the time criterion (contamination problems during long incubation periods) set at the onset of assay development (data not shown). Although contamination was detected in some instances 2-3 days after the assay, no contamination was detected during the assay period of between 0-24 hours.

Time course studies showed the sensitivity of the broth assay with respect to time and 0% inhibition reference point. The IC_{min}, $IC_{50,}$ and IC_{max} all increased with time (*Figure 1*; Table 1,p 3-12). However, after 24 hours these values remained more or less constant and subsequent measurements showed a loss of sensitivity i.e. "0% inhibition " was obtained in most wells (data not shown). The relationship between growth, peptide concentration, and

time is illustrated by the 3-dimensional graph (*Figure 1*) with maximum growth at 24 hours as reference point for 0% inhibition.

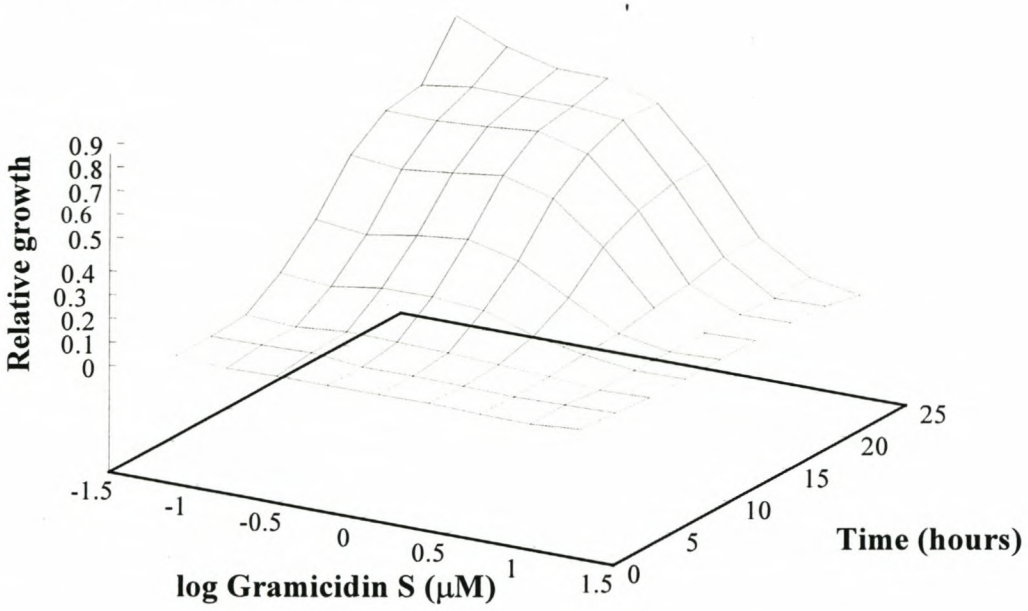

Figure 1 Effect of assay time and peptide concentration with respect to fungal growth.

The time optimised broth assay rendered satisfactory results with gramicidin S and *P. corylophilium* as the organism. Highly repeatable sigmoidal dose-responses were obtained with the microtiter plate antifungal assay. From these dose response curves the IC_{min}, IC_{50} and IC_{max} were determined at 2.81 μM, 5.29 μM, and 10.96 μM respectively (*Figure 2*, Table 1(p 3-12)). The statistical analyses of the non-linear analyses rendered $r^2 = 1$ with the absolute sum of squares = 0.000 41 and 95% confidence level for the IC_{50} of 5.2–6.3 μM.

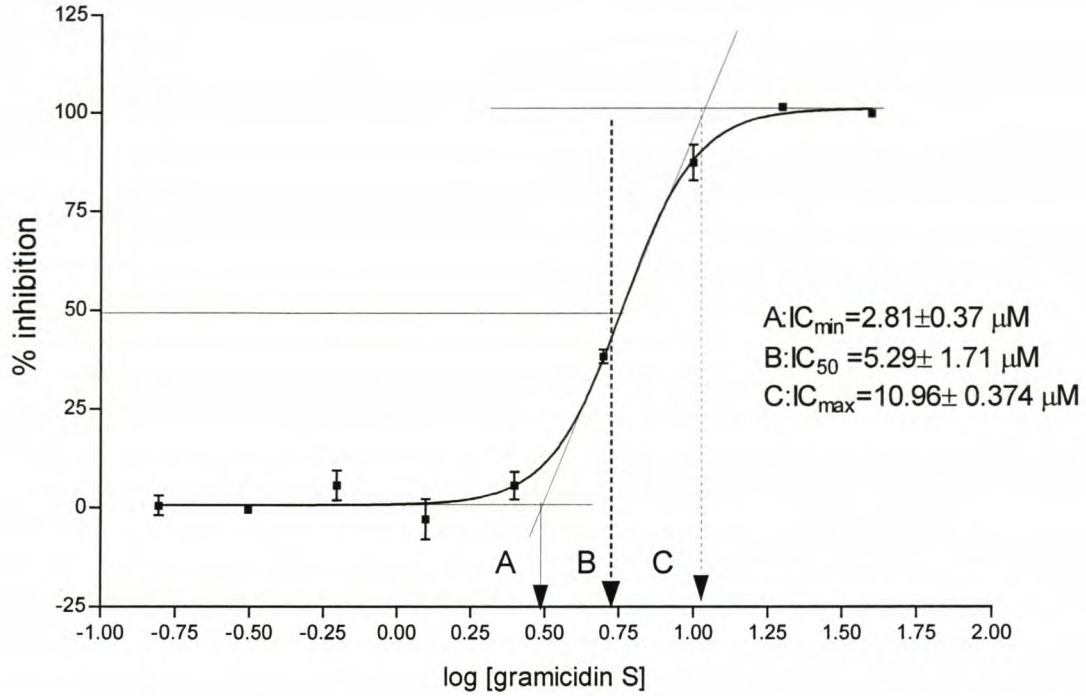

Figure 2 Log dose response curve obtained after 24 hours with the broth assay with a minimum of four determinations per data point. Statistical analysis yielded r^2 = 1.00 and absolute sum of squares = 0.000 416.

3.4.2 Microagar antifungal assay

Culture-plate based agar and agarose type assays are unsuitable for analytical evaluation of antibiotics on these organisms, as these assays are at best subjective with the added complication of peptide inactivation by the agar. We therefore developed the microtiter plate antifungal agar assay to ensure peptide-membrane interaction in the solution phase with the subsequent absorption of the solution phase into the solid phase. This allows for optimal antifungal action, yet provides a solid support with an air interface that these fungi need for successful culturing.

Standardisation of inhibition parameters is an important component in assay development and it was therefore imperative that the inhibition parameters obtained with the two assays should show a good correlation. As the agar assay allows peptide-membrane interaction in the solution phase, the inhibition parameters obtained with this assay should theoretically be in the same range as the microtiter broth antifungal assay, if the same spore count and peptide concentration is used. Therefore, the same spore count of 45 X 10^3 spores/well was used and

gramicidin S added over the same concentration range.

The microagar antifungal assay also allowed for the spectrophotometric determination of antifungal activity with agar solid support. Highly repeatable sigmoidal dose response curves were obtained with this assay and the inhibition parameters for gramicidin S on *P. corylophilium* were established as IC_{min} = 3.1 μM, IC_{50} = 4.3 μM, and IC_{max} = 7.4 μM (*Figure 3*; Table 1, p 3-12) after 16 hours. The statistical analyses of the non-linear analyses yielded r^2 = 0.999 with the absolute sum of squares = 0.0004 and 95% confidence level for the IC_{50} of 4.1–7.5 μM. A picture of a plate after 72-hour incubation is shown in *Figure 4*.

As expected, the inhibition parameters obtained with the microagar antifungal assay did show good correlation with the microtiter broth antifungal assay, although all the values were slightly lower. The differences between the IC_{min} and IC_{50} values differed with only 0.35 μM and 0.98 μM respectively. However, the IC_{max} value showed considerable deviation from the value obtained with the microtiter broth antifungal assay with a difference of 3.5 μM. These differences, especially the difference in IC_{max}, may be because the dilution effect of agar on both gramicidin S and the spores are less than that in the broth assay.

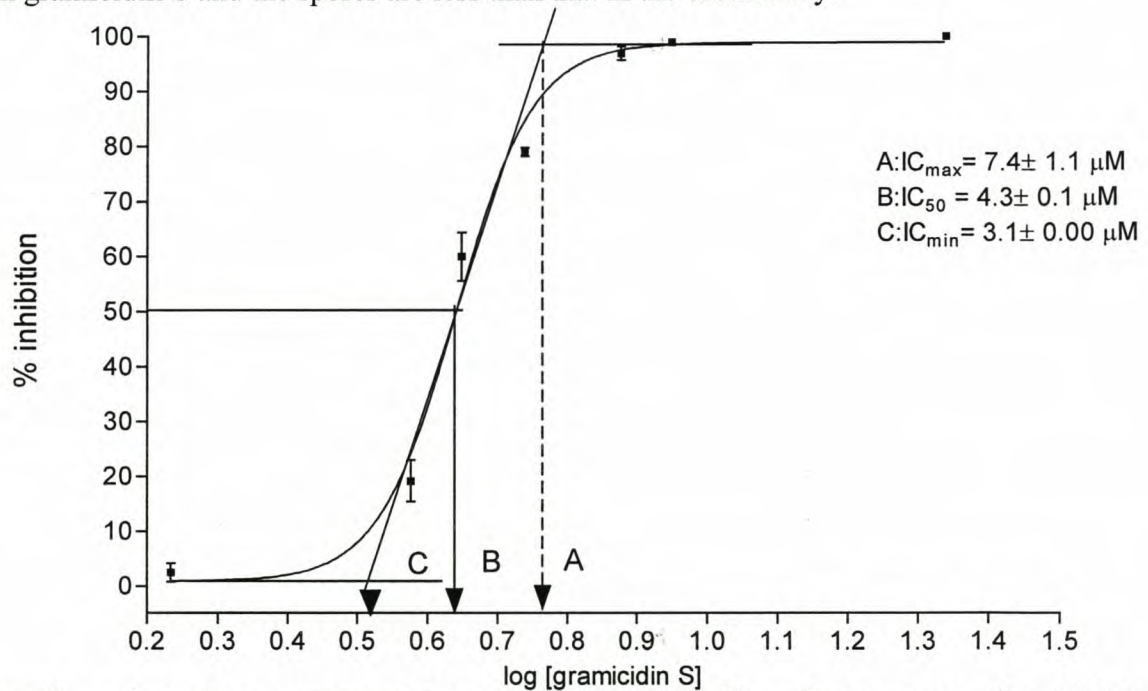

Figure 3 Log dose response curves obtained with antifungal agar assay after 16 hours with a minimum of four determinations per data point. Statistical analysis rendered r^2 = 0.999 and absolute sum of squares = 0.000 401

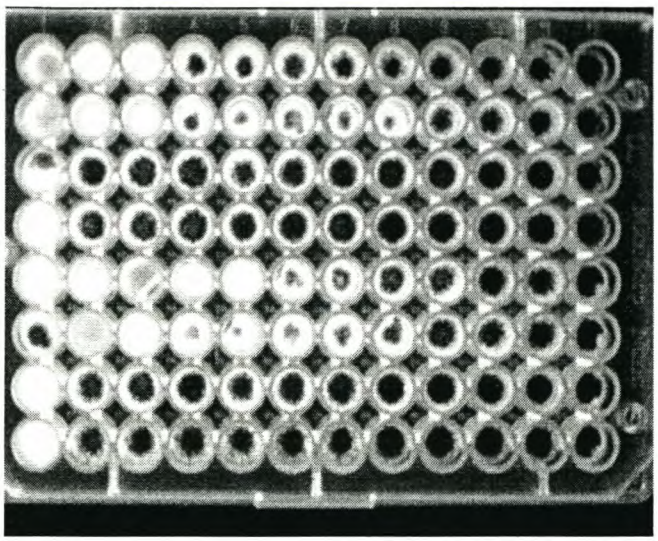

Figure 4 Visualisation of the agar assay was done by incubating the microtiter plate for 72 hours. The dark wells show the fungal growth while the white or clear well show the inhibition of the fungal growth.

Table 1 Summary of inhibition parameters against the test organisms

	IC_{min}	IC_{50}	IC_{max}
P. corylophilium (Broth Assay, 24 h)	2.81±0.1	5.29±0.4	10.96±0.1
P. corylophilium (Agar Assay, 16)	3.16±07	4.31±0.1	7.46 ±1.3

3.5 Conclusions

The broth assay gave repeatable analytical results within analytical error limits being $r^2 \geq 0.998$ and $p= 0.78$. However, the following caveat must be kept in mind when using and planning similar assays: this is a relative assay system and all values will be influenced by the reference wells. The advantage of using a relative system as opposed to an absolute system (i.e. using biomass determinations) is the ease of operation, the speed at which results can be obtained and small volumes required. Furthermore, relative systems allow for compensation with respect to solvent and environmental influence. In an absolute system, the rate of cell growth can seriously influence the IC_{min}, IC_{50} and IC_{max} values, which is not always the

case with a relative system. The advantage of a two-phase system that approximates natural conditions can be seen in the radically reduced assay time of 16 hours. Therefore, this methodology offers one day results. Furthermore, the inhibition parameters established may pave the way for direct application of the *B. brevis* product.

3.6 References

1. Kondejewski L. H., Farmer S. W., Wishart D. S., Kay C. M., Hancock R. E. W., Hodges R. S. (1996) *J. Biol. Chem.* **271**, 25261–25268

2. Tamaki M., Arai I., Akabori S., Muramatsu I. (1995) *J. Peptide Protein Res.* **45**, 299 – 302

3. Stern, A., Gibbons, W. A., Craig, L. C. (1968) *Proc. Natl. Acad. Sci. U.S.A* 61, 734 – 741

4. Pache, W., Chapman, D. and Hillaby, R. (1972) *Biochim. Biophys. Acta*, 255, 358 – 364

5. Katsu, T., Kobayashi, H. and Fujita, Y. (1986) *Biochim. Biophys. Acta*, 860, 608 –619

6. Prenner, E. J., Lewis, R. N. A. H., Neumann, K. C., Gruner, S. M., Kondejewski, L. H., Hodges, R. S. and McElhaney, R. N. (1997) *Biochemistry J.*, 36, 7906 –7916

7. Jorgenson, J. H. (1993) *J. Clin. Microbiol.*, 31, 2841 –2844

8. Rex, J.H., Cooper, C.R., Merz, W.G., Galgiani, J.N., Anaissie, E.J. (1995) *Antimicrob. Agents Chemother.* 39, 906 –909

9. Amsterdam, D. (1996) In Lorian, V. (ED.), Antibiotics in Laboratory Medicine. Williams and Wilkins, Baltimore, MD, 52 –11

10. Cooper, K.E., Woodman, D. (1946) *J. Pathol. Bacteriol,* 58, 75

11. Lehrer, R. I., Rosenman, M., Harwig, S. S. S. L., Jackson, R. and Eisenhauer, P. (1991) *J. Immun. Meth.*, 137, 167 –173

12. Barchiesi, F., Colombo, A. L., McGough, D. A., Rinaldi, M. G., 1994 *J. Clin Microbiol*, 32, 2494 –2500

13. Broekheart, W.F., Terras, F.R.G., Cammue, B.P.A., Vanderleyden, J. (1990) *FEMS Microbiol. Lett.* 69, 55-60

14. Hancock, R. E. W. (1997) Hancock Laboratory Methods, www.interchg.ubc.ca/bobh/peptides.htm

15. du Toit, E.A. and Rautenbach, M. (2000) *J. Microbiol. Methods,* **1**, 159 –165

16. Kunin, C.M. and Edmondson, W.P. (1968) *Proc. Soc. Exp. Biol. Med.*, 129, 118 –122

17. Dulbeco, R. and Vogt, M. (1954) *J Exp Med*, 98, 167

18. Steinberg, D. & Lehrer, R.I. (1997) Designer assays for antimicrobial peptides: disputing the "one size fits all" theory. In: Shafer W.M. (ed)., Methods in Microbiology. Humana Press, Totowa, NJ, 169 –187

Chapter 4

Biological activity studies on the effect of surfactin on the antimicrobial activity of gramicidin S

A revised version of this chapter will be submitted for publication to *Applied and Environmental Microbiology* (Co-authors: M Rautenbach and JL Snoep)

Abstract

Antibiotic production as defence mechanism is a characteristic of a wide variety of organisms. These defence molecules vary greatly and may take the form of extra-cellular enzymes such as proteases, enzymes and DNA replication inhibitors and antimicrobial peptides. In this study, peptides from two co-habiting bacteria were investigated. The two peptides in this study, gramicidin S from *Bacillus brevis* and surfactin from *Bacillus subtilis*, have been shown to target both membrane and intercellular components of target organisms. Evidence is presented that another function may exist for surfactin, that of a shielding molecule or anti-antibiotic. It was found that surfactin antagonises the antimicrobial action of gramicidin S in a dose-dependant manner against a variety of target cells. This antagonism is possibly the result of the formation of an inactive complex between surfactin and gramicidin S.

4.1 Introduction

In diverse ecological communities various defence strategies have evolved to effectively compete for available resources. These strategies include the utilisation of changing environmental conditions and production of compounds. The development of cellular events such as sporulation enables the organism to incorporate the physical environment in a defence strategy. Active resistance is dependent on the production of antibiotic compounds such as extra cellular enzymes, DNA replication inhibitors and antimicrobial peptides [1, 2, 3, 4]. Antibiotic production is a characteristic of many microorganisms including gram-positive bacteria from staphylococcus, streptomyces and bacilli species. A third mechanism may exist which can best be described as extra-cellular antibiotic shields or a decoy-based resistance. One possible example of this type of antibiotic shield is that of vancomycin from

Streptomyces orientalis that specifically binds to penicillin from *Penicillium* species [5]. We investigated a possible second example mechanism after antagonistic behaviour was observed between the antimicrobial peptides gramicidin S and surfactin from *Bacillus brevis* and *Bacillus subtilis* respectively.

Gramicidin S is a cyclic amphipatic decapeptide that consists of two pentapeptides, D-Phe-Pro-Val-Orn-Leu, linked between D-Phe and Leu [6]. The peptide is β-pleated with the four hydrophobic side chains of the valine and leusine residues located on one side of the ring structure and the two hydrophilic ornithine residues in the other. Interactions with alkali metal ions have also been demonstrated as well as the involvement of backbone carbonyl oxygen in this interaction [7]. It is active against gram-positive and gram-negative bacteria, fungi as well as exhibiting haemolytic activity [8, 9, 10, 11]. Association of gramicidin S with cell membranes lead to the release of phospholipids followed by a disruption of the permeability barrier and cell lyses [8, 9,]. Sporulation of *B. brevis* is also retarded by gramicidin S; this action is of special interest as gramicidin S is produced under stress conditions such as oxygen and nutrient limitation [12, 13, 14, 15]. In complex ecological communities, oxygen and nutrient limitation frequently signals fungal sporulation or rapid microbial growth.

Surfactin consists of the heptapeptide L-Glu-L-Leu-D-Leu-L-Leu-L-Val-L-Asp-D-Leu-L-Leu linked *via* a lactone bond to a β-hydroxy fatty acid with 13-15 C atoms, which forms the hydrophobic part of this molecule. Two other natural occurring forms have been isolated with either L-Val or L-Ile at position 7 in the peptide chain [16, 17, 18]. Surfactin was first recognised as a powerful biosurfactant and as such cytotoxic [16,17]. The Glu and Asp residues form an "ionic basket" that selectively binds monovalent and divalent cations and transport them across membranes [19]. Biological activity against gram-positive organisms has been demonstrated [20] as well as antifungal activity in conjunction with co-produced iturin A [21, 22]. Surfactin, like gramicidin S, exerts biological activity on the producer strain. Ahimou and co-workers [15] found that upon secretion, the molecule adsorbs onto the *B. subtilis* membrane thereby changing cell surface hydrophobicity. This may facilitate surface bacterial colonisation through enhanced bacterium-surface interactions [23]. Surfactin is also produced under stress conditions -specifically oxygen limitation at 35 ^{o}C [24, 25].

Even though a large body of scientific evidence has been gathered on the mechanism of action for both peptides, it is not yet complete. Previous studies investigated peptide-cell interaction to measure and explain peptide activity in relation to host defence. However, we believe that to explain peptide function in an ecological context, it is necessary to investigate peptide-

peptide and peptide-cell interactions of different co-existing producers. In this paper, evidence for another possible host-defence mechanism involving both gramicidin S and surfactin will be presented.

4.2 Materials

Tryptone soy broth (TSB) was supplied by Biolab Diagnostics (Midrand, RSA) and Difco Laboratories (Detroit, USA) supplied the Potato Dextrose Broth (PDB). The components for Luria Broth (LB), NaCl, tryptone and yeast extract were from Saarchem (Midrand, RSA), Unipath (Hampshire, England) and Difco Laboratories (Detroit, USA) respectively. Agar powder was from Saarchem (Krugersdorp, South Africa). Microtitre plates (Nunc™-Immuno Maxisorp) were from Nalge NUNC International (Roskilde, Denmark). Culture dishes were from Quality Scientific Plastics USA. Surfactin, gramicidin S and gramicidin D were from Sigma (St Louis, USA). The model peptide ESF1-SAGR and vancomycin were donated by JW Hastings. Acetonitrile (99.9%, far- UV grade) and casein were from BDH laboratory supplies (Poole, England). Merck (Midrand, RSA) supplied the NaH_2PO_4 and Na_2HPO_4. Analytical quality water was prepared by filtering water from a reverse osmoses plant through a Millipore Milli Q® water purification system (Milford, USA).

4.3 Methods

4.3.1 Culturing of target organisms

Eschericia coli HB 101 and *Micrococcus luteus* NCTC 8340 were cultured from freezer stocks on tryptone soy agar (TSA) and Luria agar (LA) respectively at 37°C for 48 hours before selected colonies were grown overnight in TSB and LB respectively. Both organisms were then sub-cultured in TSB at 37°C. Broth microdilution assays [26] were performed with 5 X 10^5 CFU/mL suspensions and inhibition measured spectrophotometrically after 24 hours at 620 nm on a Titertek Multiscan Plus Mk II (Flow Laboratories) microtitre plate reader. All microtitre plates were blocked with 0.5% casein in Dulbecco's Phosphate Buffered Saline (PBS) [27] and sterilised under UV light before use.

Penicillium cf. *corylophilium* spores were grown at 25°C on PDA and harvested from 14-day old cultures by flooding the plates with 10 mL sterile distilled water and gentle rubbing with a sterile spatula [28]. The harvested spores were then filtered through a double layer of gauze

before being diluted in PDA to 45 X 10^3 spores/well. Test substances were added to the spore containing wells and incubated for 24 hours at 25°C. Inhibition was measured spectrophotometricly at 620 nm with a Titertek Multiscan Plus Mk II (Flow Laboratories). All microtiter plates were blocked with 0.5% casein in Dulbeco's Phosphate Buffered Saline (PBS) and sterilised under UV light before use.

4.3.2 Electrospray Mass Spectrometry

ESMS was performed with a Micromass Quattro triple quadrupole mass spectrometer fitted with an electrospray ionisation source. Surfactin was dissolved in 50%, gramicidin S in 50% acetonitrile/water. Samples were prepared by combining the peptides five minutes before analysis. Injections into the ESMS were through a Rheodyne injector valve at 20 µL/analysis with the final carrier solvent concentration 50% acetonitrile. A capillary voltage of 3.5 kV was applied with the ionisation source temperature at 80 °C. The cone voltages for the all the analyses were 60V with the skimmer lens offset at 5V. Data acquisition was in the positive mode, scanning the mass range through m/z = 200–2000 at a scan rate of 100 atomic mass units/second.

4.3.3 Data analysis

Relative growth in the antimicrobial assays was calculated by dividing the light dispersion per well by the mean light dispersion of the wells containing growth medium, spores, and acetonitrile (taken as 100% growth or 1.00 relative growth). Subtracting the relative growth calculated from 1 and multiplying the value by 100 rendered percentage inhibition. Data were analysed using GraphPad Prism 3.0 (GraphPad Software Incorporated) for curve fits and statistical analyses. Sigmoidal dose response curves (variable slope with no weighing of data) were fitted to all assay results. Of the eight or more determinations per concentration, only the mean was considered for fitting the curve. The 50% inhibitory concentration was determined from the x- value halfway between the top and bottom plateau [29].

4.4 Results

Adding surfactin at increasing concentrations caused distinct antagonism of the antimicrobial activity of gramicidin S towards different target cells (*Figures 1-3*).

In our assay system gramicidin S had an IC_{50} of 4.2 μM against *P. corylophilium* as target organism. Surfactin caused dose-dependent antagonism of the antifungal activity of gramicidin S (*Figures 1* and *4*). At 18 μM surfactin all gramicidin activity was inhibited except at the highest gramicidin S concentration at which point approximately 60% inhibition of fungal growth was achieved and IC_{50} of gramicidin S increased by >1000%. All the surfactin concentrations used caused the inhibition curves to shift to the right, i.e. a higher concentration gramicidin S was required to obtain the same result as in the control without surfactin (*Figures 1* and *4*). Even though antagonism of gramicidin S activity diminished with decreasing surfactin concentrations the addition of 4.5 μM surfactin (approximately the IC_{50} concentration of gramicidin S) still resulted in 27% antagonism. Furthermore, the order of addition did not influence the affect the observed results. Surfactin alone was not active against *P. corilophillium* at any of the concentrations used.

Gramicidin S had an IC_{50} of 22 μM towards *E. coli* as target organism. As with the other target organisms, antagonism was also observed with this gram-negative bacterium (*Figures 2* and *4*). Unlike with *P. corylophilium,* the antagonism of gramicidin S activity on *E. coli* was not dose-dependent in the sense that a direct correlation between existed between surfactin concentration and effect on gramicidin S activity. It rather appeared that a "critical" surfactin concentration (> 10 μM) was needed to affect gramicidin S activity (*Figure 4*). The addition of surfactin above this concentration resulted in the shifting of the dose-response curve to the right. However, the gramicidin S activity could not be completely abolished - even at 40 μM surfactin, but this high concentration surfactin did cause >200% change in the IC_{50} of gramicidin S towards *E. coli.* Surfactin alone was not active against *E. coli* at any of the concentrations used. Furthermore, the order of peptide addition did not affect the antagonism profiles observed.

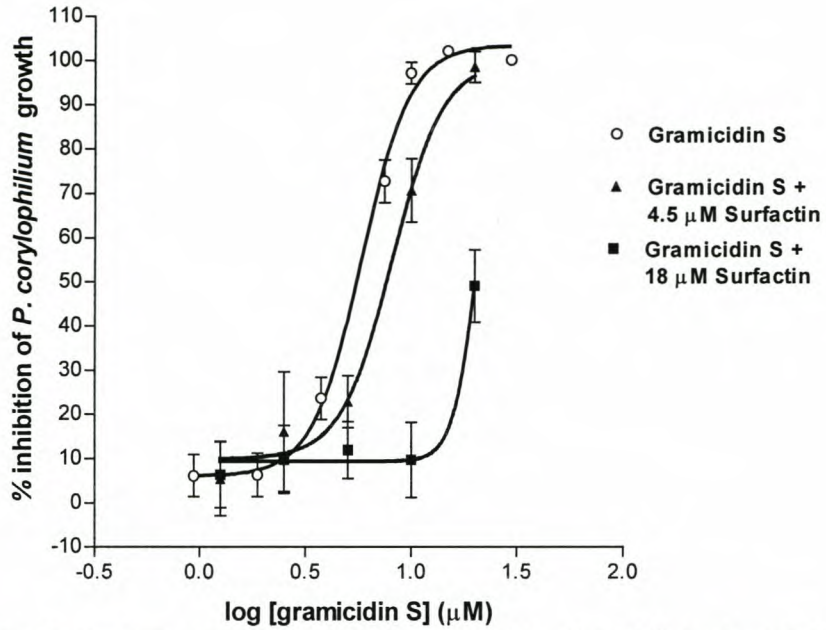

Figure 1 Dose-dependent antagonism of gramicidin S antifungal activity towards *P. corilophillium* by surfactin. Standard error of the mean for each datapoint (n = 24 for gramicidin S; n = 8 for gramicidin S + 18 μM surfactin and gramicidin S + 4.5 μM surfactin) is shown, with R^2>0.99 for all curves. The surfactin results were obtained from two independent experiments in quadroplicate and the gramicidin S results from 6 independent experiments in quadruplicate

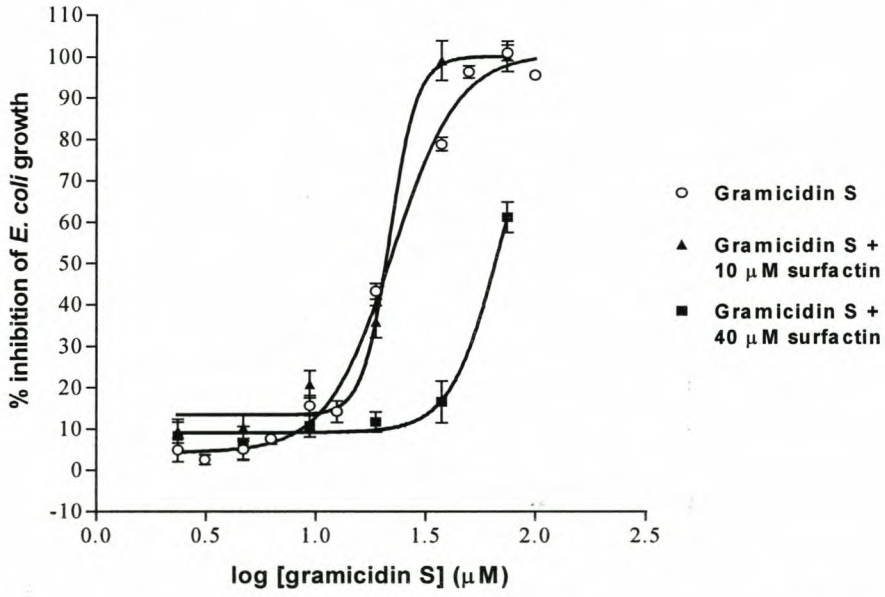

Figure 2 Surfactin induced antagonism of gramicidin S activity against the target organism *E. coli*. Standard error of the mean for each datapoint (n = 16 for gramicidin S; n = 12 for gramicidin S + 10 μM surfactin and gramicidin S + 40 μM surfactin) is shown, with R^2>0.99 for all curves. The surfactin results were obtained from three independent experiments in quadroplicate and the gramicidin S from 4 independent experiments in quadruplicate.

Gramicidin S had an IC_{50} of 6.4 μM against *M. luteus* as target organism. The antagonism (*Figures 3* and *4*) shows an interesting deviation from the profile observed with *P.*

corylophilium and *E. coli*. Unlike the other test organisms, *M. luteus* was sensitive to the order in which surfactin was added. When surfactin was added at 30 μM, after the addition of gramicidin S, only slight antagonism at the higher concentrations of gramicidin was detected (*Figure 4*, Table 1). However, when the target organism was incubated with 30 μM surfactin for 5 minutes before the addition of gramicidin S, a shift of >240 % in the IC_{50} of gramicidin S was observed. (*Figure 4*, Table 1).

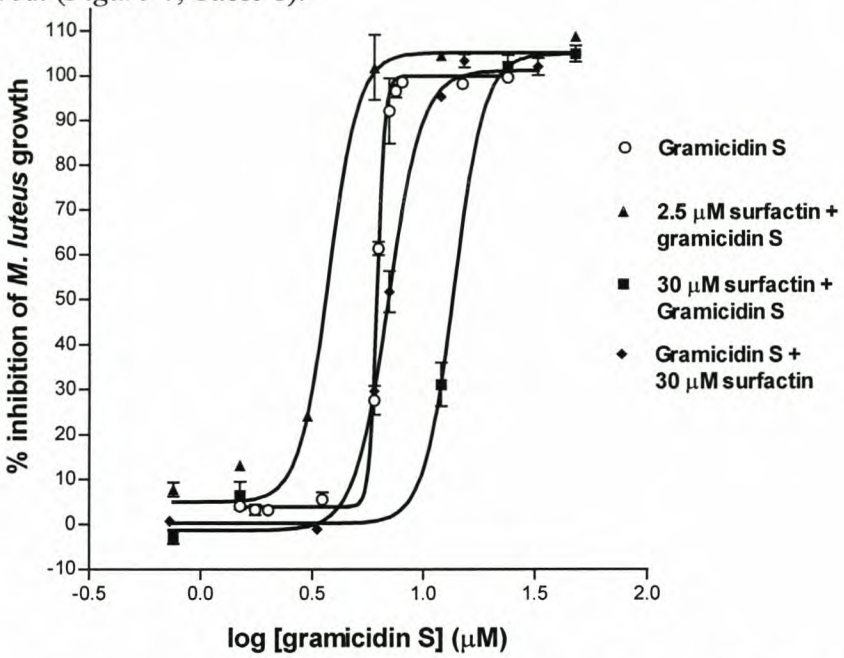

Figure 3 Antagonism of gramicidin S activity by surfactin with *M. luteus* as target organism. Standard error of the mean for each datapoint (n = 46 for gramicidin S; n = 16 for gramicidin S + 18 μM surfactin and for gramicidin S + 4.5 μM surfactin) is shown, with R^2>0.99 for all curves. The results were obtained from four independent experiments in quadruplicate.

Pre-incubation of *M. luteus* with 2.5 μM surfactin lead to >50% decrease in the IC_{50} concentration of gramicidin S (*Figures 3* and *4*). Surfactin alone was not active against *M. luteus* at any of the concentrations used. However, at 100 μM surfactin almost all gramicidin S activity against *M. luteus* was suppressed (results not shown), although at this concentration surfactin on it own showed about 20% *M. luteus* growth inhibition.

The combined action of surfactin and gramicidin S differed for each of the three target cells. The effect observed with *P. corylophilium* and *E. coli* were insensitive with respect to order of peptide addition, whereas a change in addition order had a pronounced effect on *M. luteus*. With respect to biological effect, surfactin concentrations below a 1:1 molar ratio between the peptides at the respective IC_{50} of gramicidin S resulted in synergism towards Gram-positive target cells. However, with *E. coli* and *P. corylophilium* as target cells, concentrations resulting in the same molar ratio did not result in enhanced gramicidin S activity. An increase

in surfactin concentration above the IC_{50} concentration of *P. corylophilium* resulted in an almost linear increase in gramicidin S activity antagonism (*Figures 1* and *4*).

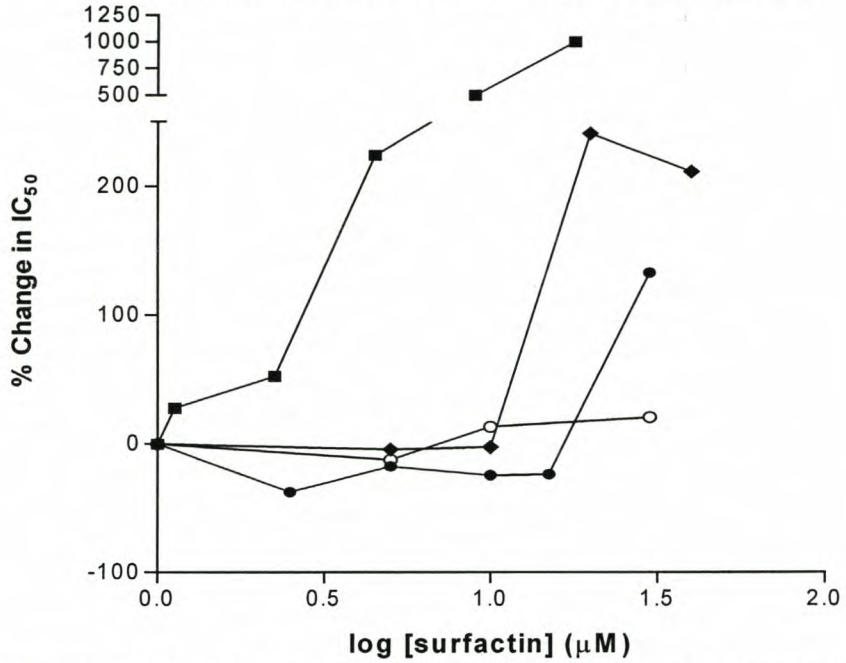

Figure 4 Change of IC_{50} values of gramicidin S towards bacterial target cells as a response to surfactin addition.

In contrast little or no effect was observed with for *E. coli* and *M. luteus* (without pre-incubation with surfactin) up to, what appears to be, a critical concentration after which a rapid increase in antagonism was observed. Similarly, after the initial synergism observed, when *M. luteus* was pre-incubated with surfactin, a small increase in antagonism was observed up to 10 μM, after which a sharp increase in antagonism was observed.

These results indicate that membrane associated interaction, as well as solution interaction between the two peptides may occur. Membrane associated surfactin will cause a localised high surfactin concentration and this may be important in the defence against gramicidin S by the surfactin producer *B. subtilis*. In order to investigate the specificity of this phenomenon, the test peptides were added to *M. luteus* in combination with other compounds (Table 1).

Table 1 Influence of various compounds on biological activity as measured by change in IC_{50} of gramicidin S towards M. luteus

Test compound or combination[1]	**IC_{50} (μM)**	**% Δ IC_{50}**
Surfactin	inactive[2]	-
30 μM[3] surfactin + Gramicidin S	13.8 ± 1.1	116
Gramicidin S	6.4 ± 0.4 [4]	-
Gramicidin S + 30 μM surfactin	6.9 ±1.0	8
0.3 mg/mL BSA	inactive	-
0.3 mg/mL BSA + Gramicidin S	7.5 ± 1.1	17
ESF1-SAGR	32.4 ± 1.1	-
30 μM surfactin +ESFI-SAGR	33.1 ± 1.1	2
Vancomycin	2.8 ± 1.0	-
30 μM surfactin + Vancomycin	2.5 ± 1.0	-11

[1] compound written first was added first and incubated for 5 minutes before addition of second compound
[2] surfactin showed about 20% inhibition of bacterial growth at 100 μM, but no effect at the concentrations used.
[3] 30 μM surfactin is equal to 0.3 mg/mL
[4] average of 17 assays in quadruplicate

Gramicidin S, together with BSA, showed that the protein did not cause a statically significant change in the IC_{50} of the peptide ($P>0.05$). The controls used for surfactin were vancomycin, a non-related glycopeptide [30] and ESF1-SAGR, a cationic α-helical model peptide [31]. The addition of surfactin did not alter the biological activity of either the glycopeptide or ESF1-SAGR.

To explain the antagonism of gramicidin S activity by surfactin, gramicidin S, surfactin, and a peptide mixture were analysed with electrospray mass spectrometry (ESMS). ESMS was used because of the soft-ionisation process that are beneficial for the detection of non-covalent interactions between bio-molecules [reviewed in 32].

The expected molecular ions for gramicidin S ($[M+2H]^{2+}$, m/z = 571; $[M+H]^{+}$, m/z = 1142) were detected (*Figure 5A*) as well as the different surfactin variants ($[M+H]^{+}$, m/z = 995, 1009, 1023, 1037,) (*Figure 5B*).

Analysis of a 1:1 molar mixture of the peptides showed the formation of doubly charged molecular ions corresponding to complexes (m/z = 1069, 1076, 1083, 1090, 1097) consisting of gramicidin S and the surfactin variant variants (*Figure 5C*).

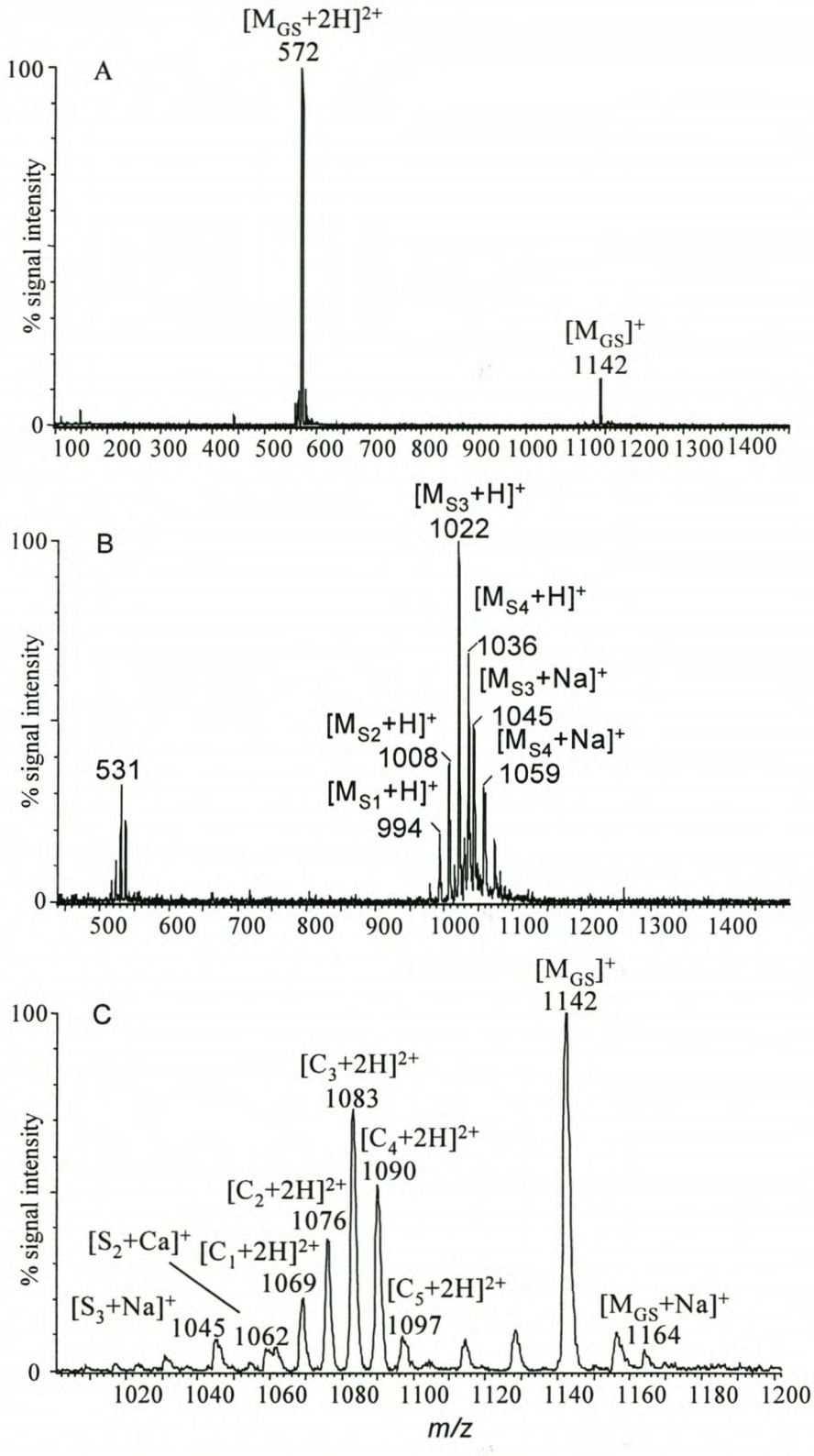

Figure 5 Electrospray mass spectrometry spectrum of (A) gramicidin S with gramicidin S ions denoted as M_{GS}, (B) surfactin with the various surfactin ions denoted as $S_{1\text{-}5}$ and the peptide mixture (C) witt the peptide complexes denoted as C_1-C_5.

Collisionally induced dissociation of the complex molecular ion with *m/z* = 1090 was performed and daughter ions corresponding to gramicidin S and one of the surfactin variants

(*m/z* = 1142 and 1036, respectively) were detected (data not shown). A detailed mass spectrometric investigation of gramicidin S and surfactin interactions will be reported in Chapter 5.

The control peptides, vancomycin and ESF1-SAGR, were also subjected to mass spectrometry and no complex formation for either of the peptides with gramicidin S was observed

4.5 Discussion

Dose-dependent modification of gramicidin S biological activity by surfactin was observed with all the target organisms used. However, the type and degree of antagonism observed with each organism differed not only with respect to order of addition but also with the degree of synergism/antagonism observed. The effect observed with *M. luteus* differed from the other target cells with respect to addition order with *M. luteus* being very sensitive to addition order. In addition, synergism between the peptides was observed at surfactin concentrations below the IC_{50} of gramicidin S. In contrast, the effect observed with *E. coli* was and *P. corylophilium*, insensitive to addition order but did not exhibit same synergism observed at low surfactin concentrations. The difference in antagonism observed is likely the result of differences in membrane composition. The synergism observed with the Gram-positive membrane is likely the result of both peptides penetrating into the lipid bilayer. Both gramicidin S and surfactin has been shown to disrupt membrane integrity and it is likely that surfactin augments gramicidin S activity through membrane destabilisation before gramicidin S addition. The lack of synergism observed with *E. coli* may be attributed to presence of the lipopolisaccharide (LPS) component of the gram-negative organism. It was previously shown that the fatty acid moiety is crucial for lipopeptide-cell membrane interaction. The presence of the LPS component may act as a barrier preventing surfactin penetration into the cell membrane and thus "priming" the membrane for gramicidin S disruption. The result obtained with the fungal target cell is significant in that surfactin is considered as an antifungal peptide in combination with iturin A [33], but in our assay it showed that surfactin can also enhance the activity of other peptides from non-related producer organisms.

With *M. luteus* as target cell, surfactin acted synergistically with gramicidin S at low surfactin concentrations and antagonistically at high surfactin concentrations. This observation is consistent with previous reports that both peptides exhibit membrane activity towards the target cell [20]. The effect of addition order shows that antagonism of gramicidin S activity is

more pronounced when *M. luteus* is incubated with surfactin. This may indicate that in this case, peptide-peptide interaction occured primarily at the membrane interface. Similarly, synergism could be the consequence of surfactin adsorption onto the target cell membranes thereby sensitising the membrane towards gramicidin S. The significantly lower antagonism observed with out pre-incubation with surfactin suggest that a) peptide-peptide interaction occurs primarily in the solution phase and b) that surfactin does not interact with gramicidin S after the latter has been immersed in the membrane. Solution phase interaction between the two peptides, as indicated by ESMS, resulted in the formation of complexes. These complexes are likely to be inactive.

Similarly, surfactin similar to iturin A, readily interacts with fungal membranes and the same mechanism for synergism and antagonism may apply. However, one can only speculate on the insensitivity of fungal membranes to addition order. A possible explanation may be that surfactin more readily interacts with fungal membranes as opposed to Gram-positive bacterial membranes.

It is unknown whether a specific surfactin-LPS interaction exists. However, it was shown that this peptide spontaneously interacts with lipid bi-layers with resultant channel formation and solubilisation of the bilayer [34, 35]. It was also found that membrane penetration was dependant on acyl chain length with the longer acyl change exhibiting the greatest penetration. It is therefore possible that the LPS component of gram-negative bacteria will allow peptide interaction without penetration into the lipid bilayer. This interaction can then lead to a localised high surfactin concentration area, which effectively prevents gramicidin S cell membrane interaction. Furthermore, surfactin-LPS interaction without lipid bilayer penetration can explain the absence of synergism between the peptides. The apparent "critical concentration" required for the antagonism of gramicidin S action may imply that a minimum number if surfactin molecules needs to be present at the cell-environment interface. However, it may also be possible that some of the solution phase antagonism was counterbalanced by synergism in the cell wall, as is the case with *M. luteus*.

The lack of antagonism observed with the non-related peptides vancomycin and ESF1-SAGR indicates that a degree of specificity exists in surfactin-peptide interactions.

It has been shown that surfactin readily adsorbs onto the gram-positive membrane of the producer organism [36]. During interaction with the *B. subtilis* membrane, surfactin is orientated with the alkane chain exposed to the environment and thus increasing cell hydrophobicity. All so, it has been shown that surfactin readily forms micelles [37] and in

addition to this it has been postulated that iturin A, with similar a structure, assemble in bilayers [38]. Therefore, we propose that at high surfactin concentrations, additional surfactin molecules interact with previously adsorbed surfactin to form a "secondary membrane" with the acidic residues orientated towards the environment. Such an assembly would generate a local high surfactin concentration at the cell-environment interface resulting in the effective antagonism of gramicidin S at membrane level. Gramicidin S will then be trapped in the bilayer and would not be able to exert either its membrane disruptive action or intracellular activity [8, 9, 10]. In addition, host immunity against the co-produced peptide, iturin A has been demonstrated [39] and this may protect *B. subtilis* against the sensitising effect of surfactin.

4.6 Conclusion

Current dogma dictates a survival of the fittest approach in the study of antimicrobial compounds, i.e. survival depends on the biological activity of the compounds produced. There is currently a growing body of evidence that this may be an oversimplified approach. The antimicrobial activity of these cyclic peptides, and others, may represent only one of a number of functions. Different functions have been proposed for gramicidin S and surfactin. The idea that gramicidin S acts as a bacterial hormone stems from the observation that *B. brevis* sporulation is retarded [40, 41], but not arrested, by gramicidin S. Surfactin has similarly been implicated in competence of *B. subtilis* spores.

Our results indicate that, in addition to numerous target cell interactions, a plethora of inter-organism molecular interactions may exist which may play a role in determining survival. The interactions encompass antibiotic activity, molecular cooperation, and antagonism. The antagonistic behaviour of surfactin as well as the cooperation with gramicidin S against susceptible organisms may point to a possible new defence strategy of *B. subtilis*. This reinforces multi-functionality of such peptides. Therefore, we propose another function for surfactin, apart from its antimicrobial and surfactant functions namely: a defence molecule against the product of another antimicrobial peptide producer i.e. an anti-antibiotic. This hypothesis is tenable if taken into account that gramicidin S is toxic to gram-positive organisms such as *B. subtilis* [20]. Furthermore, both peptides are secreted in response to oxygen stress [15, 24, 25]. *B subtilis* can survive anaerobic conditions, given a suitable electron acceptor, whereas *B. brevis* is a facultative aerobe [4]. The antagonism of gramicidin S by surfactin may therefore present a mechanism to survive the presence of its competitor's

antibiotic until anaerobic conditions result — a condition under which only *B. subtilis* can survive.

1. Bu'lock J.D. (1961) *Adv. Appl. Microbiol.*, **3**, 293–342

2. Katz E. (1977) *Bacteriol. Rev.*, **41**, 449–474

3. Schaeffer P. (1969) *Bacteriol. Rev.*, **33**, 48–71

4. Sonenshein A. L., Hoch, J. A., Losick R. (eds.) (1993) Bacillus subtilis and other gram-positive bacteria biochemistry, physiology and molecular genetics, American Society for Microbiology, U.S.A.

5. Lynen F., Borremans F., Sandra P. http://www.richrom.com/assets/CD23PDF/h27.pdf.

6. Stern, A., Gibbons, W. A., Craig, L. C. (1968) *Proc. Natl. Acad. Sci. U.S.A* 61, 734–741

7. Gross D. S. & Williams E. R. (1996) *J. Am. Chem. Soc.* **118**, 202 –204

8. Pache, W., Chapman, D. and Hillaby, R. (1972) *Biochim. Biophys. Acta*, **255**, 358 –364

9. Kondejewski, L. H., Farmer, S. W., Wishart, D. S., Kay, C. M., Hancock, R. E. W., Hodges, R. S. (1996) *J. Biol. Chem.* **271**, 25261–25268

10. Katsu, T., Kobayashi, H. and Fujita, Y. (1986) *Biochim. Biophys. Acta*, **860**, 608 –619

11. Prenner, E. J., Lewis, R. N. A. H., Neumann, K. C., Gruner, S. M., Kondejewski, L. H., Hodges, R. S. and McElhaney, R. N. (1997) *Biochemistry J.*, **36**, 7906 –7916

12. Seddon B. & Nandi (1978) *Biochem Soc. Trans.* **6**, 412 –413

13. Nandi S. & Seddon B. (1978) *Biochem. Soc. Trans.*, **6**, 409 –411

14. Azuma T. & Demain A. L. (1996) *J. Indust. Microbiol.*, **17**, 55–61

15. Demain, A. L. & Agathos, S. N. (1986) *Can. J. Microbiol.*, **35**, 208–214

16. Kakinuma A., Sugino H., Isono M., Tamura G., Arima K. (1969) *Agric Biol Chem.* **33**, 973–976

17. Baumgart F., Kluge B., Ulrich C., Vater J., Ziessow D. (1991) *Biochem. Biophys. Res. Commun.*, **177**, 998 –1005

18. Peypoux F., Bonmatin J.M., Labbé H., Das B.C., Ptak M., Michel G (1991) *Eur. J. Biochem.*, **202**, 101-6

19. Timon L., Peypoux F., Wallach J., Michel J. (1993) *Colloids Surf. B.* **1**:57 –62

20. Tsukagoshi N., Tamura G., Arima K. (1970) *Biochim. Biophys. Acta,* **196**, 204 –210

21. Ohno A., Ano T., Shoda M. (1995) *J. Ferment. Bioeng.*, **80**, 517 –519

22. Maget-Dana R., Thimon L., Peypoux F. Ptak M. (1992) *Biochimie,* **74**, 1047 – 1051

23. Ahimou F., Jacques P., Deleu M., (2000) *Enzyme and Microbial Technology*, **27**, 749 –754

24. Kim H. S., Yoon B. D., Lee C. H., Oh H. M., Katsugari T., Tani Y., (1997) *J. Ferment. Bioen.*, **84**, 41 –46

25. Roubin de M. R., Mulligan C. N., Gibbs B. F. (1989) *Can. J. Microbiol.*, **35**, 854 –859

26. Lehrer, R.I., Rosenman, M., Harwig, S.S.S.L., Jackson, R., Eisenhauer, P. (1991) *J. Immunol. Methods*, **137**, 167 –173

27. Dulbecco, R., Vogt, M., (1954) *J. Exp. Med.* **98,** 67

28. Broekheart, W.F., Terras, F.R.G., Cammue, B.P.A., Vanderleyden, J. (1990) *FEMS Microbiol. Lett.* **69**, 55-60

29. Du Toit, E.A. and Rautenbach, M. (2000) *J. Microbiol. Methods*, **1**, 159 –165

30. McCormick M. H., Stark W. M., Pittenger G. E., Pittenger R. C., McGuire J. M. In, *Antibiotics Annual*, (1955-56), 606 - 611 Medical Encyclopaedia, Inc, New York, USA

31. Dykes G.A., Aimoto S., Hastings J.W. (1998) *Biochem. Biophys. Res. Commun.*, **248**, 268-72

32. Daniel M. J., Fries D. S., Rajagopalan S., Wendt S., Zenobi R., (2002) *Int. J. Mass Spectrom.*, **216**, 1 –27

33. Maget-Dana R., Thimon L., Peypoux F. Ptak M. (1992) *Biochimie,* **74**, 1047 – 1051

34. Maget-Dana R., Ptak M., (1995) *Biophys. J.*, **68**, 1947 –53

35. Grau A., Gomez-Fernandez J.C., Peypoux F., Ortiz A. (1999) *Biochim Biophys Acta*, **1418**, 307 –19

36. Ahimou F., Jacques P., Deleu M., (2000) *Enzyme and Microbial Technology*, **27**, 749 –754

37. Ishigami Y., Osman M., Nakahara H., Sano Y., Ishiguro R., Matsumoto M. (1995) *Colloids Surfaces B: Biointerfaces* **4**, 341 –348

38. Grau A., Gómez-Fernández J. C., Peypoux F, Ortiz A., (2001) *Peptides*, **22**, 1 –5

39. Maget-Dana R. & Peypoux F. (1994) *Toxicology* **87**, 151 –174

40. Seddon B. & Nandi S. (1978) *Biochem Soc. Trans.*, **6**, 412 –413

41. Nandi S. & Seddon B. (1978) *Biochem. Soc. Trans.*, **6**, 409 –411

Chapter 5

An electrospray mass spectrometry investigation of the nature of gramicidin S - surfactin interaction

A revised version of this Chapter will be submitted for publication to *Journal of the American Society of Mass spectrometry* (Co-authors: M Rautenbach and MJ van der Merwe)

Abstract

We have previously shown (Chapter 4) that surfactin antagonises the antimicrobial action of gramicidin S. In this chapter we report on the possible mechanism of antagonism as investigated through electrospray mass spectrometry. We observed the formation of surfactin-gramicidin S complexes in 1:1 and 2:1 ratios with complex formation favoured by an increase in the organic component of the carrier solvent. Dissociation *via* cone voltage and collisionally induced dissociation experiments showed the relative stability of the peptides and peptide complexes. Competition studies indicated that neither Na^+ nor Ca^{2+} affect the stability of preformed complexes, and that metal ion association does not occur after complex formation. Titration of ion-associated surfactin (Na^+ or Ca^{2+} adducts) showed that gramicidin S associates with both surfactin and the ion-complexed surfactin.

5.1 Introduction

A number of established analytical techniques are available to investigate non-covalent interactions of macromolecules. Solution phase techniques include surface plasmon resonance [1], optical spectrometry, nuclear magnetic resonance [2], differential scanning calorimetry, isothermal thermal titration [3, 4], and light scattering techniques [5]. Mass spectrometry has been added to this repertoire of solution phase techniques [6] in the form of electrospray mass spectrometry (ESMS). The "soft ionisation" in ESMS has been used with great success in the investigation of peptide and protein structure–function relationships, and DNA sequencing (reviewed in [7]). Furthermore, metal ion–ligand and interactions has been studied extensively through mass spectrometry (reviewed in [8]) as well as host-guest interactions in biomolecules [9, 10]. The investigation of non-covalent interactions with mass spectrometry

also benefited from the recent advances in "soft ionisation" and detection technology (reviewed in [11]).

The investigation of electrostatic interactions between metal ions and biomolecules is of particular importance as these interactions have been implicated in many biochemical processes, and are therefore inextricably linked to life itself. Examples of the interactions include Mg^{2+} stabilisation of nucleotide complexes; Zn^{2+} participation in the catalytic mechanisms of several enzymes and Ca^{2+} mediated secondary messenger systems. Furthermore, the redox pair Fe^{2+}/Fe^{3+} is utilised in electron transfer systems. Osmoregulation of cells as well as nerve impulse transmittance is dependent on the alkali metal ions Na^{+} and K^{+}. Disturbances in the ion-biomolecule homeostasis or interactions that do not naturally occur in the cell could potentially have disastrous consequences on cell vitality. The mechanism of action of ionophores, such as the cyclic antibiotic peptide valinomycin, involves the disruption of the osmotic balance by specifically complexing with K^{+} ions [12] and transporting it over the cell membrane [13]. The chelating of alkali metal ions is analogous to the metal ion complexes formed by crown ethers by capturing the metal ions in its ring structure with the oxygen atoms as chelating atoms [8, 14].

In Chapter 4 the broad-spectrum antagonistic effect of surfactin on the biological activity of gramicidin S was described. Preliminary results indicated that this phenomenon might be the result of inactive complex formation between surfactin and gramicidin S. In this study we explore the complex formation, and specifically the effect of Na^{+} and Ca^{2+} on complex formation, using electrospray mass spectrometry (ESMS). Gramicidin S [15, 16] and surfactin are known to complex metal ions [17, 18, 19]. Gramicidin S has β-pleated sheet conformation that contains two type II β-turns [20]. The hydrophobic residues (L-Val and L-Leu) are orientated towards one side of the plane and the charged Orn residues on the opposite side of the plane [20, 21, 22]. Biological activity of gramicidin S is dependent on the Orn and D-Phe residues [23]. Surfactin's conformation has been elucidated through NMR and molecular modelling [24] and found to be a β-sheet with a "horse saddle" topology for the ring atoms. The L-Glu and L-Asp residues were found apposite the aliphatic chain and in a "claw" conformation. The conformation allows the chelating of metal ions for transport across membranes [19]. Furthermore, interactions with metal ions are essential for stabilisation of the ring structure, which is necessary for micelliation [25].

5.2 Materials and methods

5.2.1 Materials

Surfactin was supplied by Fluka Chemie (GmbH) and gramicidin S by (St Louis, USA). Acetonitrile (99.9%, far- UV grade) was from BDH laboratory supplies (Poole, England). Calcium chloride was from Associated Chemical Enterprises (Glenvista, RSA) and NaCl from Saarchem (Midrand, RSA). Analytical quality water was prepared by filtering water from a reverse osmoses plant through a Millipore Milli Q® water purification system (Milford, USA).

5.2.2 Electrospray Mass Spectrometry

ESMS was performed with a Micromass Quattro triple quadrupole mass spectrometer fitted with an electrospray ionisation source The peptides as well as the salts were dissolved in 50% acetonitrile/water. Solvent concentration before injection was 50% acetonitrile/water. Samples were prepared by incubating surfactin and the respective salts overnight. Gramicidin S was added five minutes before analysis. Samples were injected into the ESMS through a Rheodyne injector valve at 20 μL/analysis with the final carrier solvent concentration 50% acetonitrile. A capillary voltage of 3.5 kV was applied with ionisation source temperature at 80 °C. The cone voltage for all analyses, except for CV experiments, was 60V the skimmer lens offset at 5V. Data acquisition was in the positive mode through the *m/z* = 200–2000 at a scan rate of 100 atomic mass units/second. Cone voltage (CV) driven dissociation was performed as above with the cone voltage varied between 20V and 120V. Collisionally induced dissociation (CID) of selected molecular ions was executed at a gas pressure of $2X10^{-3}$ mbar argon in MS_2 with collision energy of 45eV. Fragment ions were detected by scanning the second analyser from *m/z* = 10 to about 100 atomic mass units (amu) above the *m/z* value of the parent ion. Data was acquired in the multiple channel acquisition mode. CID experiments were also performed under above conditions with the collision energy varied from CE=15–75 eV. The first and second mass analysers were set to the selected parent ions and chromatograms recorded of the change in parent-ion signal intensity.

5.3 Results and Discussion

To explain the previously observed antagonism of gramicidin S activity, mass spectrometry was performed on the compounds, to determine purity (results not shown, see Chapter 2) as well as on a peptide mixture. It was found that both compounds were of high purity containing only minor contaminants. With gramicidin S, both the doubly charged ($[M+2H]^{2+}$) and the singly charged ($[M+H]^{+}$) species were detected, as well as sodiated gramicidin S with the expected *m/z* ratios of 571.7, 1142.1, and 1165.46 respectively (*Figure 1*). Analysis of surfactin showed singly charged species of the variant surfactin forms (*m/z* = 994.72, 1008.74, 1022.77, 1036.8 and 1049.82) (Table 1). In addition to the different surfactin species, their Na^{+} and Ca^{2+} adducts were also detected. However, no doubly charged surfactin species were detected under the ESMS conditions.

5.3.1 Identification of surfactin-gramicidin S complexes

A mixture of gramicidin S and surfactin contained, in addition to the specific peptide species, a range of molecular species corresponding to the *m/z* ratios of doubly charged surfactin-gramicidin S complexes (C_1–C_5 in *Figure 1*, Table 1). In addition to the 1:1 complexes, 2:1 surfactin:gramicidin S complexes also were detected (*Figure 2*, Table 2).

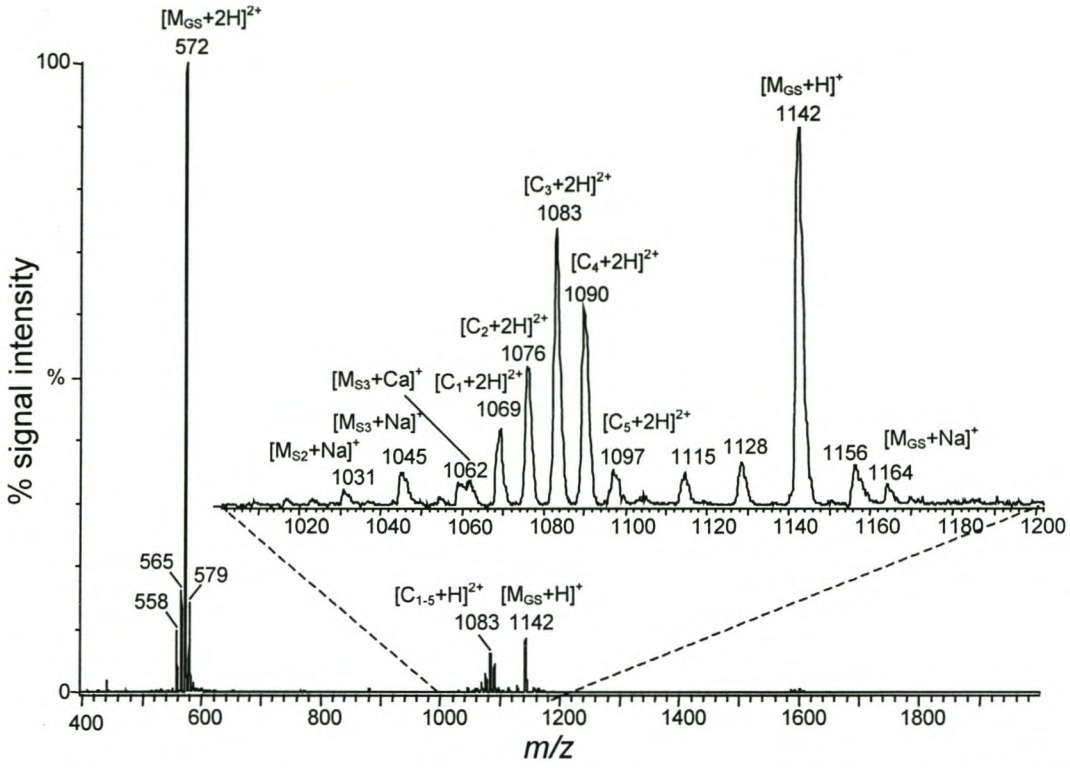

Figure 1 Mass spectra of a 1:1 surfactin-gramicidin S mixture. Both singly (*m/z* = 572) and doubly charged (1142) gramicidin S ions were detected. Five different doubly charged 1:1 surfactin-gramicidin S complexes (complexes 1 –5) were detected. The complexes formed from different surfactin forms are denoted C_1–C_5. Gramicidin S species are denoted M_{GS}.

Table 1 Summary of the different peptide and 1:1 complex species detected with ESMS in a gramicidin S-surfactin mixture

Peptide or complex	**M_r**	**Specie**	**Expected *m/z***	**Detected *m/z***
Gramicidin S [#]	1141.24	$[M+H]^+$	1142.24	1142.47
		$[M+2H]^{2+}$	571.62	571.84
Surfactin1 [1]	994.27	$[M_1]^+$	994.27	994.73
Surfactin2 [2]	1008.30	$[M_2]^+$	1008.30	1008.71
Surfactin3 [3]	1022.33	$[M_3]^+$	1022.33	1022.81
Surfactin4 [4]	1036.36	$[M_4]^+$	1036.36	1036.79
Surfactin 5 [5]	1050.39	$[M_5]^+$	1050.39	1049.76
Complex 1	2135.51	$[M+M_1+2H]^{2+}$	1068.75	1068.61
Complex 2	2149.54	$[M+M_2+2H]^{2+}$	1075.77	1075.59
Complex 3	2164.24	$[M+M_3+2H]^{2+}$	1082.78	1082.58
Complex 4	2177.60	$[M+M_4+2H]^{2+}$	1089.80	1089.57
Complex 5	2191.63	$[M+M_5+2H]^{2+}$	1096.81	1096.18

\# cyclo[D-Phe-L-Pro-L-Val-L-Orn-L-Leu]

1 cyclo[L-Glu-L-Leu-D-Leu-L-Val-L-Asp-L-Leu-L-Val-($C_{14}H_{28}O_2$)]
cyclo[L-Glu-L-Leu-D-Leu-L-Ala-L-Asp-L-Leu-L-Leu-($C_{14}H_{28}O_2$)]
cyclo[L-Glu-L-Leu-D-Leu-L-Ala-L-Asp-L-Leu-L-Ile-($C_{14}H_{28}O_2$)]

2 cyclo[L-Glu-L-Leu-D-Leu-L-Val-L-Asp-L-Leu-L-Leu-($C_{13}H_{26}O_2$)]
cyclo[L-Glu-L-Leu-D-Leu-L-Val-L-Asp-L-Leu-L-Ile-($C_{13}H_{26}O_2$)]
cyclo[L-Glu-L-Leu-D-Leu-L-Val-L-Asp-L-Leu-L-Val-($C_{15}H_{30}O_2$)]

3 cyclo[L-Glu-L-Leu-D-Leu-L-Val-L-Asp-L-Leu-L-Leu-($C_{14}H_{28}O_2$)]
cyclo[L-Glu-L-Leu-D-Leu-L-Ala-L-Asp-L-Leu-L-Val-($C_{14}H_{28}O_2$)]
cyclo[L-Glu-L-Leu-D-Leu-L-Val-L-Asp-L-Leu-L-Ile-($C_{14}H_{28}O_2$)]

4 cyclo[L-Glu-L-Leu-D-Leu-L-Val-L-Asp-L-Leu-L-Leu-($C_{15}H_{30}O_2$)]
cyclo[L-Glu-L-Leu-D-Leu-L-Val-L-Asp-L-Leu-L-Ile-($C_{15}H_{30}O_2$)]

5 cyclo[L-Glu-L-Leu-D-Leu-L-Val-L-Asp-L-Leu-L-Leu-($C_{16}H_{32}O_2$)]

It must be noted that even although a 1:1 molar mixture in 50% acetonitrile was subjected to ESMS, a considerably lower surfactin signal was detected. This was expected, as surfactin

is anionic and the ESMS was performed in the positive mode. No triply charged ($[M+3H]^{3+}$) or quadruply charged ($M+4H]^{4+}$) complex species corresponding to three surfactin molecules and gramicidin S were detected. However, if these species exist exclusively as doubly charged ions detection was not possible as the data acquisition was done over the *m/z* = 200 –2000 range.

To determine the stoichiometry of complex formation, mixtures of gramicidin S and surfactin were analysed at different surfactin-gramicidin S molar ratios. It was found that optimal complex formation is at a 1:1 ratio (*Figure 3*). Analysis of the spectra recorded indicated that no complexes were formed at a 1:2 surfactin:gramicidin S ratio.

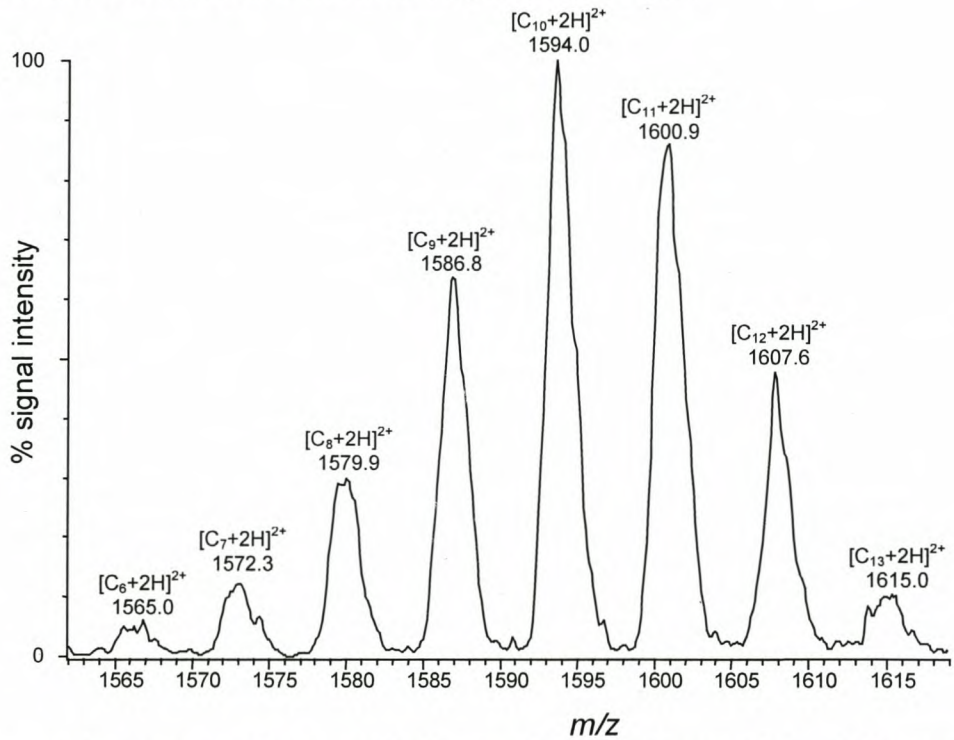

Figure 2 Mass spectra of a 1:1 surfactin-gramicidin S mixture. Eight different doubly charged 2:1 surfactin-gramicidin S complexes (C_6-C_{13}) were detected.

Table 2 A summary of the different peptide and 1:2 complex species detected with ESMS in a gramicidin S-surfactin mixture (S = surfactin; G = gramicidin S)

Peptide or complex	M_r	Specie	Expected *m/z*	Detected *m/z*
Complex 6	3129.78	$[S1+S1+G+2H]^{2+}$	1565.89	1565.00
Complex 7	3143.80	$[S1+S2+G+2H]^{2+}$	1572.90	1572.34
Complex 8	3157.84	$[S1+S3+G+2H]^{2+}$; $[S2+S2+G+2H]^{2+}$	1579.92	1579.99
Complex 9	3171.86	$[S1+S4+G+2H]^{2+}$; $[S2+S3+G+2H]^{2+}$	1586.93	1586.80
Complex 10	3185.52	$[S1+S5+G+2H]^{2+}$; $[S2+S4+G+2H]^{2+}$; $[S3+S3+G+2H]^{2+}$	1593.76	1594.01
Complex 11	3199.48	$[S2+S5+G+2H]^{2+}$; $[S3+S4+G+2H]^{2+}$	1600.74	1600.90
Complex 12	3213.56	$[S3+S5+G+2H]^{2+}$;$[S4+S4+G+2H]^{2+}$	1607.78	1607.66
Complex 13	3227.9	$[S5+S5+G+2H]^{2+}$	1614.95	1615.01

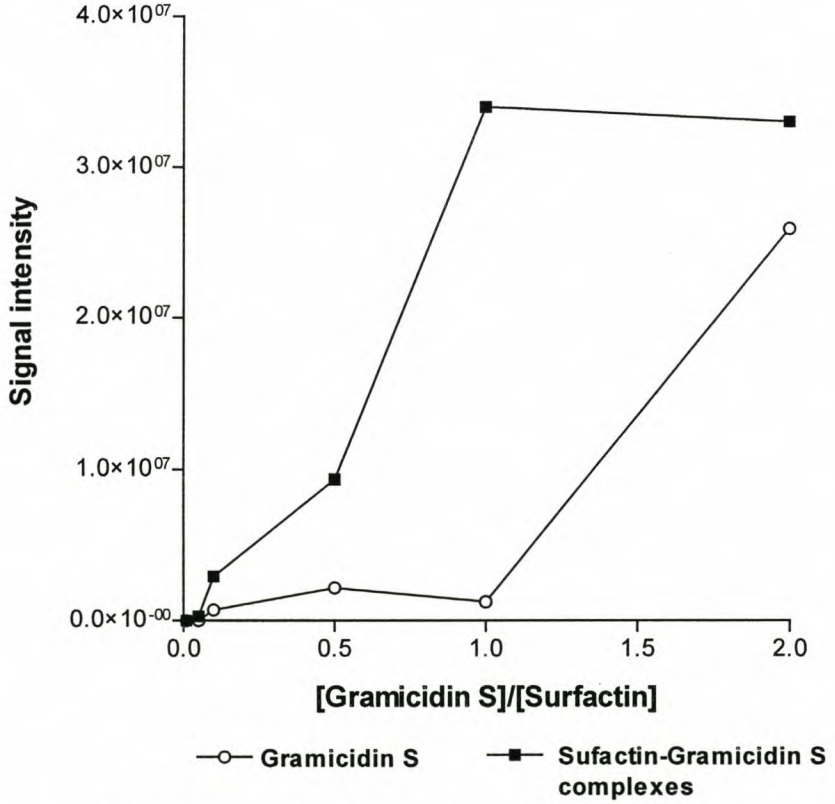

Figure 3 Change in signal intensity of gramicidin S and gramicidin S:surfactin complexes with change in molar ratio.

5.3.2 Stability of surfactin-gramicidin S complexes

Collisionally induced dissociation (CID in MS_2) of C_3 (*m/z* 1089) showed that this molecular species is composed of gramicidin S and the surfactin variant with M_r = 1036.8. In addition to molecular ions corresponding to gramicidin S and surfactin with M_r = 1036.8 the parent ion was also detected (*Figure 4*). Collisionally induced dissociation of the molecular ion with *m/z* =1600.84 shows that the ion is composed of surfactin 2–5 and gramicidin S.

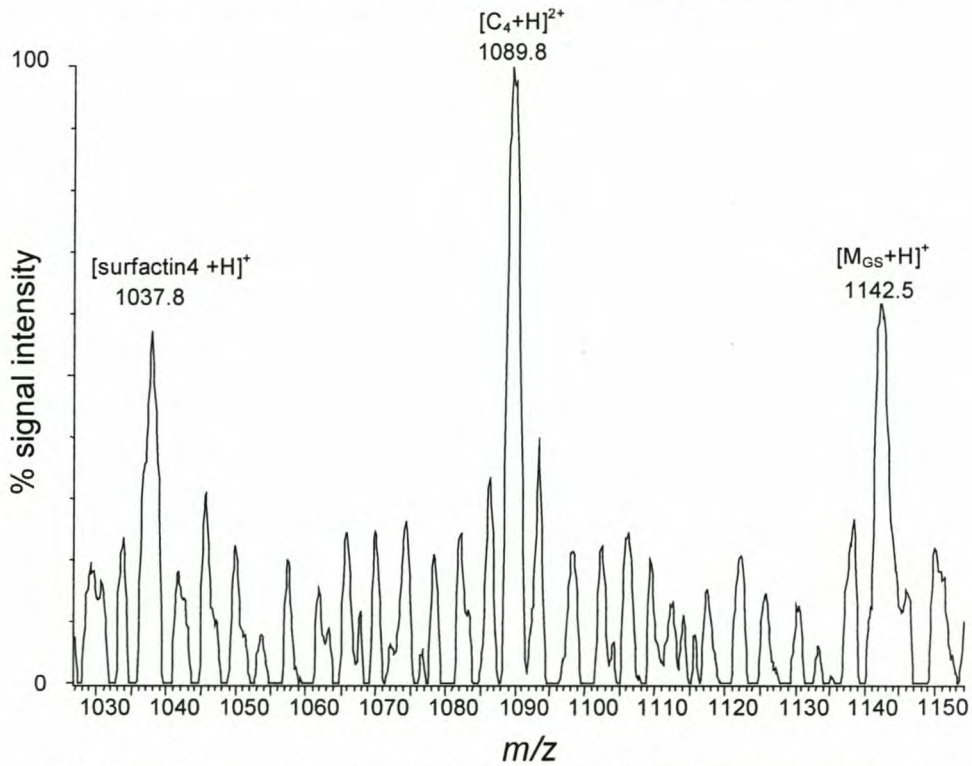

Figure 4 Collisionally induced dissociation of gramicidin S-surfactin complex 3 (*m/z* = 1089.41). Cone voltage was set at 60 V and the collision energy to 20 eV.

Since slightly different conformations were reported for the different surfactin variants, cone-voltage driven dissociation experiments were performed to evaluate the relative gas-phase stability of the peptides and complexes (*Figure 5*). The cone voltage was varied from 20–120V at a source temperature of 85° C. Surfactin variants 1–5 had an optimum signal between 50 and 80V with rapid deterioration of the signal intensity at cone voltage higher than 100V, due to fragmentation. Close inspection of the results showed that optimum signal for surfactin 1 was 60V, and for surfactin 2-4 at 80 V (results not shown). This surfactin 1 specie showed the weakest ionisation over the cone voltage range, but and was stable over the range 60-100V. It is interesting to note that the strongest signal was found for surfactin 3, but that an equal signal was not detected for surfactin 2, which differs only with respect to fatty acid

chain length indicating that surfactin 3 possibly contains the highest concentration of surfactin molecules (results not shown). The average CV optimum for the surfactin species was between 50 and 80V and that of gramicidin S was found to be stable up to 100V (*Figure 5*).

Gramicidin S-surfactin complexes were subjected to identical ESMS conditions (*Figure 5*) and the results show that the stability of the complex mirrors that of the peptide constituents. Complexes 1-5 had similar stabilities with the highest signal at 60V (*Figure 5*), with complex 2 slightly more stable that the other complexes (results not shown). Complexes 6-13 showed the same stability as complexes 1-5 with highest signal at CV of 60V. However, complex 6 was the most unstable and degraded at CV>40V (results not shown). The highest signal was observed for complex 10 that consists of a combination of five different surfactin variants (Table 2) followed by complex 11 and 9 (composed of 4 different surfactin forms respectively) (results not shown). Analyses of surfactin-gramicidin S complexes indicate that optimal signal was achieved for all the complexes, except complexes 6 and 7, at 60V, indicating that the complexes were more unstable than the individual peptides.

During the cone voltage driven dissociation experiments we observed an initial sharp increase in total ion current up to 60 V for all the complexes, where after it decreased again. This decrease in signal intensity can therefore be reasonably ascribed to gas-phase dissociation rather than fragmentation, at least up to CV of 80V. The variation in cone voltage to study relative stability is problematic given the influence of cone voltage on ionisation. However, CID has also been used to induce a unimolecular decay of selected ions with sufficient internal energy upon collision with a neutral gas. Several previous studies showed that binding energies calculated from CID experiments reflect solution phase binding energies [26, 27]. Therefore, we performed CID on the peptides and complexes to gain more accurate information regarding the relative stabilities of the peptides and complexes (*Figure 6*).

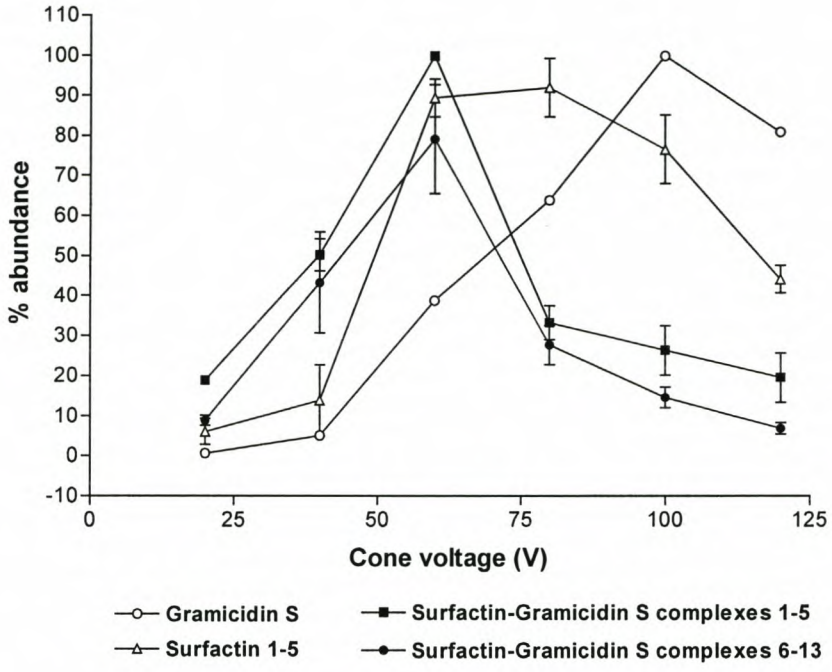

Figure 5 The influence of changing cone voltage on gramicidin S, surfactin (average of surfactin 1-5), and surfactin-gramicidin S complexes (average of complexes 1-5; 6-13).

When the optimal CV and eV setting for maximum signal for each of the analytes were reached, the increase in collision energy (CE) caused dissociation and fragmentation of the analytes comparable to the stability of the analyte (*Figure 6*). The results indicated that all the surfactin forms needed similar CE_{50} (the collision energy to dissipate 50% of the molecular ion specie [11]) with an average of 36.7±1eV. Gramicidin S ions were significantly more stable (CE_{50} = 42.8±1eV) than surfactin ions and this difference can be attributed to the rapid decomposition of the lactone bond (*Figure 6*).

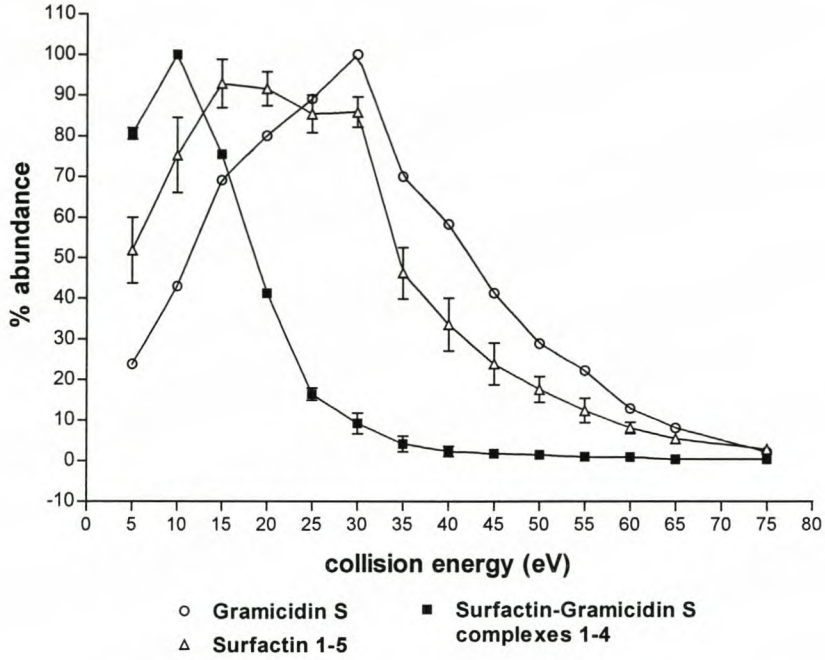

Figure 6 Collisionally induced dissociation of gramicidin S, surfactin 1-5 (average values) and complexes 1-4 (average values from CE =5 –75 eV with cone voltage set to 60V.

CID of gramicidin S-surfactin complexes showed the complexes were much more unstable than the individual peptides with average CE_{50} of 18.7±1eV (*Figure 6*). These results confirmed the lower stability of the complexes detected with varying CV.

5.3.3 Type of interaction between surfactin and gramicidin S

5.3.3.1 Influence of solvent

To investigate the type of interaction, the sample solvent, as well as the carrier solvent, was varied from 10% (v/v) to 90% (v/v) acetonitrile. If electrostatic interactions were involved, a non-polar environment would favour complex formation with a resultant higher complex signal. On the other hand, if the hydrophobic moieties of the peptides were responsible for the interaction, a higher complex signal would be obtained with the polar solvents.

We observed that signal intensities of the surfactin-gramicidin S complexes increases with a decrease in solvent polarity (*Figure 7*). This result suggests the involvement of electrostatic interactions rather than hydrophobic interactions in formation of the surfactin-gramicidin S

complexes.

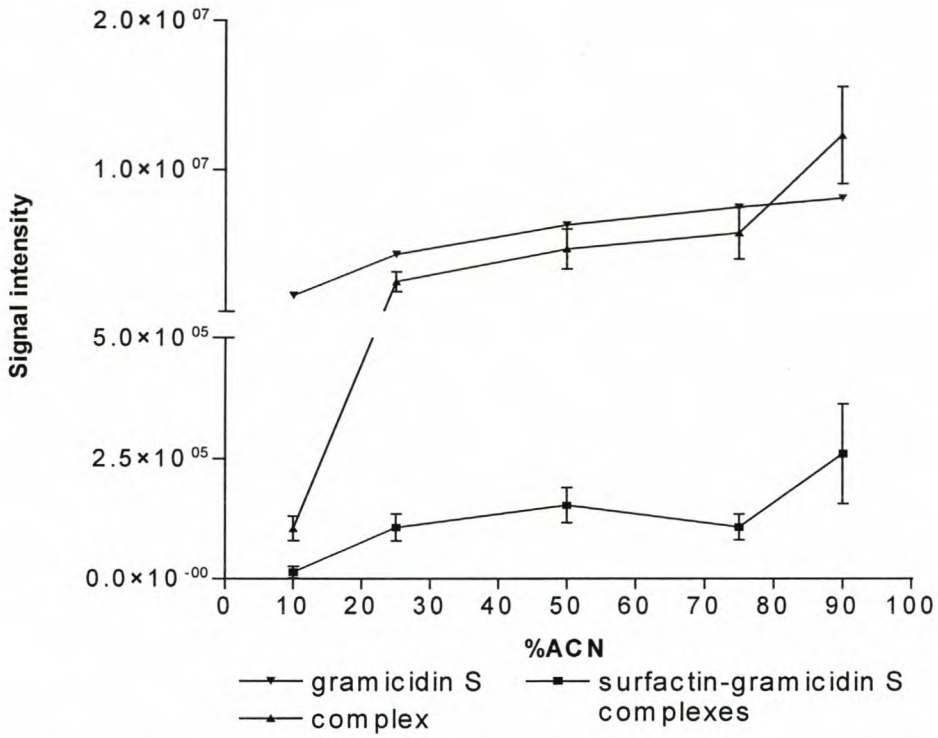

Figure 7 Relationship between change in signal intensity and acetonitrile content of sample/analysis solvent for surfactin (all species), gramicidin S and the surfactin-gramicidin S complexes (total signal). The signal intensity has been calculated in terms of the total molecular ion intensity in the sample with 10% acetonitrile)

It must be noted that solvent polarity is one of the determining factors of ionisation. All the molecular ion signal intensities showed a slight increase up to 50% acetonitrile/water, where after the signal decreased slightly from 50–75% acetonitrile/water. All the free peptide molecular ions showed a slight increase (<10%) in signal intensity at 90% acetonitrile water. In contrast, surfactin-gramicidin S complex signal continuously increased over the solvent polarity range, and showed particularly significant increase of 35% from 80% to 90% acetonitrile. Therefore, we conclude that an apolar environment probably favours surfactin-gramicidin S interaction.

5.3.3.2 Influence of mono- and divalent ions

It was previously shown that the L-Glu_1 and L-Asp_5 residues of surfactin complexes with both mono– and divalent cations, resulting in either partial or complete neutralisation of the acidic residues [18]. Since metal ion binding neutralises the acidic residues, it offers a tool to investigate the possibility of an ionic interaction with these residues through competition

studies.

Addition of NaCl to surfactin-gramicidin S mixtures did not affect the pre-formed complex up to 35.6 mM NaCl (400 times molar excess) (*Figure 8*). The complexes formed with all variants of surfactin. All remained reasonably constant over the concentration range. Similarly gramicidin S signal intensity was unaffected by increasing NaCl concentrations. Signal intensities of various surfactin forms showed minor fluctuations over the NaCl concentration range with a slight drop in intensity at 35.6 mM NaCl. Furthermore, sodiated gramicidin S (data not shown) and sodiated surfactin (*Figure 8*) showed an increase over the concentration range. However, no sodiated surfactin-gramicidin S complexes were detected. A molecular ion with *m/z* corresponding to a sodiated complex (*m/z* = 1101.5) was fragmented and found not to consist of either gramicidin S or surfactin (data not shown). The signal intensities of the various surfactin and surfactin-gramicidin S complexes exhibited the same general trend. Therefore, the individual signal intensities were summed and the data presented as total intensities (*Figure 8*).

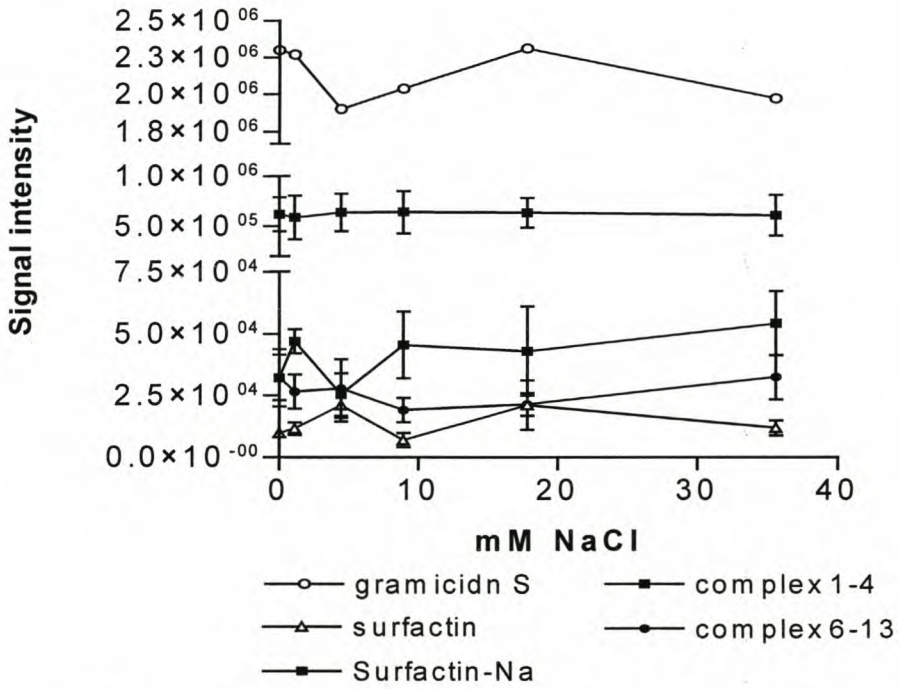

Figure 8 Influence of NaCl addition of to a 1:1 mixture of gramicidin S and surfactin (89 μM each)

The increase in sodiated surfactin and gramicidin S signal (*Figure 9*) intensity over the NaCl concentration range confirmed that sodium-peptide interaction was uninhibited. The results indicate that Na^+ does not interact with surfactin after gramicidin S interaction. Furthermore,

Na^+ does not affect the stability of preformed surfactin-gramicidin S complexes and therefore does not displace gramicidin S from the surfactin molecule.

The influence of sodium interaction with surfactin was investigated by pre-incubating approximately 134 μM surfactin (calculated from variant with highest M_r) with 1.33 mM NaCl (10 times molar excess). The mixture was diluted to approximately 89 μM surfactin and titrated with Gramicidin S over 8.9–89 μM concentration range. Ion chromatograms were recorded to monitor the effect of increasing gramicidin S concentration on signal intensity. The results obtained for the different surfactins and surfactin complexes exhibited the same trends and were therefore added to present the total signal observed (*Figure 9*). Surfactin-gramicidin S signal intensity increased extensively over the gramicidin S concentration range, as did the gramicidin S signal. The free surfactin signal increased at low concentrations of gramicidin S, indicating that some complexes may have formed by displacing sodium and then dissociated to produce free surfactin. The sodiated and free surfactin signal decreased at the highest gramicidin S concentration; an indication that surfactin was chelated in the complexes, regardless if it was bound to sodium or not. However, again no sodiated surfactin-surfactin or sodiated mixed complexes were detected.

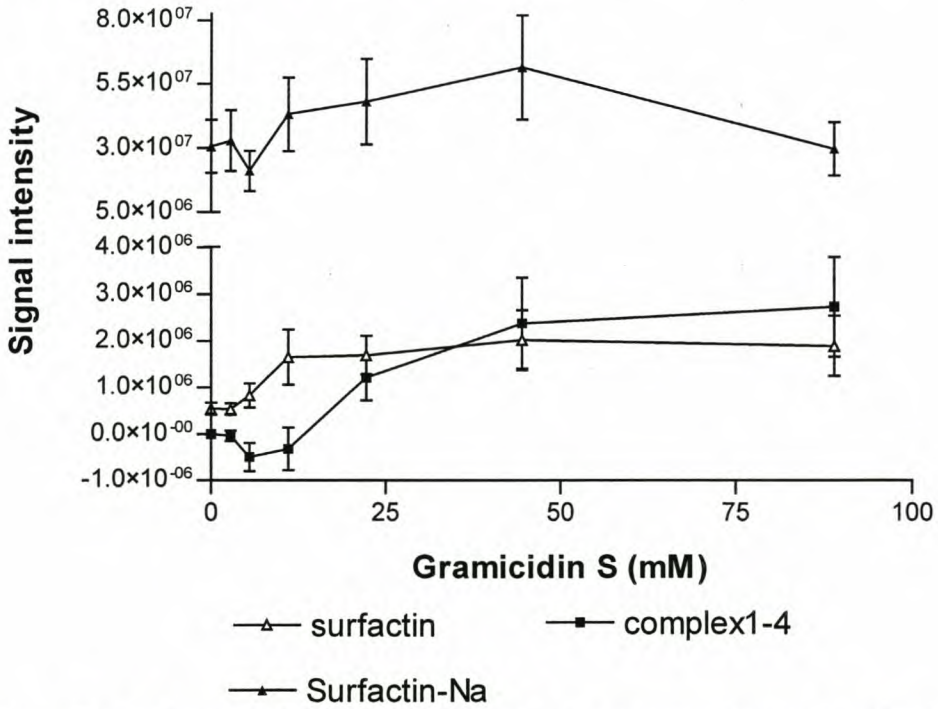

Figure 9 The influence of increasing gramicidin S concentrations on surfactin and gramicidin S-surfactin complexes. Gramicidin S was titrated against Na^+-incubated surfactin.

As with Na^+, the effect of Ca^{2+} on complex formation was investigated through gramicidin S titration of surfactin pre-incubated with $CaCl_2$. In the samples without gramicidin S, we observed calcium-induced surfactin complexes consistent with other reports [17, 18, 25]. These complexes all consisted of surfactin:Ca^{2+} in a 1:1 ratio.

When the calcium-incubated surfactin was the titrated with gramicidin S, the ESMS results indicated, as in the case with sodium-incubated surfactin, that complex formation is uninhibited by surfactin–Ca^{2+} interaction (*Figure 10*). The presence of calciated surfactin may even have benefited the formation of complexes, as the increase of complexes 1-5 was much more pronounced than with the sodium pre-incubation. The signals detected for double surfactin gramicidin S complexes (complexes 6-13) increased over the gramicidin S concentration range, but not as pronounced as the 1:1 complexes. The free surfactin increased over the whole gramicidin S concentration range, probably because of gramicidin-induced dissociation of calciated surfactin.

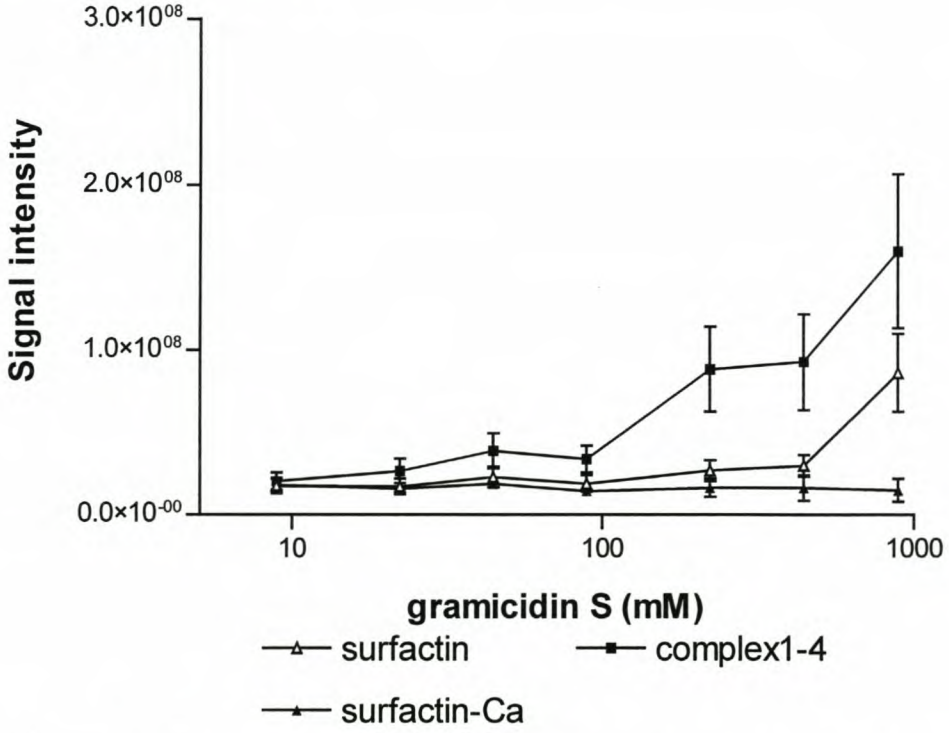

Figure 10 The influence of increasing gramicidin S concentrations on surfactin and gramicidin S-surfactin complexes. Gramicidin S was titrated against Ca^{2+}-incubated surfactin.

In total 33 surfactin complexes, complexed either with Ca^{2+}, surfactin, and/or gramicidin S was clearly detected (results not shown). The addition of gramicidin S generated molecular ions with *m/z* ratios within 1 amu of the surfactin species (see Addendum, Tables 1 and 2 for

complete analysis of the molecular ions detected). Therefore, only eight of the species (four each of $[2S+2Ca+2H]^{2+}$ and $[3S+3Ca+2H]^{2+}$) with distinct and strong signals were selected to represent each group (*Figure 11*). All the selected ions from each group exhibited the same behaviour. Similar to the other ions monitored, the addition of gramicidin S caused an initial increase in signal intensity. Initially, signals of all the calciated surfactin species increased (*Figure 11*). This increase cannot be explained, but interaction with gramicidin may have liberated surfactin from surfaces to which it adsorbed. However, after 22.5 μM of gramicidin S has been added the calciated multi-surfactin complexes showed a sharp decline and the mono-calcium surfactin complex remained relatively constant. The results again indicate that calcium ion interaction does not interfere with complex formation. Furthermore, gramicidin S does interfere with calcium induced surfactin-surfactin complexes.

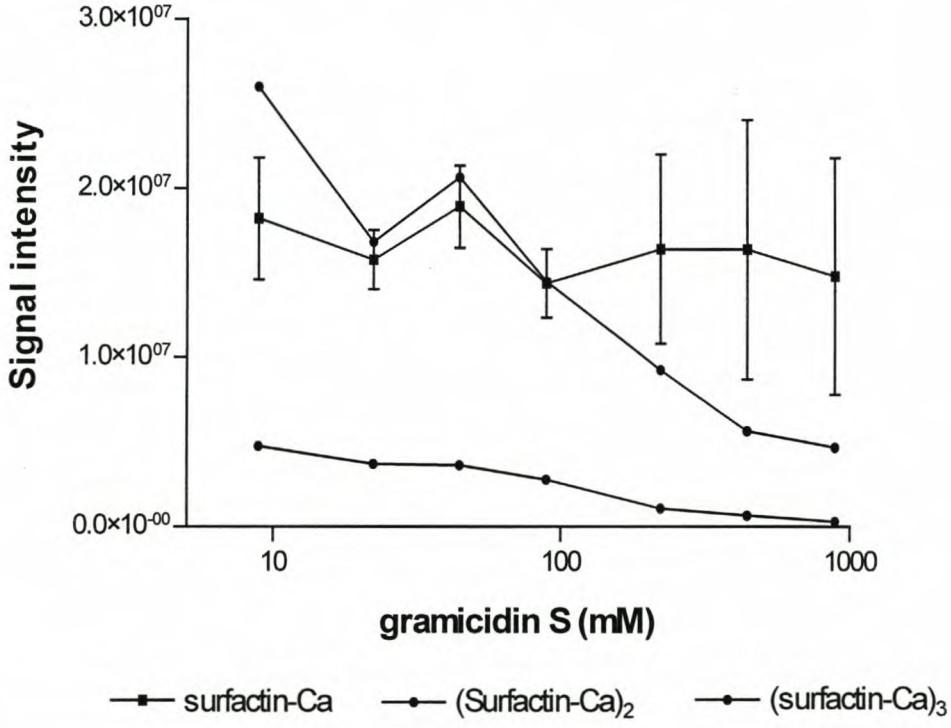

Figure 11 The influence of increasing gramicidin S concentrations on calcium induced surfactin-surfactin complexes

Analyte complexity makes conclusive kinetic deductions difficult. However, the following is noteworthy: 1) surfactin-gramicidin S interaction is not limited to free surfactin –if this was the case the free surfactin would have declined over the gramicidin S concentration range; 2) a dynamic equilibrium seems to exist between surfactin and calcium-associated surfactin as both signals maintained similar trends in signal across the gramicidin S concentration range and 3) gramicidin S dissociates calcium induced surfactin-surfactin complexes. Given that the

surfactin-surfactin complexes only forms upon Ca^{2+}-surfactin interaction, it is conceivable that gramicidin S interferes with Ca^{2+}-surfactin interaction. Furthermore, single surfactin gramicidin S complexes (complexes 1-5) increased up to 225 μM gramicidin S after which the signal remained constant. In contrast, double surfactin-gramicidin S complexes increased continuously. Therefore, it appears that a saturation point exists for single surfactin-gramicidin S complex formation and that a second surfactin molecule is then added to the 1:1 complex.

During both experiments with NaCl and $CaCl_2$ as modifying agents, an initial increase in signal intensity for all molecular ions monitor were observed. Considering the relationship between analyte ionisation and detection in a mass spectrometer, it is possible that the addition of a polar compound, such gramicidin S, may influence the ionisation characteristics of the other compounds in solution. In addition, as proposed above, gramicidin S may liberate surfactin from surfaces to which it may have absorbed. This may explain the initial increase in signal intensity of the monitored species.

5.4 Conclusions

Our results indicate that previously observed antagonism of the antimicrobial activity of gramicidin S by surfactin is likely the result of direct gramicidin S-surfactin interactions. Surfactin interaction with gramicidin S was observed in a 1:1 and a 2:1 ratio. However, if higher complexes exist exclusively as doubly charged ions, these ions could not be detected in this study due to analyses constraints. We found that neither the minor conformational differences reported for surfactin variants nor the acyl chain length had any major influence on the gas phase or the collision stability of surfactin. Minor differences, however, reflected in the stability of the corresponding surfactin-gramicidin S complex. Investigations into the influence of solvent polarity showed that complex formation is favoured by a high organic component in the solvent. This may indicate that the interaction is of an electrostatic nature. Titration of preformed complexes showed that complex formation is probably unaffected by salts such as NaCl. Furthermore, the absence of ion-associated complexes indicates that surfactin-ion interaction is not favourable after surfactin-gramicidin S complex formation. Titration of Ca^{2+} incubated surfactin specifically indicated that complex formation is unaffected or even assisted by surfactin-calcium interaction. Furthermore, we observed a rapid decrease in calcium induced surfactin-surfactin complexes over the gramicidin S

concentration range, indicating that gramicidin S interferes with the surfactin-surfactin interactions. As the Ca^{2+} association drives surfactin-surfactin interactions, it is conceivable that gramicidin S interferes with Ca^{2+} interaction. It may also be possible that the calcium-induced conformation of surfactin will induce binding of gramicidin S in exchange for the Ca^{2+}. It is unlikely that the mechanism of this interference is a direct competition for the glutamic acid carboxyl groups by the ornitines of gramicidin S. It has been shown that calcium associates with the carboxyl groups [17, 18, 19]. However, the significance of peptide ring β-turns in alkali metal ion chelating has previously been demonstrated for the analogues peptide, iturin A [28, 29]. Therefore, we propose that the ornithine residues of gramicidin S interact with surfactin in one or both of the β-turns. Furthermore, this interaction may result in a conformational change in the spatial orientation of the acidic residues of surfactin in such a way that surfactin-calcium ion interaction is no longer possible.

5.5 References

1. Leonard P., Hearty S., Brennan J., Dunne L., Quinn J., Chakraborty T., O'Kennedy R. (2003) *Enzyme and Microbial Technology*, **32,** 3 –13

2. Wider G. (2000) *BioTechniques*, 29, 1278 –1294

3. Cooper A. (1999) *Curr. Opin Chem. Biol.*, **3,** 557–563

4. Weber P. C. & Salemme F. R. (2003) *Current Opinion in Structural Biology*, **13**, 115 –121

5. Hensley P., *Structure*, (1996) **4**, 367 –73

6. Smith D. L., Deng, Y., Zhang Z. (1997) *J. Mass Spectrom.*, **32**, 135 –146

7. Siuzdak G. (1994) *Proc. Natl. Acad. Sci. U.S.A.*, **91**, 11290 –7

8. Brodbelt J. S. (2000) *Int. J. Mass Spectrom.*, **200**, 57 –69

9. Fändrich M., Tito M. A., Leroux M. R., Rostom A. A., Hartle F. U., Dobson C. M., Robinson C. V. (2000) *Proc. Natl. Acad. Sci. U.S.A.* **97**, 14151 –5

10. Lim H-K., Hsieh Y. L., Ganem B., Henion J. (1998) *J. Mass Spectrom.* **30**, 708 –714

11. Daniel M. J., Fries D. S., Rajagopalan S., Wendt S., Zenobi R., (2002) *Int. J. Mass Spectrom.*, **216**, 1 –27

12. Marrone T. J. & Kenneth M. M. Jr. (1995) *J. Am. Chem Soc,* **117,** 779 –91

13. Franklin T. J. & Snow G. A., *Biochemistry of Antimicrobial action*, 3rd Ed, Chapman and Hall: London, 1981; pp 67 –72

14. Wang K., & Gorkel G. W. (1996) *Pure Appl. Chem*, **68**, 1267 –1272

15. Gross D. S. & Williams E. R. (1996) *J. Am. Chem. Soc.*, **118**, 202 –204

16. Pankiewicz R., Gurzkowa A., Brzezinski B., Zundel G., Bartl F. (2002) *Journal of Molecular Structure*, **xx**, 1 –8

17. Maget-Dana R. & Ptak M. (1992) *J. Colloid. Interface Sci.*, **153**, 285 –291

18. Thimon L., Peypoux F., Wallach J., Michel G. (1993) *Colloids Surfaces B: Biointerfaces* **1**, 57 –62

19. Sheppard J.D., Jumarie C., Cooper D.G., Laprade R. (1991) *Biochem Biophys. Acta* **1064**, 13 –23

20. Stern A., Gibbons W. A., Craig L. C. (1968) *Proc. Natl. Acad. Sci. U.S.A* **61**, 734 –741

21. Hodgekin D. C., & Oughton B. M. (1957) *Biochem. J.* **65**, 752 –756

22. Ovchinikov Y. V. & Ivanov V.T. (1975) *Tetrahedron* **31**, 2177 –2209

23. Kondejewski L. H., Farmer S. W., Wishart D. S., Hancock R. E. W., Hodges R. S. (1996) *J. Biol. Chem.* **271**, 25261 –25268

24. Bonmatin J. M., Labbé H., Ptak M. (1994) *Biopolymers* **34**, 975 –986

25. Osman M., Høiland H., Holmson H., Ishigami Y. (1998) *J. Peptide Sci.* **4**, 449 –458

26. Penn S.G., He F., Green M. K., Lebrilla C. B., (1997) *J. Am. Soc. Mass Spectrom.*, 8, 244 –252

27. Jørgensen T. J. D., Delforge D., Remacle J., Bojensen G., Roepstorff P. (1999) *Int. J. Mass Spectrom.*, **188**, 63 –85

28. Maget-Dana R., Ptak M., Peypoux F., Michel G (1992) *J. Colloid. Interface Sci.*, **149**, 174 –183

29. Rautenbach M., Swart P., van der Merwe M. J. (2000) *Bioorg. Med. Chem.*, **8**, 2539 –2548

5.6 Addendum

Table 1 Molecular ions of surfactin and surfactin-calcium complexes detected during ESMS analysis of a mixture of gramicidin S and surfactin.

Complex	Specie	M_r	*m/z*	Detected *m/z*
[S1+Ca]2+	[S1+Ca]2+	1034.3	517.1	517.1
[S2+Ca]2+	[S2+Ca]2+	1048.3	524.1	524.1
[S3+Ca]2+	[S3+Ca]2+	1062.3	531.2	531.0
[S4+Ca]2+	[S4+Ca]2+	1076.3	538.2	538.0
[S5+Ca]2+	[S5+Ca]2+	1090.4	545.2	545.2
S1	[S1]+	994.3	994.3	994.7
S2	[S2]+	1008.3	1008.3	1008.6
S3	[S3]+	1022.3	1022.3	1022.7
S4	[S4]+	1036.4	1036.4	1036.7
S5	[S5]+	1050.4	1050.4	1050.7*
[S1+Ca]+	[S1+Ca+H]+	1034.3	1035.3	1035.5
[S2+Ca]+	[S2+Ca+H]2+	1048.3	1049.3	1049.1
[S3+Ca]+	[S3+Ca+H]2+	1062.3	1063.3	1063.2
[S4+Ca]+	[S4+Ca+H]2+	1076.4	1077.4	1077.4*
[S5+Ca]+	[S5+Ca+H]2+	1090.4	1091.4	1091.3*

*Molecular ions detected from spectrum list because the ion signal was obscured by other signals in the spectrum.

Table 2 Molecular ions of double surfactin and surfactin-calcium complexes detected during ESMS analysis of a mixture of gramicidin S and surfactin. The shaded rows indicate the molecular ions that are indistinguishable from gramicidin S-surfactin complexes. Surfactin are denoted as S.

Complex	Specie	M_r	*m/z*	Detected *m/z*
SS1	[2S1+2Ca+2H]2+	2070.6	1035.3	1035.0
SS2	[S1+S2+2Ca+2H]2+	2084.6	1042.3	1042.0
SS3	[2S2+2Ca+2H]2+; [S1+S3+3Ca+2H]2+	2098.6	1049.3	1049.1
SS4	[S1+S4+2Ca+2H]2+; [S2+S3+2Ca+2H]2+	2112.6	1056.3	1055.8
SS5	[3S1+3Ca+2H]2+	3102.8	1552.4	1552.3
SS6	[2S1+S2+3Ca+2H]2+	3116.8	1559.4	1559.0
SS7	[2S2+S1+2Ca+2H]2+; [2S1+S3+3Ca+2H]2+	3130.9	1566.4	1566.5
SS8	[2S2+S3+3Ca+2H]2+; [S1+S2+S4+2Ca+2H]2+; [2S1+S5+3Ca+2H]2+; [2S3+S1+3Ca+2H]2+	3158.8	1580.4	1580.8
SS9	[2S2+S4+3Ca]2+; [2S3+S5+3Ca]2+; [S1+S3+S4+3Ca]2+	3172.9	1587.5	1587.3
SS10	[2S2+S5+3Ca+2H]2+; [2S4+S1+3Ca+2H2+; [3S3+3Ca+2H]2+; [S2+S3+S4+3Ca+2H]2+	3186.9	1594.5	1594.0
SS11	[2S3+S4+3Ca+2H]2+; [S4+S2+3Ca+2H]2+; [S2+S3+S5+3Ca+2H]2+	3201.0	1601.5	1600.9
SS12	[2S4+S3+3Ca+2H]2+; [2S1+S5+3Ca+2H]2+; [2S5+S1+3Ca+2H]2+	3215.0	1608.5	1609.0
SS13	[2S5+S2+3Ca+2H]2+; [S3+S4+S5+3Ca+2H]2+; [3S4+3Ca+2H]2+	3229.0	1615.5	1615.0

Chapter 6

Preliminary investigation into the interaction of iturin A and two synthetic linear analogues with gramicidin S

6.1 Introduction

In Chapters 4 and 5 it was shown that surfactin antagonises the antimicrobial action of gramicidin S in a dose-dependent manner. Furthermore, this antagonism was shown to possibly be the result of direct gramicidin S-surfactin interactions, of which the latter is independent of surfactin-metal ion interactions [1, 2, 3, 4]. The lack of antagonism by surfactin on non-related peptides vancomycin and ESF1-SAGR indicates that a degree of specificity exists in the peptide-peptide interaction.

Afore mentioned results (Chapter 4 and 5) prompted the decision to investigate some of the other *Bacillus subtilis* peptides. Surfactin is co-produced with iturin A in some *B. subtilis* strains. In addition to a pronounced synergistic effect of surfactin on iturin A biological activity [5, 6], surfactin shares some structural similarities with the iturins. Both surfactin and the iturins are cyclic lipopeptides with fatty acid chain length of $C_{13\text{-}16}$ (surfactin) [7, 8] and $C_{14\text{-}16}$ (iturins) [9, 10, 11]. The inclusion of D-amino acids in the primary structures of both peptides facilitates the folding of the peptide backbone to form β-turns. The iturins have two β turns [12, 13] where surfactin has only one [14]. In both cases the polar residues are orientated toward one side of the molecule and the fatty acids toward to other side. This arrangement confers a pronounced amphipatic character on the peptides. Unlike surfactin with two acidic residues (Glu and Asp) [15] polar component of iturin A consists of three Asn residues at positions 2, 4, and 7, and a Gln at position 5 [9, 10, 11]. This difference resulted in surfactin having true surfactant ability but no antifungal activity [16] whereas iturin A possesses pronounced antifungal activity but less surfactant ability [17] In both cases the molecular orientation allows for interaction with both an aqueous phase and apolar environments. Iturin C on the other hand possesses no antimicrobial activity. This complete loss of biological activity can only be attributed to the mutation if Asn_2 to Asp_2 [9].

11]. This difference resulted in surfactin having true surfactant ability but no antifungal activity [16] whereas iturin A possesses pronounced antifungal activity but less surfactant ability [17] In both cases the molecular orientation allows for interaction with both an aqueous phase and apolar environments. Iturin C on the other hand possesses no antimicrobial activity. This complete loss of biological activity can only be attributed to the mutation if Asn_2 to Asp_2 [9].

These similarities with surfactin made iturin A a prime choice to extend this study. A number of previous studies have demonstrated that peptide analogues can be used to elucidate the structural characteristics that are important in peptide mechanism of action [9-18]. The syntheses of both iturin A and C are accomplished through the cyclisation of a linear precursor and this afforded the opportunity to investigate the influence of both primary and secondary structure on peptide-peptide interaction.

In this chapter the possibility that structural similarity between iturin A and surfactin may lead to gramicidin S antagonism is explored using iturin A and the linear analogues, 8-Beta and 8-$Beta_c$ (see Chapter 2). Due to limited amount and impurity of cyclic 8-$Beta_c$ (synthetic iturin C), only linear 8-$Beta_c$ was investigated, while both iturin A and its linear analogue 8-Beta were evaluated. Biological experiments, with gramicidin S and *Micrococcus luteus* as target cell, were performed with the linear analogues and compared to iturin A. The interaction of these lipopeptides with gramicidin S biological was explored with mass spectrometry.

6.2 Materials

Tryptone soy broth (TSB) was supplied by Biolab Diagnostics (Midrand, RSA), the components for Luria Broth (LB), NaCl, tryptone and yeast extract were from Saarchem (Midrand, RSA), Unipath (Hampshire, England) and Difco Laboratories (Detroit, USA)

broth (LB) and sub-cultured in tryptone soy broth (TSB). Broth microdilution assays [28] were performed with 5 X 10^5 CFU/mL suspensions and inhibition measured spectrophotometrically after 24 hours at 620 nm on a Titertek Multiscan Plus Mk II (Flow Laboratories) microtiter plate reader. All microtiter plates were blocked with 0.5% casein in Dulbeco's Phosphate Buffered Saline (PBS) [29] and sterilised under UV light before use.

6.3.2 Mass spectrometry

ESMS was performed in positive mode with a Q-TOF Ultima® mass spectrometer using an electrospray ionisation source. All samples were prepared in 50% acetonitrile/water at 20 μM before being injected into the mass spectrometer using an Agilent 1100 HPLC system at 50 μL/minute acetonitrile with a final injection volume of 10 μL. A capillary voltage of 3.2 kV was applied with a source temperature of 80°C. The cone voltage was set at 60 V.

6.3.3 Data analysis

Percentage inhibition was calculated by first expressing the growth observed with the test substance present as a percentage of the total growth observed in the control wells without test substance (i.e. (growth observed with test substance/growth in control well without test substance) X 100). This value was subtracted from 100 to render percentage inhibition. Data were analysed using GraphPad Prism 3.0 (GraphPad Software Incorporated) for curve fits and statistical analyses. Sigmoidal dose response curves (variable slope with no weighing of data) were fitted to all assay results. Of the eight or more determinations per concentration, only the mean was considered for fitting the curve.

Statistical analyses of data performed with GraphPad Prism include, the absolute sum of squares, and standard error of the mean. The 50% inhibitory concentration was calculated from the X-value halfway between the top and bottom plateau of the log dose-response curve [30].

6.4 Results and discussion

6.4.1 Influence of the iturins on M. Luteus *activity of gramicidin S*

As observed for surfactin, iturin A also antagonised the biological activity of gramicidin S (*Figure 1*). The antagonism of gramicidin S by iturin A was, however, much less pronounced than that of surfactin. The antagonism profile is complicated by some antibiotic activity of iturin A at the concentrations used. For example, 50% inhibition of *M. luteus* growth was found at 30 μM iturin A, whereas no activity was detected at lower concentrations. Iturin A caused a 100% increase in the IC_{50} value of gramicidin S 30 μM, 10 μM, and 5 μM iturin A (*Figures 1* and *2*).

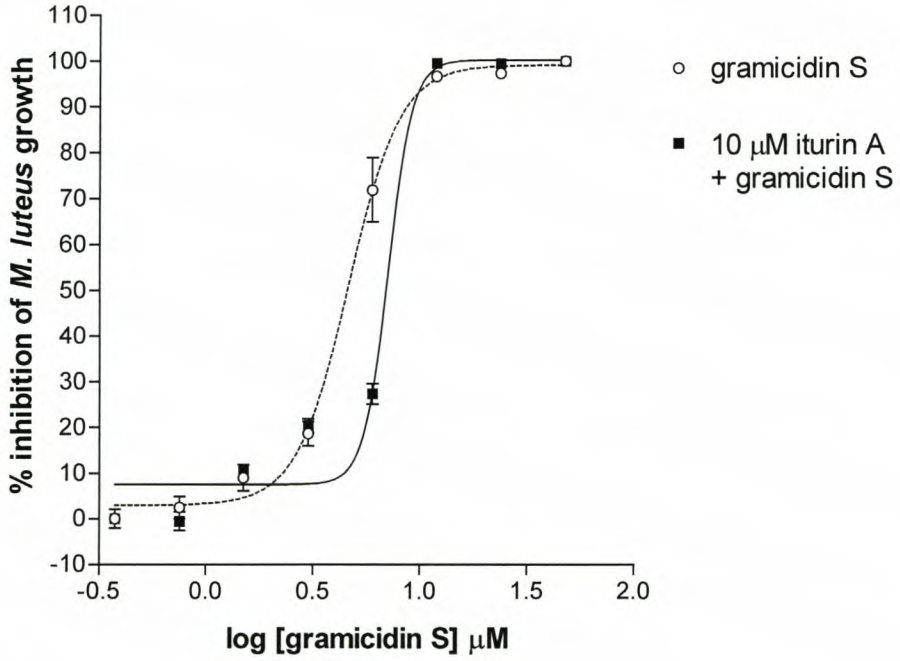

Figure 1 The influence of 10 μM iturin A on gramicidin S activity. The standard error of the mean (SEM) is shown for each data point, with eight determinations per data point, $r^2 > 0.995$ was found for both curves. Results obtained from two independent experiments in quadruplicate.

Gramicidin S activity was retained at 2.5 μM iturin A. Synergism between gramicidin S was not observed at iturin A concentrations below the IC_{50} of gramicidin S, as found with surfactin in Chapter 4. This lack of synergism might be related to the difference in surfactant activity with surfactin being the better surfactant [31, 32] resulting a more pronounced membrane destabilisation of lower concentrations.

An exponential relationship was found between antagonism of gramicidin S activity and iturin A concentration. The influence of iturin A on the biological activity of gramicidin S at concentrations close to the IC_{50} (6 μM; IC_{50} = 4.9 μM) (*Figure 2*) is most pronounced over the concentration range 2.5 –5 μM with a dramatic decrease at higher concentrations

Comparing this result to the results obtained with surfactin (Chapter 4; *Figure 1*), which showed an almost linear increase in antagonism with *P. corylophilium* over the entire concentration range, it is evident that the dynamics of peptide-peptide interaction at cellular level is markedly different. It appears that the antagonism observed is counterbalanced by the activity of iturin A towards this organism resulting in a decrease in the effectivity of iturin A induced antagonism with increasing iturin A concentrations. Furthermore, it is clear that gramicidin S also antagonises the antibiotic activity of iturin A. Less than 19% inhibition was found at 30 μM iturin A, when 6 μM gramicidin S was present. If both peptides were fully active at these concentrations, total inhibition of *M. luteus* growth would be expected; therefore more than 80% activity was lost.

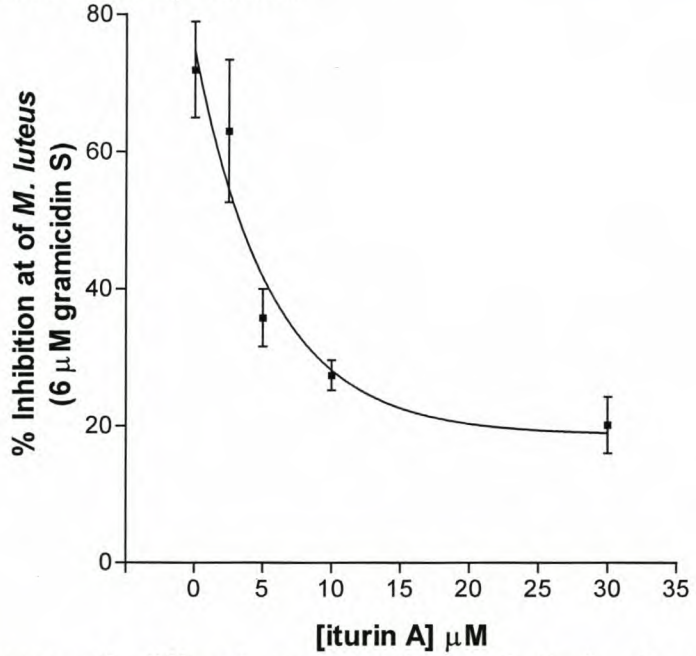

Figure 2 Influence of different concentrations of iturin A on gramicidin S at approximately its IC_{50} concentration. In addition to the progressive loss of gramicidin S activity with increasing iturin A concentrations approximately 60% of iturin A activity was lost at 30 μM iturin A.

6.4.2 Influence of linear analogues on M. Luteus *activity of gramicidin S*

It was found that 8-Beta have little on no activity on *M. luteus* after 18 hours, similar to previously obtained results for 8-Beta I and II [33]. No effect on the activity of gramicidin S

was found if 8-Beta was added of a brad concentration range (2.5-30 μM) (*Figure 3*). It is therefore clear that the cyclisation of 8-Beta is essential for antagonism. The addition of 8-Beta$_c$, over the same concentration range as iturin A, however, did result in a subtle change in the dose-response profile of gramicidin S, especially at the high concentrations of gramicidin S (*Figure 3*). This subtle difference indicated that some antagonism of gramicidin S activity does occur at the highest peptide concentration used.

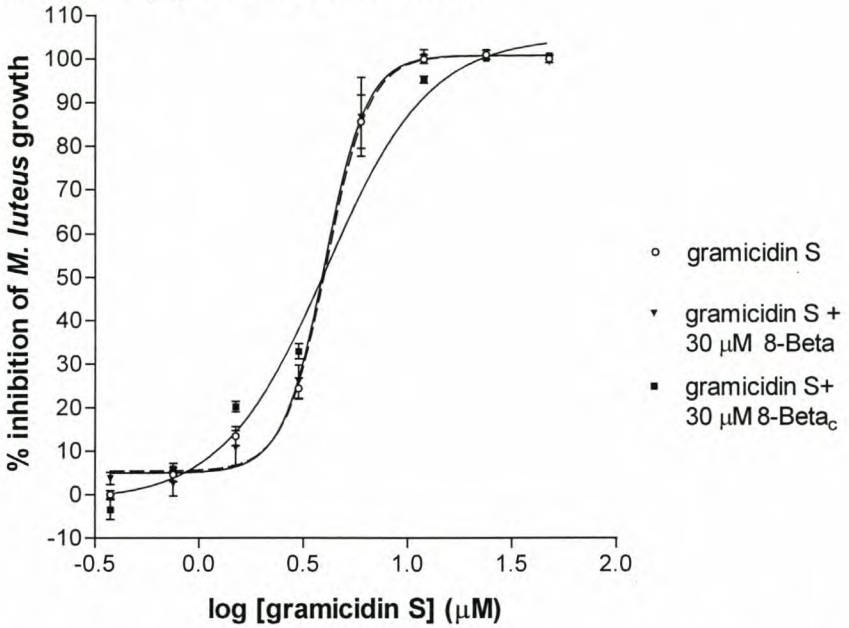

Figure 3 Influence of 30 μM linear analogues on the biological activity of gramicidin S. SEM = ±1.1 μM (8 Beta^c), 1.0 μM (8 Beta) and 1.0 μM (gramicidin S) with r^2 = 0.992, 0.998 and 0.995 respectively, a minimum of 8 determination per data point were taken. Results obtained from four independent experiments in quadruplicate.

6.4.3 Mass spectrometry analysis of mixtures of gramicidin S and iturins

The mass spectrum of gramicidin S (obtained from Sigma) showed, in addition to the singly and doubly charged species (with *m/z* = 1141.24 and 570.72 respectively), the presence of two isotopic species of gramicidin S with *m/z* = 1142.28 and 1143.38 respectively (*Figure 4*A). A fragmentation ion (b_8) with *m/z* = 881.34 was also detected. The doubly charged ion of the isotope with *m/z* = 1142.28 were detected at 572.16. Three known forms of iturin namely, iturin A_2 (*m/z* = 1043.75), iturin A with C_{15} β-amino fatty acid (iturin A C_{15}; *m/z* =1057.76), and iturin A_L (*m/z* = 1071.71), were detected (*Figure 4*B) in the commercial sample from Sigma (only the major isotope *m/z* values are given). In addition, sodiated and doubly charged species were observed.

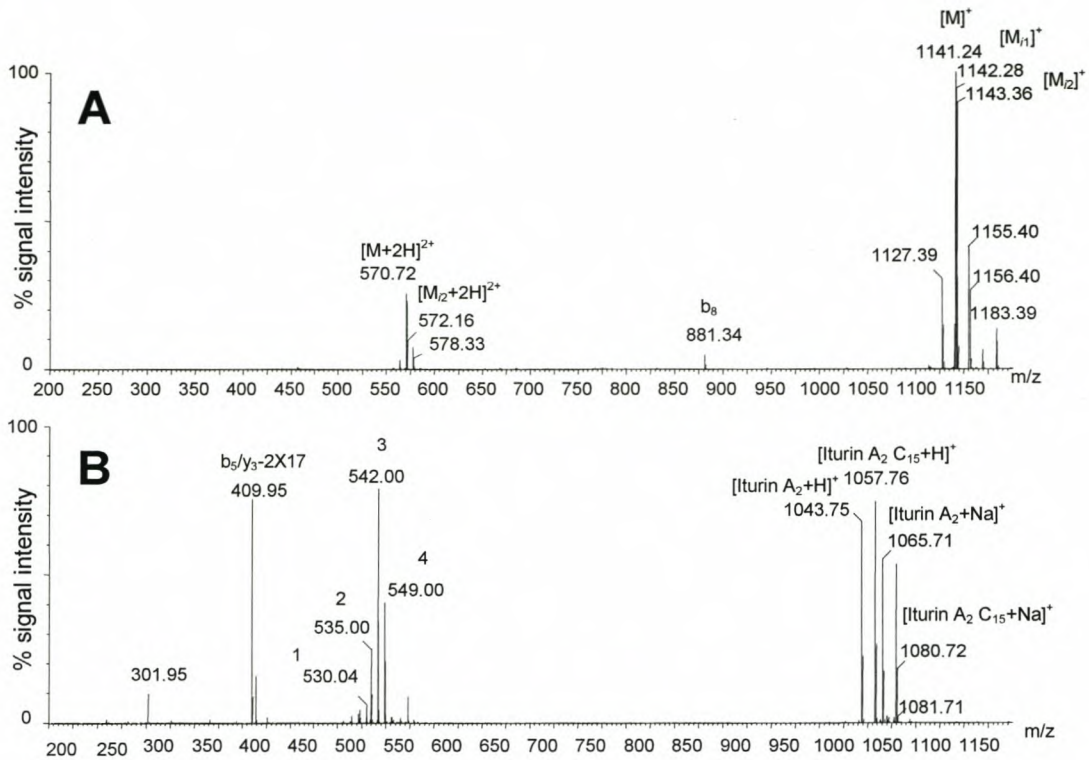

Figure 4 ESMS-TOF mass spectra of gramicidin S (A) and iturin A (B) obtained from Sigma. The gramicidin S isotope signals are denote M, M_{i1}, and M_{i2} respectively. The doubly charged ions were identified as: 1) iturin A C_{15}, 2) iturin A_2+Na, 3) iturin A C_{15}+Na and 4) iturin A_L+Na.

As with surfactin, all variants of iturin A formed complexes with gramicidin S (*Figure 5*) with *m/z* = 1092.90, 1099.90 and 1106.92. The isotope variation of gramicidin S was reflected in the formed complexes rendering complexes with C, C+0.5amu C+1amu, and C+2amu (C=complex, amu=atomic mass units). The signal intensity of the complexes was, however, much lower than that found for surfactin-gramicidin S.

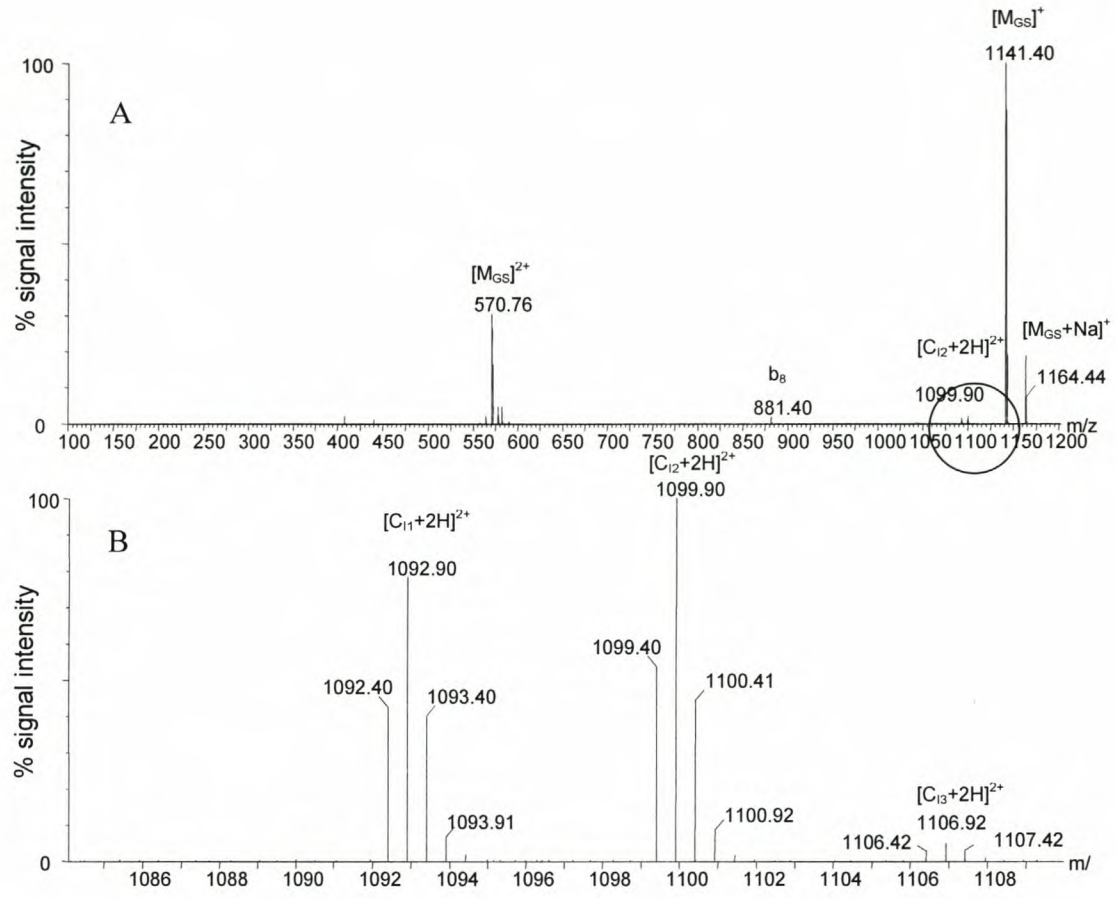

Figure 6 ESMS-TOF mass spectra of complexes between gramicidin S and iturin A. The encircled region in A is expanded in B. The different complexes are denoted as C_{I1} –C_{I3} with I1, I2 and I3 as iturin A_2, iturin A C15 and iturin A_L respectively. The annotated peaks are those of the dominant isotope with the other isotopes differing with increments 0.5 amu from the dominant signal.

Gramicidin S was mixed with the linear peptides 8-Beta and 8-Beta$_c$ in approximately a 1:1 molar mixture and subjected to mass spectrometric analysis. Mass spectra of the mixtures on the Waters Q-TOF Ultima mass spectrometer did not reveal any complex species with gramicidin S for either 8-Beta$_c$ (*Figure 7*A) or 8-Beta (*Figure 7*B), with the correct *m/z* ratios (*m/z* = 1102.59 for complexes of gramicidin S with 8-Beta$_c$ and 1102.10 for 8-Beta), under similar analysis conditions used for iturin A. Since the analysis conditions resulted in the excessive fragmentation of gramicidin S in presence of 8-Beta or 8-Beta$_c$ the lowest energy conditions possible with the ESMS-TOF (CV of 35V, collision energy 10V), was used. Previously we also found complex formation between the linear analogues and gramicidin S using the Micromass mass spectrometer.

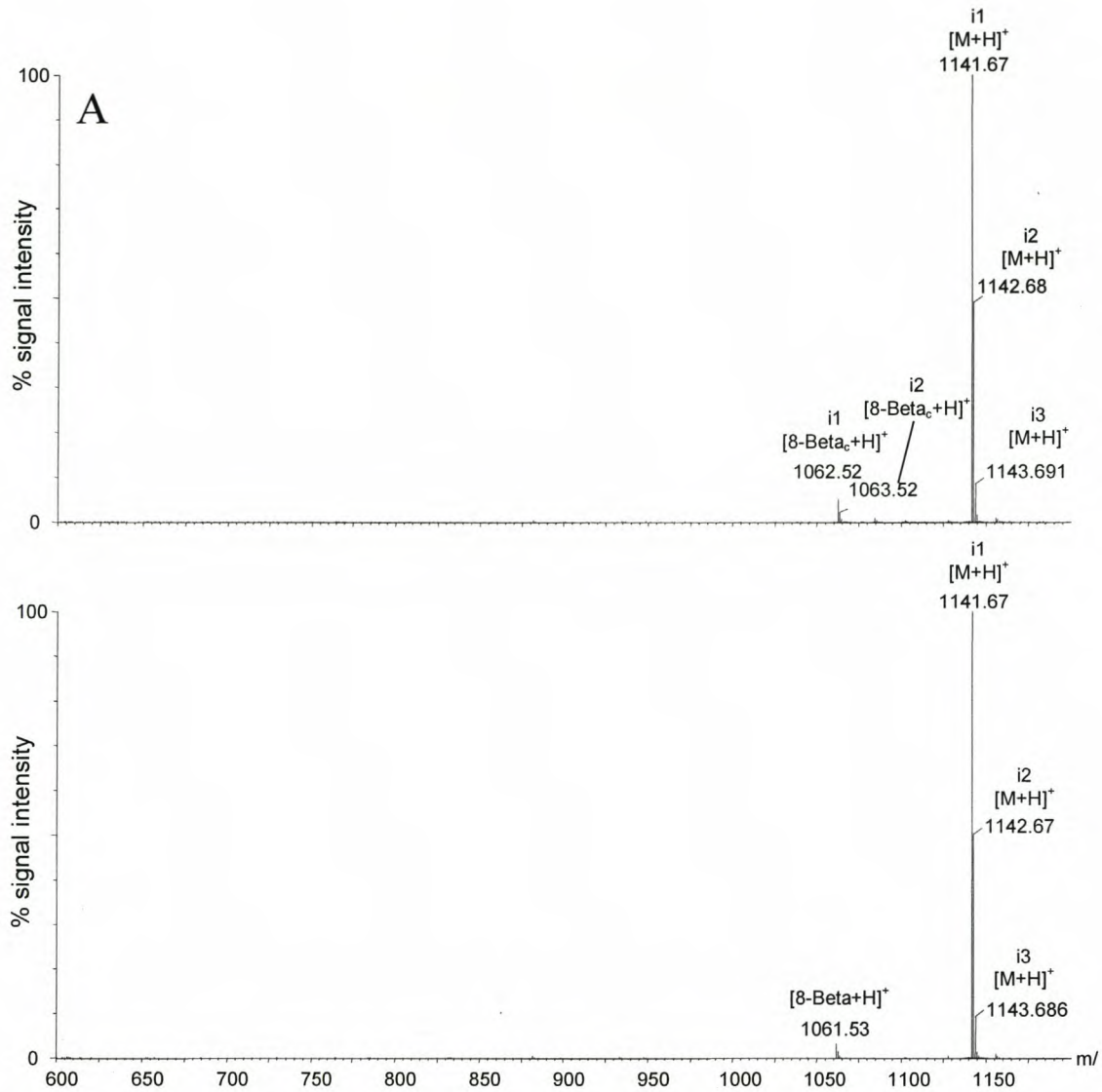

Figure 7 Mass spectrum of gramicidin S mixed with 8-Beta$_c$ (A) and 8-Beta and gramicidin S (B). The isotope peaks are denoted *i*1-3.

6.5 Conclusions

As we found with surfactin, the structurally similar iturin A also influenced the biological activity of gramicidin S. However, the interpretation of the antagonism results was more complex, because of the activity exhibited by iturin A against the target cell. Unlike surfactin, a dose-dependent antagonism of gramicidin S biological activity was not observed with the lowest concentration iturin causing maximal antagonism. In addition, no synergism was observed between iturin A and gramicidin S, but a mutual antagonism of biological activity exists between iturin A and gramicidin S. The combination of gramicidin S (6 μM) and iturin A at 30 μM resulted in an >80% decrease in iturin A activity. Of the two linear analogues tested only 8-Beta$_c$ caused a change in the dose-response profile indicating that some

antagonism of gramicidin S activity did occur. It is thus possible that as with iturin A and 8-Beta, that cyclisation of 8-Beta$_c$ to form iturin C, may lead to pronounced antagonism of gramicidin S, but this remains to be tested.

Previously obtained results indicated that at least one of the β-turns in iturin A_2 [34, 35] are conserved in the linear 8-Beta [33] and this is also possibly true for 8-Beta$_c$. We postulated in Chapter 5 that a β-turn of surfactin may be involved in the interaction with gramicidin S and surfactin. If the same argument holds true for the interaction of iturin A (and iturin C) with gramicidin S, three possible scenarios exist to explain the lack of complex formation between gramicidin S and the linear analogues: a) the conserved β-turn in 8-Beta/8-Beta$_c$ is not as stable as one in the cyclic peptide; b) interaction occurs at the disrupted β-turn or c) both β-turns are involved in stable complex formation. When comparing iturin A and surfactin that dramatically influenced the biological activity of gramicidin S with the linear analogues 8-Beta and 8-Beta$_c$, it is clear that cyclic peptides formed complexes with gramicidin S that readily detectable by ESMS.

These findings support our original hypothesis in Chapters 4 and 5 that antagonism of the antimicrobial action of gramicidin S is related to stable, inactive complex formation with the "shield" lipopeptide, surfactin. Furthermore, the interaction between the peptides is dependent on the conserved secondary structure of the *B. subtilis* peptides as illustrated by the inability of 8-Beta and the limited ability 8 Beta$_c$ to antagonise the antimicrobial action of gramicidin S. Irrespective of the mechanism of interaction, it is clear that stable complex formation is dependent on a highly conserved secondary structure.

These preliminary findings indicate that the iturins may also be "shield" lipopeptides. The apparent correlation between structural characteristics and antagonism indicates that the other *B. subtilis* lipopeptides such as mycosubtilin may also form inactive complexes with gramicidin S. Future studies should be directed at the investigation of these peptides to establish the generality of inactive complex formation as defence mechanism. Furthermore, it underscores the importance of the development of an optimised synthesis protocol for the production of iturin C in order to investigate this peptides biological role. These results, in combination with the results obtained with surfactin, illustrate the complexity of both the microbial environment and the interaction between species and warrants further multi-disciplinary investigation.

6.6 References

1. Timon L., Peypoux F., Wallach J., Michel J. (1993) *Colloids Surf. B.* **1**:57 –62
2. Maget-Dana R. & Ptak M. (1992) *J. Colloid. Interface Sci.,* **153**, 285 –291
3. Sheppard J.D., Jumarie C., Cooper D.G., Laprade R., (1991) *Biochim Biophys Acta*, **1064**, 13-23
4. Osman M., Hoiland H., Holmson H., Ishigami Y. (1998) *J. Peptide Sci.,* **4**, 449 – 458
5. Ohno A., Ano T., Shoda M. (1995) *J. Ferment. Bioeng.,* **80**, 517 –519
6. Maget-Dana R., Thimon L., Peypoux F. Ptak M. (1992) *Biochimie,* **74**, 1047 – 1051
7. Kakinuma A., Sugino H., Isono M., Tamura G., Arima K. (1969) *Agric Biol Chem.* **33**, 971–972
8. Besson F., Tenoux I., Hourdou M.L., Michel G., (1992) Biochim Biophys Acta, 1123, 51-8
9. Maget-Dana R. & Peypoux F. (1994) *Toxicology,* **87**, 151 –174
10. Winkelmann G., Allgaier H., Lupp R., Jung G. (1983) *J. Antibiotics* **36**, 1451 – 1457
11. Peypoux F., Besson F., Michel G., Delcambe L., Das B. C. (1978) *Tetrahedron,* **34**, 1147 –1152
12. Garbay-Jaureguiberry C., Roques B. P., Delcambe L., Peypoux F., Michel M. (1978) *FEBS Lett.* **93**, 151 –156
13. Bonmatin J. M., Labbé H., Ptak M. (1994) *Biopolymers* **34**, 975 –986
14. Ferré G., Besson F., Buchet R. (1997) *Spectrochemica Acta Part A.*, 53, 632 – 635
15. Kakinuma A., Sugino H., Isono M., Tamura G., Arima K. (1969) *Agric Biol Chem.* **33**, 973–976
16. Peypoux F., Bonmatin J. M., Wallach J. (1999) *Appl Microbiol Biotechnol.,* **51**, 553 –563
17. Klich M. A., Arthur K. S., Lax A. R., Bland J. M. (1994) *Mycopathologia*, **127**, 123 –127
18. Kondejewski L. H., Farmer S. W., Wishart D. S., Hancock R. E. W., Hodges R. S. (1996) *J. Biol. Chem.,* **271**, 25261 –25268
19. Setsuko A., Nishikawa H., Takiguchi H., Lee S., Sugihara G. (1993) *Biochim Biophys Acta,* **1147**, 42–49
20. Jelokhani-Niaraki M., Kondejewski L. H., Farmer S. W., Hancock R. E. W., Kay C. M., Hodges R. S. (2000) *Biochem. J.,* **349**, 747 –755
21. Ovchinikov Y. V. & Ivanov V.T. (1975) *Tetrahedron* **31**, 2177 –2209

22. McInnes C., Kondejewski L. H., Hodges R. S, Sykes B. D. (2000) *J. Biol. Chem.*, **275**, 14287 –14294

23. Gibbs A. C., Bjorndahl T. C., Hodges R. S., Wishart D. S. (2002) *J. Am. Chem. Soc.*, **124**, 1203 –1213

24. Besson F., Peypoux F., Quentin M. J, Michel G. (1984) *J. Antibiotics,* **37**, 172 – 177

25. Rautenbach M., Swart P., van der Merwe M. J. (2000) *Bioorg. Med. Chem.*, **8**, 2539 –2548

26. Rautenbach M., Swart P., van der Merwe M. J. (2001) *J. Am. Mass Spectrom.*, **12**, 505 –516

27. Morikawa M., Hirate Y., Imanaka T., (2000) *Biochim. Biophys. Acta*, **1488**, 211 –218

28. Lehrer, R.I., Rosenman, M., Harwig, S.S.S.L., Jackson, R., Eisenhauer, P. (1991) *J. Immunol. Methods*, **137**, 167 –173

29. Dulbeco, R., Vogt, M., (1954) *J. Exp. Med.* **98,** 67

30. Du Toit, E.A. and Rautenbach, M. (2000) *J. Microbiol. Methods*, **1**, 159 –165

31. Thimon L., Peypoux F., Maget-Dana R., Michel G. (1992) *J. Am. Oil. Chem Soc.,* **62**, 92 –93

32. Peypoux F., Bonmatin J. M., Wallach J. (1999) *Appl Microbiol Biotechnol.,* **51**, 553 –563

33. Rautenbach M. (1999) The synthesis and characterisation of analogues of the antimicrobial peptide iturin A_2, Ph.D. – Thesis (Biochemistry) University of Stellenbosch,

34. Garbay-Jaureguiberry C., Roques B. P., Delcambe L., Peypoux F., Michel M. (1978) *FEBS Lett.* **93**, 151 –156

35. Bonmatin J. M., Labbé H., Ptak M. (1994) *Biopolymers* **34**, 975 –986 Bonmatin J. M., Labbé H., Ptak M. (1994) *Biopolymers* **34**, 975 –986

Chapter 7

Conclusions, preliminary results and future prospects

This is the first investigation into the effect of surfactin and iturin A on the biological activity of gramicidin S. The broad aim of this ongoing project is to elucidate the influence of different peptides from competitive, cohabiting organisms on each other, which may eventually impact on organism survival. The objectives of this study were: 1) to evaluate the impact of surfactin on the biological activity of gramicidin S, 2) to investigate inter-molecular interactions involved with ESMS and 3) to evaluate the possibility of a general defence against gramicidin S toxicity using iturin A and synthetic iturin analogues in a preliminary study. An ancillary objective to the investigation into the influence on biological activity was the development of sensitive antifungal assay systems.

7.1 Experimental conclusions

The identity of the various surfactin forms present in the commercially available mixture as well as the fidelity of gramicidin S, iturin A and synthetic analogues were determined as reported in Chapter 2. It was determined that surfactin and gramicidin S met the purity stated by the manufacturer, but iturin A did not fully comply. In addition, for example, the commercially obtained iturin contained trace amounts of what appears to be the related peptide mycosubtilin. Similarly, a surfactin sample obtained from Sigma (not used in this study) contained trace amounts of iturin A_2. These findings underlines the importance of validating commercial peptides even those acquired from reputable suppliers. Although successful syntheses of the linear iturin precursors were performed the synthetic methods available for this study did not allow for the successful, large scale for the synthesis of iturin C. Results obtained with the linear analogues validated purification through the unique method of self-assembly, which is partially related to crystallisation as separation technique. Peptides were further purified by HPLC and final analyses of the peptides indicated that both analogues were of suitable high purity for use in biological experiments (92.6% and 95.5% pure for 8-$Beta_c$ and 8-Beta respectively).

In the antifungal assay development section (Chapter 3) we were able to develop two assays which rendered repeatable, analytical results within analytical error limits being $r^2 \geq 0.998$ and $p = 0.78$ for the broth assay and $r^2 \geq 0.998$, and $p = 0.78$ for the agar based assay. The inhibition parameters determined for gramicidin S against *P. corylophilium* with the broth assay were $IC_{min} = 2.4$ μM, $IC_{50} = 5$ μM and $IC_{max} = 11$ μM. The agar based assay rendered $IC_{min} = 2.4$ μM, $IC_{50} = 4.5$ μM and $IC_{max} = 11$ μM. The drastic reduction in assay time observed for the microagar assay indicates the importance of oxygen diffusion rate. However, the influence of the agar as nutrition source cannot be discounted. Furthermore, the similar inhibition parameters obtained with the microagar assay showed that peptide inactivation by the agar did not take place and therefore cell-peptide interaction did occur in the solution phase.

Investigation into the biological effect of gramicidin S and surfactin mixtures showed that surfactin had a pronounced antagonistic effect on gramicidin S activity. This antagonism was monitored with biological activity studies using *Escherichia coli*, *Micrococcus luteus,* and *Penicillium corylophilium* as target organisms. A dose-dependent antagonism was observed with all the test organisms. A markedly different antagonism profile was observed with *M. luteus* as target organism with respect to the profiles obtained with *E. coli* and *P. corylophilium*. The results obtained indicate that a degree of synergism may exist between the peptides at low concentration with regard to the Gram-positive target cell and that antagonism at higher concentration is limited to the solution phase. This may indicate that surfactin and gramicidin S work synergistically with respect to gram-positive organisms at low surfactin concentrations. This may seem to contradict the hypothesis, since the producer organism is also Gram-positive. However, host-immunity to antibiotics has been demonstrated [1, 2, 3] and therefore this effect may not extend to the surfactin producer. Furthermore, it has been shown that surfactin and iturin A adsorbs onto the *B. subtilis* membrane with the fatty acid moiety orientated to the environment [4]. This adsorption may protect the producer against the antimicrobial action of gramicidin S, especially if surfactin assembles in a "secondary membrane" on the cell surface orientating the gramicidin S binding area towards the environment.

Electrospray mass spectrometry revealed that the loss of gramicidin S activity is most probably the result of non-covalent complexes formation between gramicidin S and surfactin.

Results indicate that surfactin interacts with gramicidin S in a 1:1 and 2:1 ratio. Collisionally induced dissociation (CID) showed the complexes to consist of gramicidin S and surfactin. Whether the 2:1 complex formation is the result of two separate surfactin molecules each interacting with an Orn-residue or a surfactin dimer interacting with a gramicidin S molecule, is unclear at this stage. Cone voltage driven dissociation and CID of the complexes showed that the complexes were less stable than the composite peptides. Minor differences in surfactin conformation were previously reported [5]. Although minor differences were observed for both the surfactin forms and peptide complexes, this was most probably due to the acyl chain length rather than peptide ring conformation as the surfactin variant with the shortest acyl chain showed the greatest stability. Furthermore, the stability of this specie was reflected in the stability of the corresponding complex. Therefore, differences in surfactin composition are not reflected in gramicidin S binding ability or selectivity. The increase in complex formation with the increase of acetonitrile concentrations indicated that the interactions between these amphipathic peptides are most probably of polar character and not the consequence of hydrophobic interactions.

Titration of preformed surfactin-gramicidin S complexes with NaCl revealed that the presence of the metal ion had little or no influence on complex stability. Furthermore, no sodiated complexes were detected, indicating that ion interaction is not favourable after complex formation. The influence of alkali or earth metal ion interaction with surfactin on complex formation was investigated by incubating surfactin with NaCl and $CaCl_2$ before titration with gramicidin S. Results show that complex formation was uninhibited by the presence of these metal ions. Furthermore, the interaction of gramicidin S and metal ions with surfactin were found to be mutually exclusive, as no ion-peptide-peptide complexes were detected. In addition, gramicidin S had a pronounced effect on calcium-induced surfactin-surfactin interactions. The signals observed for these species decreased after the addition of the *B. brevis* peptide. The absence of a reciprocal increase in surfactin-Ca^{2+} or the formation of calcium-associated complexes may indicate that these complexes are formed through the displacement of the metal ion rather than through a "detergent" effect. At this stage it is unclear exactly what type of electrostatic force or forces are involved in complex formation, but it is unlikely that the mechanism involves only a direct competition of gramicidin S with Ca^{2+}. However, the displacement of calcium may indicate that peptide-peptide interaction results in a conformational change that prevents surfactin-metal ion interaction. In this case,

the most likely additional area of interaction is one of the β-turns in the peptide ring.

Biological experiments with iturin A indicate that antagonism of gramicidin S activity also extends to this related lipopeptide. The evaluation of the iturin data was complicated by the biological activity of iturin A. However, clear antagonism of gramicidin S activity was observed at concentrations as low as 5 μM iturin A and no synergism between gramicidin S and iturin was observed, as with surfactin. The interpretation of the biological results obtained was complicated by the membrane activity of iturin A. Iturin A caused a 50% inhibition of *M. luteus* growth at 30 μM. The activity of iturin A decreased with decreasing iturin A concentrations and no activity were observed at 2.5 μM. Furthermore, iturin A caused 50% inhibition of M. luteus growth at 30 μM but in the presence of 6 μM only 19% inhibition was observed for iturin A. These results indicate that 80% of iturin A activity was lost and that mutual antagonism if biological activity takes place. Clear antagonism of gramicidin S biological activity could not be shown for the linear iturin analogues. However, subtle changes observed in the dose-response profile when 8-Beta$_c$ was present indicates that some antagonism occurs at high gramicidin S concentrations, which may be a strong indication indicates that antagonism of gramicidin S activity may also extend to iturin C.

Mass spectrometry of peptide mixtures reinforced the conclusion derived from the surfactin data that antagonism is related to the formation of inactive complexes. Gramicidin S formed complexes with al the forms of iturin A, whereas no complex formation was observed for the linear analogues, 8-Beta and 8-Beta$_c$ under the same ESMS conditions as the iturin A-gramicidin S analysis. However, complexes were observed at extremely low energy conditions. Both the linear analogues influenced the mass spectrometric character of gramicidin S resulting excessive gramicidin S fragmentation in the presence either 8-Beta$_c$ or 8-Beta. This indicates that interaction between the molecules do exist under ESMS conditions but this interaction is not reflected in biological activity. The inability of the analogues to form stable complexes points to rigid conformational requirements. The linear analogues retain at least one of the two β-turns of the native molecule [6], whether this indicates that both β-turns are involved in complex formation or that backbone rigidity is required for stable complex formation may be the topic of a further investigation. Furthermore, this also supports the exclusion of hydrophobic interaction as the sole contributor to complex formation.

A concern in this investigation was the possibility of non-specific interactions especially under ESMS conditions. These concerns were addressed by investigating two control peptides, the glycopeptide vancomycin, [7] and the ESF1-SAGR, a model with a symmetrical α-helical structure [8]. Surfactin did not enhance or antagonise the activity of either peptide. Furthermore, no interaction between the peptides and surfactin was observed under MS conditions. These results further illustrate that a degree of specificity exists between gramicidin S and surfactin. Furthermore, this specificity is not only dependant charge but may be related to the β-turn structure and the spatial arrangement of the positive residue. Although ESF1-SAGR (ESF1 with Ala substituted for Ser and Arg substituted for Gly) carries the same polarity as Orn the spatial arrangement of the atoms might preclude interactions based on charge *and* atomic geometry. A more appropriate control peptide may be the model KLK peptide [9], which was not available at the time this study was performed. As Lys is analogous to Orn (R = $(CH2)_4NH_3^+$ for Lys and R = $(CH2)_3NH_3^+$) this might give a better indication of the spatial orientation requirements of the polar groups involved. However, the combined results of the interaction of gramicidin S with surfactin, iturin A, and other iturin analogues do indicate that a) electrostatic interactions are involved in peptide-peptide interaction, b) that a fixed stoichiometry is involved in these interactions and c) that the structural integrity of the peptide is necessary for complex formation. As the β-turns are a common denominator in both surfactin and iturin structures, it is conceivable that gramicidin S interaction with both peptides may revolve round the presence if these structures. If interactions occur in the β-turns, it indicates a degree of specificity in peptide-peptide interaction. Therefore, the formation of complexes between the *B. subtilis* products and gramicidin S does appear to form part of the host defence of *B. subtilis*. This extends the concepts of synergism and biological activity beyond the augmentation of antibiotic activity and the ability to induce cell death.

7.2 New preliminary results

This study has raised a number of questions regarding specificity and area of interaction. Unfortunately time constraints did not allow the full investigation of these questions. However, several pilot studies have been launched and the preliminary results will be discussed briefly.

Central to the hypothesis of an "anti-antibiotic" or "shield" peptide is compound specificity. The control peptides showed that this interaction is not a non-specific peptide-peptide interaction. The question that remained is whether this phenomenon is limited to interaction of gramicidin S with surfactin and iturin. Therefore, a. pilot study was initiated using gramicidin D (a mixture of gramicidins A-C and E). Initial biological experiments, using *M. luteus* as target cell, indicate that surfactin increased the IC_{50} concentration of the peptide mixture with >100% (from 6.7 μM to 15.2 μM). The inactive complex hypothesis was tested with mass spectrometry using tyrothricin – a mixture of gramicidin D, gramicidin S, and the tyrocidines. Results indicated that surfactin not only formed complexes with all the gramicidins present, but also with all the forms of tyrocidin present. It is therefore likely that surfactin-induced antagonism of biological activity extends to all the *B. brevis* peptides. The tyrocidins, with only one Orn residue and varying number of Phe residues, offer an opportunity to explore the relative contribution of the polar/hydrophobic interactions in complex formation. Future studies will necessitate the purification to homogeneity of these compounds. In addition to the iturins, another *B. subtilis* peptide may have been present in trace amounts in the commercially obtained peptide mixture. This compound's mass to charge ratio corresponds to that of a related peptide, mycosubtilin. Complex formation was observed between this specie and gramicidin S. This compound needs to be positively identified as mycosubtilin, and if it is indeed mycosubtilin this will further extend the specificity of these interactions. These preliminary results indicate that complex formation between the *B. subtilis* peptides and the *B. brevis* peptides may indeed by a general defence mechanism.

Ancillary to the issue of specificity is the interaction environment i. e. whether the interaction takes place in solution phase or at membrane-environment interface with surfactin being membrane bound. By extension, this will determine whether intra-cellular targets are affected or not. The emergence of atomic force microscopy (AFM) as an analytical tool in biological sciences [10] offered an exciting, visual way of investigating possible membrane effects. In previous studies Holroyd *et al.* [11] and Rautenbach *et al.* [12] clearly showed peptide-induced changes in membrane topology in erythrocytes and *E. coli* respectively. The authors found the formation of legions on the surface erythrocytes and showed the difference in cell surface vesiclisation induced by different peptides including gramicidin S. We have found in preliminary studies that the surfactin coated both the *E. coli* cell surface as well as the silica slide used for sample preparation. Upon the addition of gramicidin S, the silica bound

surfactin formed vesicles and the cell surface topology changed slightly, but membrane vesiclisation was not observed. Therefore, it seems that gramicidin S is "trapped" at the cell wall-membrane interface and is not available to intracellular targets. However, the effect on the Gram-positive organisms is likely to be more complicated given that surfactin does possess membrane activity against Gram-positive cells.

Another aspect of the specificity of interaction is molecular specificity i.e. how do the molecules "fit". Tandem mass spectrometry has successfully been used to elucidate the structure surfactin and iturin A_2 [13]. Furthermore, MS/MS was successfully used to study the interaction of the peptides and peptide analogues with metal ions [13, 14]. We used tandem mass spectrometry in a preliminary study on the molecular interaction of surfactin with gramicidin S. Collisionally induced dissociation of the peptide complex with m/z = 1082 resulted in a number of unique fragments that cannot be ascribed to the primary sequence of either surfactin or gramicidin S. In particular, a fragment with *m/z* = 450.00 were assigned to a doubly charged, hydrated, fragment ion complex between gramicidin S b_4 and surfactin b_6y_7 (calculated *m/z* =450.02). In addition, a surfactin fragment was observed with *m/z* =569.8 (b_6/y_7; calculated *m/z* = 569.65), that was not generated upon CID of surfactin alone. However, this sodiated fragment (b_6y_7+Na+H) was observed upon CID of sodiated surfactin (*m/z* = 594.0; calculated *m/z* = 593.65). These results point to the protection of the β-turn during CID when surfactin is complexed with either Na^+ or gramicidin S, similar to what Rautenbach *et al.* found for linear 8-beta and sodium [14]. Although this data needs to be confirmed with further MS experiments the results indicate that: 1) mass spectrometry can successfully be used to characterise non-covalent interaction between the peptides, 2) that the interaction is sequence specific and it is unlikely that non-specific (non-polar) interactions are the primary contributors to complex formation, and 3) that the β-turn of surfactin is a probable site for interaction with gramicidin S.

7.3 Future prospects

An immediate and specific area of future research would involve both the determination the type of interaction involved, as well as the testing of the hypothesis that this phenomenon represents a novel, defence mechanism. A multitude of analytical techniques such as nuclear magnetic resonance, surface plasmon resonance, Fourier transform infrared spectroscopy,

circular dichroism and mass spectroscopy exists to investigate the physical characteristics molecular interactions. These techniques, together with chemical manipulation and/or the generation of synthetic analogue libraries, can be used to elucidate the nature of peptide interaction. Monitoring bacterial growth in mixed peptide producer cultures, under different culture conditions, will reveal the significance of peptide interaction in terms of organism survival.

Establishing the generality of antibiotic-antibiotic interaction as defence mechanism is a long-term research prospect that may proof to be of paramount importance as this may aid in our understanding of bacterial resistance, especially in relation to human pathogenesis.

7.4 Hypothesis

The results of this study indicated that a novel defence mechanism might exist for *Bacillus subtilis* i.e. a mechanism that involves the synthesis and secretion of peptides to act as molecular shields against the toxic product of a competitor. In addition to shielding B. subtilis surfactin acts cooperatively with gramicidin S against other Gram-positive bacteria. Furthermore, should the cooperative behaviour not lead to sufficient resources for both bacteria, the molecular shield or anti-antibiotic will allow *B. subtilis* to survive until it can enter an anaerobic phase. A condition that it's competitor, *Bacillus brevis*, cannot survive. The hypothesis is illustrated in *Figure 1* with the simplified life cycle of the *B. brevis* (A), *B. subtilis*, (B) and the hypothetical mixed culture (C).

An anomaly seems to exist within the hypothesis in that fungi and Gram-negative bacteria are protected from the antibiotic action of gramicidin S. The origin of the contradiction might be found on the source data of the hypothesis. *In vitro* systems were used to gather the data, and these systems cannot give a true reflection of *in vivo* behaviour. The apparent protection might therefore be an experimental artefact created by concentration effect and membrane characteristics. However, the anomalies observed should not detract from the basis on which this hypothesis was build: surfactin causes a dose-dependent antagonism of gramicidin S, possibly through the formation of stable, inactive complexes. Furthermore, it appears that this interaction occurs at membrane level, which is consistent with reports stating that surfactin readily adsorbs onto the producer membrane upon secretion [15]. In addition, the synergism observed between gramicidin S and surfactin casts a new light on the intricacies and

complexity of the microbial environment – an environment where symbioses and antibiosis are two sides of the same coin.

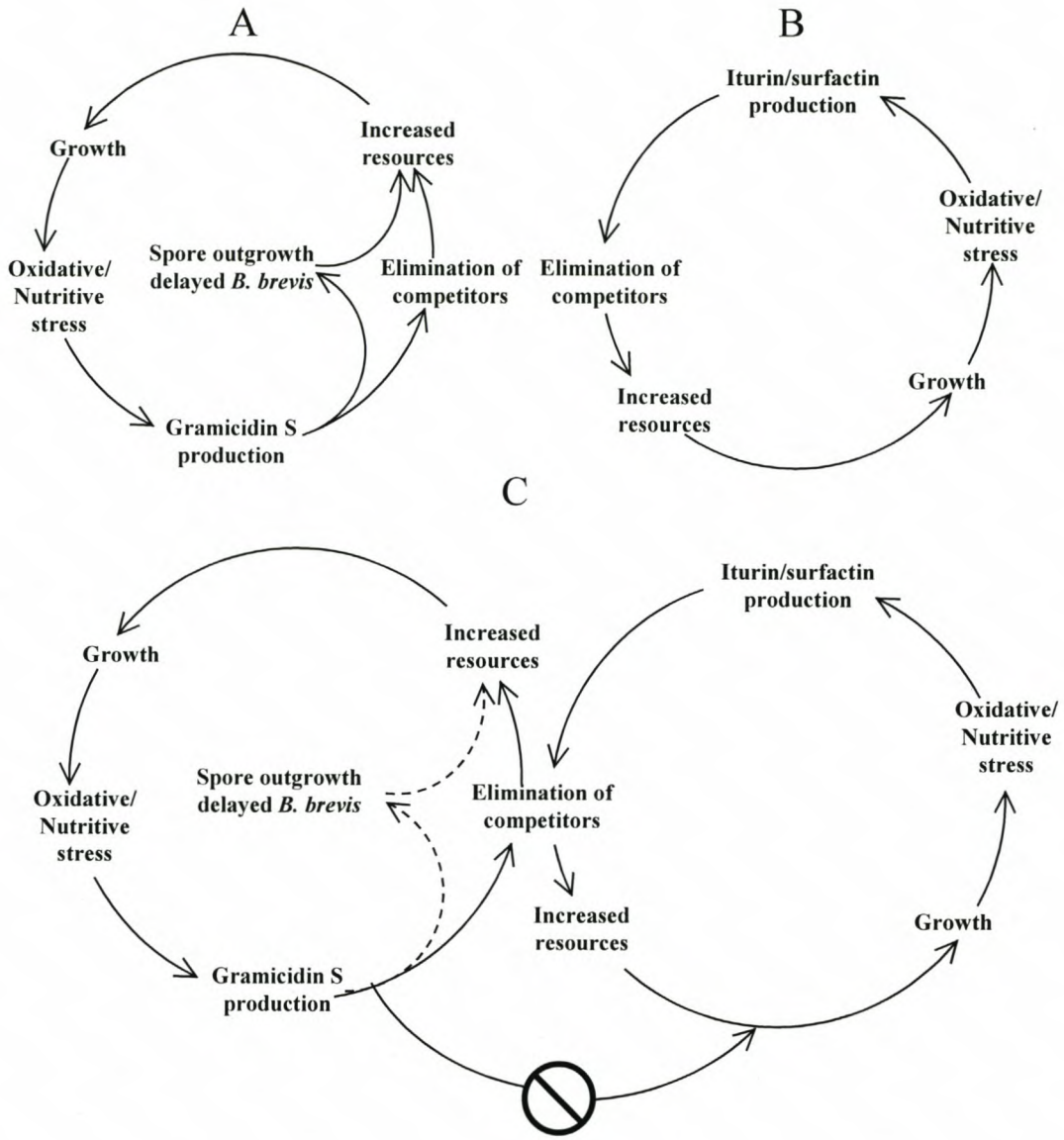

Figure 1 A Simplified illustration of the anti-antibiotic hypothesis with the *B. brevis* cycle (A) and the *B. subtilis* cycle (B). The hypothetical mixed culture as illustrated in (C) shows cooperation between surfactin and gramicidin S when the action of gramicidin S is directed at organisms other than B. subtilis. The effect of gramicidin S on B. subtilis is negated by surfactin (indicated with ⊘).

7.5 References

1. Azuma T. & Demain A. L. (1996) *J. Indust. Microbiol.*, **17**, 55 –61

2. Seddon B. & Nandi S. (1978) *Biochem Soc. Trans.*, **6**, 412 –415

3. Nandi S. & Seddon B. (1978) *Biochem. Soc. Trans.*, **6**, 409 –411

4. Ahimou F., Jacques P., Deleu M., (2000) *Enzyme and Microbial Technology*, **27**, 749 –754

5. Ferré G., Besson F., Buchet R. (1997) *Spectrochemica Acta Part A.*, 53, 632 –635

6. Rautenbach M. (1999) The synthesis and characterisation of analogues of the antimicrobial peptide iturin A_2, Ph.D. – Thesis (Biochemistry) University of Stellenbosch

7. McCormick M. H., Stark W. M., Pittenger G. E., Pittenger R. C., McGuire J. M. In, *Antibiotics Annual*, (1955-56), 606 - 611 Medical Encyclopaedia, Inc, New York, USA

8. Dykes G.A., Aimoto S., Hastings J.W. (1998) *Biochem. Biophys. Res. Commun.*, **248**, 268-72.

9. Oren Z., Homg J., Shai Y. (1992) J. Biol. Chem., 272, 14643 –14649

10. Dufrêne Y. F., (2003) *Current Opinion in Microbiology*, **6**, 317–323

11. DL Holroyd, MSc Analysis of the interaction of antimicrobial peptides with specific target-membranes. April 2003, M. Sc. Thesis, University of Stellenbosch

12. Meincken M, Holroyd DL, Sanderson RD, Rautenbach M (2004) An AFM study of the membranolytic effect of antimicrobial peptides on /Escherichia coli/, SPM2004 Conference, Beijing, China

13. Williams S. M. & Brodbelt J. S. (2004) *J. Am. Soc. Mass Spectrom.*, **15**, 1039 –1054

14. Rautenbach M., Swart P., van der Merwe M. J. (2001) *J. Am. Mass Spectrom.*, **12**, 505 –516

15. Ahimou F., Jacques P., Deleu M., (2000) *Enzyme and Microbial Technology*, **27**, 749 –754